

Activity of leg motoneurons during single leg
walking of the stick insect:
From synaptic inputs to motor performance

Inaugural-Dissertation zur Erlangung des Doktorgrades
der Mathematisch-Naturwissenschaftlichen Fakultät
der Universität zu Köln

vorgelegt von

Jens Peter Gabriel
aus Bielefeld

Köln
2005

Berichterstatter: Prof. Dr. Ansgar Büschges

Prof. Dr. Holk Cruse

Tag der letzten mündlichen Prüfung: 13.1.2006

Abstract

In the single middle leg preparation of the stick insect, leg motoneurons were recorded intracellularly during stepping movements on a treadmill. This preparation allows investigating the synaptic drive from local sense organs and central pattern generating networks to motoneurons. The synaptic drive comprises rhythmic ('phasic') excitation and inhibition and a sustained ('tonic') depolarization. This general scheme was found to be true for all motoneurons innervating the muscles of the three major leg joints. A comparison e.g. with results obtained from deafferented and pharmacologically activated preparations of the stick insect suggests that both tonic depolarization and phasic inhibition originate from central networks, while the phasic excitation is mainly generated by local sense organs.

Recruitment of motoneurons was studied on the flexor tibiae muscle as an example of a complexly innervated muscle. It is innervated by ~14 slow, semifast and fast motoneurons that are firing action potentials during the stance phase of the step cycle. During slow steps or steps under small load, less motoneurons are recruited than during fast steps or steps under high load. Fast flexor motoneurons are recruited later during stance phase than slow motoneurons. All motoneurons receive substantial common synaptic drive during walking. They are recruited in an orderly fashion due to the more negative resting membrane potential of the fast motoneurons, which thus require a larger and longer lasting depolarization to reach the threshold for the generation of action potentials.

Because walking is not invariable but needs to be adjusted to the behavioral requirements, it was investigated how these adjustments are implemented at the motoneuronal level. The activity of flexor and extensor tibiae motoneurons was analyzed during steps with different velocities. Extensor motoneuron activity during the extension phase of the step cycle (i.e. swing phase) is rather stereotypic and invariant with stance velocity. Flexor motoneurons show two distinct periods of depolarization at the beginning of stance. The initial depolarization is also stereotypic and most likely generated by a release from inhibition that allows the underlying tonic excitation to depolarize the neuron. The subsequent depolarization is larger and faster during fast steps than during slow steps. This indicates that in the single insect leg during walking, mechanisms for altering stepping velocity are becoming effective only during already ongoing stance phase motor output. Since a large portion of the phasic excitation arises from sense organs, it is conceivable that for the generation of different stepping velocities the effectiveness of these pathways are centrally modulated, for example by variations in the degree of presynaptic inhibition.

Zusammenfassung

In der Mittelbein-Einbeinpräparation der Stabheuschrecke wurden während Schreitbewegungen auf einem Laufband Motorneurone der Beinmuskeln intrazellulär abgeleitet. Diese Präparation ermöglicht eine Analyse der synaptischen Eingänge die Motorneurone von lokalen Sinnesorganen und zentralen rhythmusgenerierenden Netzwerken erhalten. Diese Eingänge bestehen aus einer rhythmischen (phasischen) Erregung und Hemmung und einer persistierenden (tonischen) Depolarisation. Dieses Grundmuster wurde in allen Motorneurongruppen gefunden die die Muskeln der drei wichtigsten Beinelenke innervieren. Ein Vergleich z.B. mit Ergebnissen von deafferentierten oder pharmakologisch aktivierten Präparationen der Stabheuschrecke deutet darauf hin, dass sowohl die tonische Depolarisation als auch die phasische Hemmung in zentralen Netzwerken generiert wird, während die phasische Erregung auf Signalen von lokalen Sinnesorganen beruht.

Die Rekrutierung von Motorneuronen wurde am Flexor tibiae als Beispiel für einen komplex innervierten Muskel untersucht. Er wird von ~14 sog. langsamen, intermediären und schnellen Motorneuronen innerviert, die Aktionspotentiale während der Stemmphase des Schrittes erzeugen. Während langsamer Schritte oder Schritten mit geringer Last werden weniger Motorneurone rekrutiert als bei schnellen Schritten oder solchen mit hoher Last. Schnelle Flexor-Motorneurone werden später während der Stemmphase rekrutiert als langsame Motorneurone. Alle Motorneurone erhalten zum großen Teil gemeinsame synaptische Eingänge während der Schreitbewegungen. Die geordnete Rekrutierung erfolgt durch das negativere Ruhemembranpotential der schnellen Neurone, die dadurch eine längere und stärkere Depolarisationsphase benötigen um das Schwellenpotential zur Erzeugung von Aktionspotentialen zu erreichen

Weil es sich beim Laufen nicht um ein invariantes Bewegungsmuster handelt, sondern ständige Anpassungen an Umwelt und Verhaltenssituation erforderlich sind, wurde untersucht wie diese Anpassungen auf der Ebene der Motorneurone verwirklicht werden. Die Aktivität von Flexor- und Extensor tibiae-Motorneuronen wurde während Schritten mit unterschiedlichen Schreitgeschwindigkeiten verglichen. Die Aktivität der Extensor-Motorneurone während der Schwingphase ist stereotyp und invariant mit der Bandgeschwindigkeit während der Stemmphase. Flexor-Motorneurone zeigen zwei Depolarisationsphasen zum Beginn der Stemmphase. Die anfängliche Depolarisation ist auch stereotyp und wird wahrscheinlich durch das Ende der phasischen Hemmung bei gleichzeitiger tonischer Depolarisation erzeugt. Die darauf folgende Depolarisation hat während schneller Schritte eine größere Amplitude und einen schnelleren Zeitverlauf als

während langsamer Schritte. Dies deutet darauf hin, dass während der Schreitbewegungen Mechanismen zur Erzeugung unterschiedlicher Stemmgeschwindigkeiten erst dann effektiv werden, wenn die Muskelkontraktion schon begonnen hat. Weil ein Großteil der phasischen Erregung von sensorischen Bahnen erzeugt wird ist es denkbar, dass zur Erzeugung unterschiedlicher Schreitgeschwindigkeiten die Effektivität dieser Bahnen zentral moduliert wird, z.B. durch Variationen im Grad der präsynaptischen Inhibition.

Table of Contents

1. Introduction	8
1.1. <i>Synaptic drive to motoneurons</i>	8
1.1.1. Central pattern generators	9
1.1.2. Afferent signals from sense organs	10
1.1.3. Higher brain centers	10
1.2. <i>Intrinsic properties of motoneurons</i>	12
1.2.1. Significance for recruitment	12
1.2.2. Bistable properties	12
1.3. <i>Control of stepping velocity</i>	13
1.3.1. Mechanisms for changing swimming speed	13
1.3.2. Mechanisms for changing walking speed	13
1.3.3. Advantages of the single leg preparation	14
1.4. <i>Objectives</i>	15
2. Materials & Methods	16
2.1. <i>Preparation</i>	16
2.2. <i>Treadmill</i>	16
2.3. <i>Electrophysiology</i>	18
2.3.1. Extracellular recordings	18
2.3.2. Intracellular recordings	18
2.4. <i>Data recording and evaluation</i>	19
2.5. <i>Statistics</i>	20
3. Results	21
3.1. <i>Basic description of walking movements and motor pattern</i>	21
3.1.1. Leg anatomy	21
3.1.2. Walking movements	21
3.1.3. Motor pattern	23
3.2. <i>Synaptic drive to flexor tibiae MNs</i>	26
3.2.1. Modulation of membrane potential during stepping	26
3.2.2. Input resistance shows synaptic drive	28
3.2.3. Current injection shows reversal potentials	32
3.2.4. Voltage-clamp recordings	40
3.2.5. Functional significance of the tonic depolarization	41
3.2.6. Other leg motoneurons	44
3.2.7. Summary	49

3.3.	<i>Recruitment of slow and fast flexor MNs</i>	50
3.3.1.	Muscle structure	50
3.3.2.	Functional requirements	50
3.3.3.	Consecutive recruitment	51
3.3.4.	Membrane potential depolarization in slow and fast flexor motoneurons	51
3.3.5.	Common synaptic inputs	54
3.3.6.	Activity at different frictional levels	55
3.3.7.	Resting membrane potential and spike threshold	55
3.3.8.	Conclusions	57
3.4.	<i>Control of stepping velocity</i>	58
3.4.1.	Correlation of cycle period and belt velocity	58
3.4.2.	Amplitude of membrane potential modulation and spike frequency	58
3.4.3.	Time course of membrane potential modulation in flexor motoneurons	63
3.4.4.	Time course of membrane potential modulation in extensor motoneurons	66
4.	Discussion	69
4.1.	<i>Synaptic drive to leg MNs</i>	69
4.1.1.	Tonic depolarization	69
4.1.2.	Phasic modulation	71
4.2.	<i>Recruitment of slow and fast flexor MNs</i>	72
4.2.1.	Activity control in slow and fast Flex-MNs during stance	72
4.2.2.	Influence of belt friction	73
4.3.	<i>Control of stepping velocity</i>	75
4.3.1.	Cycle period of single leg stepping movements and varying stepping velocity	75
4.3.2.	Time course of membrane potential modulation of flexor motoneurons	76
4.3.3.	Antagonistic synaptic drive to flexor and extensor MNs and organization of the leg muscle control system for the single leg	78
	Literature	81
	Appendix	92

1. Introduction

Animals locomote through muscle contractions that move legs, wings or fins or change the body shape. In some cases, especially in “lower” invertebrates, muscles are antagonized by a hydroskeleton (e.g. pseudocoel of nematodes) or the body wall (e.g. mesoglea of medusae [Cnidaria]). In most invertebrates as well as vertebrates however, locomotion requires coordinated, rhythmical contractions of antagonistic, striated muscles that often move multi-jointed limbs and appendages. With the exception of myogenic mechanisms, e.g. in asynchronous flight muscles of dipteran and hymenopteran insects, contractions in striated muscle are elicited by one or more action potentials in the associated motoneurons. In extreme cases, in invertebrates just one excitatory motoneuron innervates a muscle (crayfish: opener muscle of walking legs, Cooper & Ruffner, 1998; locust: coxal adductor and levator tarsi muscle, Sasaki & Burrows, 1998), but usually it is 2-15 motoneurons. In vertebrates the number of motoneurons is much higher (13 in the human eye muscle rectus lateralis to 750 in the human biceps brachii; Blickhan, 1996). All motoneurons that innervate the same muscle belong to a common motor pool; a single motoneuron in conjunction with the innervated muscle fibers is termed a motor unit. In order to control the speed and amplitude of a contraction, there has to be an orderly recruitment of the motor units within the motor pool, and the action potential frequency of each motoneuron has to be well-tuned.

1.1. Synaptic drive to motoneurons

The motoneurons represent the ultimate site of integration for signals from the central nervous system and the periphery. The main sources of synaptic inputs (directly or indirectly via intercalated interneurons) are central pattern generating networks, sense organs and higher brain centers. Broadly spoken, synaptic drive to motoneurons can either persist over several locomotor cycles (tonic drive) or be confined to a certain phase of the locomotor cycle (phasic drive). For a motor output that is underlying rhythmic movements like swimming, walking flying, chewing, breathing, swallowing etc. (reviewed in Stein et al., 1997), motoneurons

innervating antagonistic muscles are required to fire one or more action potentials (in the latter case termed a burst) followed by a quiescent period during which antagonistic motoneurons are firing. Such a firing pattern is often based on rhythmical alternation of phasic excitatory and inhibitory synaptic to motoneurons (lamprey: Russel & Wallén, 1983; Dale, 1986; zebrafish: Buss & Drapeau, 2001; rodent: Cazalets et al., 1996; cat: Orsal et al., 1986; stick insect: Büschges et al., 2004). A tonic depolarization of motoneurons is also a prominent feature of many preparations (*Xenopus*: Soffe & Roberts, 1982; *Tritonia*: Getting & Degin, 1985; stick insect: Büschges et al., 2004).

1.1.1. Central pattern generators

At the core of the neuronal architecture that generates a rhythmic motor pattern in many cases one or more neuronal ensembles termed “central pattern generator” (CPG; Grillner & Zangger, 1975) have been identified. Brown (1911) first suggested that central circuits are generating the alternating flexion and extension of leg muscles in the cat. Since then such networks have been discovered in a large number of motor systems. In the absence of sensory feedback or descending inputs from higher brain centers, CPGs can generate rhythmic activity in motoneurons (reviewed in Pearson, 1993; Stein et al., 1997). In some preparations the rhythmic activity is very close to the pattern observed in the intact animal (crayfish stomatogastric nervous system: Selverston, 1977; leech heartbeat: Stent et al., 1979). In other systems, the rhythm generated in the isolated nervous system is still similar to that in the intact animal, but shows clear differences, e.g. a longer cycle period (Grillner, 1981; Chrachri & Clarac, 1990; Johnston & Levine, 1996), which has been explained with the lack of excitation from sense organs (Grillner, 1981; Pearson & Wolf, 1987; Chrachri & Clarac, 1990; cf. Cruse, 2002). It is generally assumed that in motor systems and under situations with small contribution of sensory feedback (e.g. due to very quick movements) the centrally generated rhythm is more similar to and of greater significance for the rhythm observed in the intact animal (Prochazka & Yakovenko, 2001; Cruse, 2002).

In the deafferented nervous system of the stick insect, CPG-like networks that control motoneuron activity can be activated by tactile stimulation of the head or abdomen (Bässler & Wegener, 1983; Büschges et al., 2004) or by application of the muscarinic agonist pilocarpine (Büschges et al., 1995). The motor pattern that was generated showed only some features of intact locomotor patterns, like switching between antagonistic motoneuron pools. No cycle-to-cycle coupling between neighboring leg joints or segments (Bässler & Wegener, 1983;

Büschges et al., 1995) was observed. This indicates that in the stick insect there may exist an individual CPG for each joint (a concept termed *unit-burst generator* by Grillner [1981] to describe the modular organization of pattern generating networks in the cat hind limb) which are coupled through central pathways and/or peripheral signals to ensure interjoint as well as intersegmental coordination (Cruse, 1990; Büschges, 2005; see below).

1.1.2. Afferent signals from sense organs

The experiments on the deafferented thoracic nerve cord of the stick insect mentioned in chapter 1.1.1 (Bässler & Wegener, 1983; Büschges et al., 1995; Büschges et al., 2004) show that in this system sensory signals are necessary for the cycle-to-cycle coupling of individual joint oscillators. Many influences that serve interjoint coordination have been identified (Hess & Büschges, 1997, 1999; Akay et al., 2001; Bucher et al., 2003; Akay et al., 2004) which together are sufficient to generate coordinated stepping movements of a stick insect middle leg when implemented in a neuro-mechanical simulation (Ekeberg et al., 2004; Büschges, 2005). Also, afferent signals from neighboring segments are an important mechanism to ensure a proper intersegmental coordination of leg movements (Cruse et al., 2003; Ludwar, 2003; Ludwar et al., 2005a). In order to maximally benefit an animal, the motor rhythm has to meet two prerequisites. It has to be stable and regular, but also flexible enough to allow compensations for sudden perturbations and also variations in walking gait, speed and direction. To ensure both stability and flexibility, proprioceptors play an important role. They signal joint position, load to a leg, muscle length or muscle strain to the CPG and/or directly to the motoneurons (monosynaptic reflex; human: Mendell & Hennemann, 1971; crayfish: Le Ray et al., 1997) and thereby influence the strength and timing of muscle contractions. Thus, signals from sense organs can e.g. lengthen step phases or facilitate phase transitions (reviewed in Pearson, 1993) or serve intersegmental coordination (Hill et al., 2003) as it is required for an effective locomotion (Marder & Calabrese, 1996; McCrea, 2001).

1.1.3. Higher brain centers

Descending signals from higher brain areas play an important role in the selection, initiation and adaptation of the motor pattern. Descending neurons can make direct connections with motoneurons (e.g. vertebrate corticospinal neurons; Preston & Whitlock, 1961) or have an indirect action by influencing CPG networks (Pagget et al., 2004). The segmental spinal networks in vertebrates are the target of descending supraspinal drive from higher brain

centers. In cats it has been shown that electrical stimulation of a site in the midbrain that has been termed mesencephalic locomotor region (MLR) can evoke locomotion (Shik et al., 1966; reviewed in Jordan, 1998). As in command systems of invertebrates (see below), the rhythm of the locomotor pattern is unrelated to the pattern of MLR stimulation. Similar experiments suggest the existence of a MLR in all vertebrates, since it has been found in birds, tetrapods, fish and cyclostomes (reviewed in Grillner et al., 1997). Neurons in the MLR and in another locomotor region in the lateral hypothalamus project to reticulospinal neurons that activate the locomotor CPGs. Obviously, the relatively simple, tonic activity pattern in the brain stem nuclei cannot account for all subtleties of vertebrate locomotion. For example for goal-directed locomotion, the participation of cortical (motor cortex) and subcortical structures (basal ganglia, cerebellum) is required (Gordon, 1991). In invertebrates, command neurons in the brain have been found that can evoke coordinated motor activity (e.g. crayfish swimmeret beating: Wiersma & Ikeda, 1964; cricket stridulation: Bentley, 1977; locust flight: Pearson et al., 1985; Heinrich, 2002). For example, in the cricket an identified interneuron in the protocerebrum can activate the pattern generator for stridulation when it is tonically firing action potentials (Hedwig, 2000). It is again important to note that activity in command neurons is unrelated to the motor rhythm itself (Bentley, 1977), which is produced by the pattern generating networks that are actuated. However, descending neurons can integrate sensory information of different modalities and convey this information to the thoracic pattern generating networks (Heinrich, 2002).

In the stick insect, cutting the circumesophageal connectives increases walking activity without substantially altering walking movements (Graham, 1979a,b; reviewed in Bässler, 1983; Graham, 1985), suggesting an inhibitory influence of the supraesophageal ganglion. After cutting of the neck connectives the animals show no organized walking movements, suggesting an excitatory influence of the subesophageal ganglion (Graham, 1979a; reviewed in Bässler, 1983; Graham, 1985). Similar to the command neurons that are involved in stridulation of the cricket, neurons in the subesophageal ganglion seem to have a “nonspecific stimulatory effect”, since their influence can be replaced by an especially strong abdominal stimulation (Bässler, 1983). Also, studies in locusts found that descending interneurons originating in the subesophageal ganglion are active during leg movements, but show extensive variability in their response properties (Altman & Kiehn 1979; discussion in Ridgel & Ritzmann, 2005). It has been suggested that descending inputs from the brain partly act to release neuromodulators that activate thoracic neuronal networks (Johnston et al., 1999; Ridgel & Ritzmann, 2005).

1.2. Intrinsic properties of motoneurons

1.2.1. Significance for recruitment

Motoneurons in vertebrates and invertebrates comprise a very variable population of neurons that differ in intrinsic properties such as size, membrane currents, amount and probability of transmitter release etc. In invertebrates, so-called slow, semifast and fast motoneurons can be distinguished that often innervate different sections of the muscle (Bässler et al., 1996; Sasaki & Burrows, 1998). Although vertebrate motoneurons are usually not termed fast or slow motoneurons, they also have different sizes and intrinsic properties that are important for the generation of a functional motor pattern. Intrinsic properties determine the neurons' response to synaptic inputs. For example, different thresholds for action potential generation (Burrows, 1996) can be responsible for one neuron firing action potentials while another one is not as a reaction to identical synaptic inputs. Another mechanism that has been discovered in vertebrates is termed the 'size principle' (Henneman et al., 1965), which states that differences in membrane resistance due to corresponding differences in cell body size are responsible for the differential consecutive recruitment of neurons from a motor pool that receive common synaptic inputs.

1.2.2. Bistable properties

In some cases, the motoneurons themselves possess the array of different ion channels that is required to generate the oscillations that underlie rhythmic motor pattern. For example in the stomatogastric ganglion of decapod crustaceans (STG), motoneurons can act as endogenous bursters (Bal et al., 1988, reviewed in Hooper & DiCaprio, 2004). In other cases, motoneurons can generate some features of the oscillations (reviewed in Nusbaum & Beenhakker, 2002). Among these features are the ability of motoneurons to sustain a depolarization in the absence of excitatory inputs (*plateau potential*; Llinas & Sugimori, 1980; Hounsgaard et al., 1984; reviewed in Kiehn & Eken, 1998), an increased excitability after inhibition (*post-inhibitory rebound*; Friesen, 1994; Angstadt et al., 2005) or the escape from inhibition (Kiehn et al., 2000). In vertebrate motoneurons, persistent inward currents have been found that increase the excitability for synaptic inputs (reviewed in Heckmann et al., 2005).

1.3. Control of stepping velocity

In a diverse and often non-predictable environment, the motor output of an animal needs to be adjusted at all time in order to fulfill the current requirements of a behavioral task. In walking, for example, such adjustments include changing the direction and the speed of locomotion. At present detailed knowledge exists on the generation of a basic locomotor output for a variety of locomotor behaviors, like swimming (reviewed in Friesen, 1994; Arshavsky et al., 1998; Grillner, 2003), walking (reviewed in Bässler & Büschges, 1998; Pearson & Gordon, 2000) and flying (reviewed in Robertson, 2003). However, when it comes to the neural mechanisms that underlie the patterning of motoneuron activity during modifications of the motor output, e.g. changing the speed of locomotion, the picture is less clear.

1.3.1. Mechanisms for changing swimming speed

For swimming in vertebrates and invertebrates considerable information is available on the mediation of changes in speed of locomotion. An increase in swimming speed results from an increase in the frequency of the rhythmic tail, fin or body movements. The lamprey, for example, swims by means of undulatory trunk movements that are generated by alternating contractions of the myotomes along its body axis. Within each body segment there is a CPG network that receives tonic glutamatergic excitation from reticulospinal neurons in the brainstem (Buchanan et al., 1987, reviewed in Grillner et al., 1997). The more tonic excitatory drive the CPG interneurons receive, the faster the networks oscillate which in turn provide alternating excitation and inhibition to the motoneurons (summary in Orlovsky et al., 1999). With increasing locomotor output not only the frequency, but to some extent also the magnitude of motoneuron activation and muscle contractions increases (Sirota et al., 2000), which in a freely moving animal would lead to an increase of swimming velocity. Results on fictive swimming in the *Xenopus* embryo (Sillar & Roberts, 1993; Roberts et al., 1998) and the marine mollusc *Clione* (Satterlie 1993; reviewed in Orlovsky et al., 1999) point in a similar direction.

1.3.2. Mechanisms for changing walking speed

For walking, less is known about the neural mechanisms in charge of modifying the activation pattern of motoneurons. In general walking systems are multi-legged with two, four, six or

more limbs. With changing speed interlimb coordination changes (Wendler, 1964; Graham, 1972; Cruse et al., 1994). In quadrupeds, for example, there is a change in gait from walk to trot to gallop when the speed of locomotion increases (summary in Orlovsky et al., 1999). The walking pattern of the single limb can contribute to an increase in locomotor speed in different ways, e.g. by an increase of step length, a decrease of cycle period or a combination of both. Although for example in the cat stride length of the stance phase increases to some extent with faster speeds of locomotion, it is primarily the decrease in cycle period that is responsible for the increase in speed (Halbertsma, 1983; Yakovenko et al., 2005, reviewed in Orlovsky et al., 1999). The same is true for walking in arthropods, e.g. in crayfish (Clarac & Chasserat, 1986) and stick insects (Wendler, 1964; Graham, 1972; Graham & Cruse, 1981). In turn, the decrease in cycle period is generally achieved by a decrease in stance phase duration, while swing duration varies little or not at all (stick insect: Wendler, 1964; Graham, 1972; locust: Burns, 1973; lobster: Ayers & Davis; 1974; cat: Halbertsma, 1983; reviewed in Orlovsky et al., 1999).

In insects it has been suggested that descending drive from the brain provides tonic excitation, the strength of which can influence walking speed (Roeder, 1937; Ridgel & Ritzmann, 2005). Similarly, in the cat the cycle period of the walking motor output changes with tonic background excitation from the brainstem. It is noteworthy that these descending signals appear not to directly control cycle period but instead determine the intensity of muscle contractions (Shik et al. 1966), suggesting that the changing afferent feedback from the limb is responsible for changing the cycle period (Yakovenko et al., 2005).

1.3.3. Advantages of the single leg preparation

How exactly the synaptic drive to motoneurons and their activity pattern in a walking animal are affected in the course of changes in walking speed, in particular *in vivo* is however still a largely unknown issue. Compared to the investigations reported above, the semi-intact single leg preparation of the stick insect endogenously expresses a locomotor rhythm varying in cycle period, speed or strength (Bässler, 1993; Fischer et al. 2001). The findings provide insights into the neural mechanisms that may be responsible for the generation of different walking speeds *in vivo*, and which also have implications for the design of robots utilizing biological principles of locomotion (Dürr et al., 2002; Ritzmann et al., 2004) or behavior-based computer simulations (Cruse et al., 1998; Dürr et al., 2004). The results may allow conclusions on the modifications in the premotor network that contribute to changes in

walking speed and enable us to develop specific hypotheses that can be tested in subsequent sets of experiments under more reduced conditions.

1.4. Objectives

As the interface between nervous system and musculature, motoneurons are the site of integration for synaptic drive from the CPG, afferent signals from sense organs and descending information from higher brain centers. Their intrinsic properties are responsible for the translation of these inputs into an appropriate firing pattern to drive the muscles. The single middle leg preparation of the stick insect (Bässler, 1993; Fischer et al. 2001) allows an in-depth intracellular analysis of the activity pattern of leg motoneurons during the execution of stepping movement in order to answer the following questions:

- What is the synaptic drive the motoneurons receive during the execution of rhythmic locomotor activity?
- Do the neurons in one motor pool receive similar or different synaptic drive during walking?
- What are the mechanisms that are responsible for an orderly recruitment of motoneurons? Do intrinsic properties play a role in this?
- What are the mechanisms that act at the level of the motoneurons to produce variations in motor output, e.g. different stepping velocities?

2. Materials & Methods

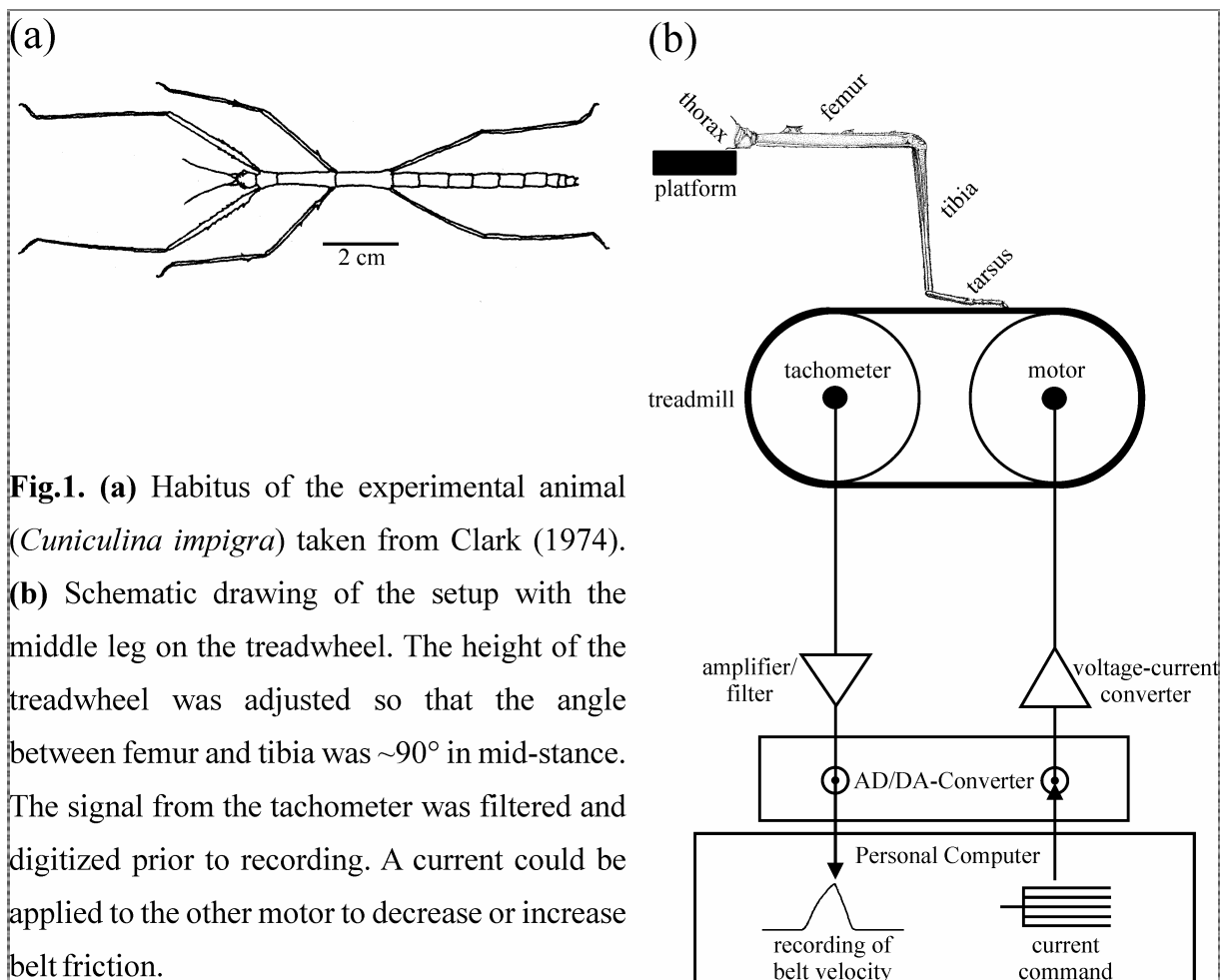
2.1. Preparation

The experiments were performed on adult female individuals of the stick insect species *Cuniculina impigra* (syn. *Baculum impigrum*) from a colony maintained at the University of Cologne (**Fig.1a**). All legs except one middle leg were severed at the level of mid-coxa. The thorax was glued to a foam platform dorsal side up with dental cement (*Protemp II*, 3M ESPE, Seefeld, Germany). Pro- and retraction of the remaining leg was blocked also with dental cement. A window was cut dorsally through the cuticle spanning from the middle of the meso- to the middle of the metathorax. The gut was moved aside and fat and connective tissue were removed in order to expose the mesothoracic ganglion and the lateral nerves. Care was taken to leave the main trachea intact. The lateral nerves 2 and 5 (nl2/nl5, nomenclature according to Marquardt, 1940) on the ipsilateral side of the remaining leg, innervating the pro- and retractor coxae muscles, respectively, were crushed with a fine forceps. The mesothoracic ganglion was lifted on a movable waxed platform and the surrounding connective tissue was pinned down with small cactus spines. To improve electrode penetration, small crystals of a proteolytic enzyme (*Pronase E*, MERCK, Darmstadt, Germany) were placed on the ganglionic sheath for 60-90s. The enzyme was thoroughly washed out and the thoracic cavity was filled with saline (NaCl 180mM; sucrose 30mM; HEPES 10mM; CaCl₂ 5mM; KCl 4mM; MgCl₂ 1mM).

2.2. Treadmill

The treadmill consisted of two styrofoam drums (diameter 40mm; width 28mm) each mounted on a micro DC-motor (*DC1516*, FAULHABER, Schönaich, Germany) that had a center distance of 50mm. Around them a belt made of light crepe paper (35g/m²) was placed. The tangential force that had to be applied to overcome belt friction was 4.0 ± 0.3 mN. The

moment of inertia of the system, which is determined by the effective mass of the treadmill, was 1.1g and thus equal to the mass of an adult animal ($1.1 \pm 0.3\text{g}$; $N=10$; mean \pm SD). One of the DC-motors served as a tachometer. The output voltage, which was proportional to belt velocity, was smoothed (first order low-pass filter, time constant 20ms) in order to eliminate voltage spikes. With the other motor, belt friction could be varied. By a computer-controlled voltage-current converter (Peter Heinecke, self-construction) a current could be applied that generated a torque and thereby changed the force required to move the belt without moving the belt itself. By this, belt friction could be altered in a range from 1.5 to 6.5mN. The treadmill was positioned below the leg perpendicularly to the longitudinal axis of the animal. The height was adjusted so that the angle of the joint between femur and tibia was $\sim 90^\circ$ in mid-stance (**Fig.1b**).



2.3. Electrophysiology

2.3.1. Extracellular recordings

Recordings were carried out under dimmed light conditions at room temperature (20-22°C). Both animal and electrodes were placed on an air table that dampened vibrations and minimized movement especially of the intracellular recording electrode relative to the animal. Electromyogramms (EMGs) of the femoral muscles were recorded by inserting two copper wires (diameter 50µm, insulated except for the tips) closely together through the cuticle of the proximal femur. Depending on the insertion site, muscle potentials from the flexor tibiae were recorded individually or (due to the vicinity of both muscles) together with extensor tibiae potentials. Potentials from these antagonists could be distinguished by amplitude and correlation with leg movements on the treadmill (cf. Fischer et al., 2001). In some figures, the flexor EMG was displayed twice: one on full scale (EMG 'Flex') and one on an enlarged scale to show the extensor potentials more clearly (EMG 'Ext'; see arrows in **Fig.3a**). Because of the innervation by several excitatory motoneurons (MNs) (~14 in the closely related species *Carausius morosus*; Storrer et al., 1986; Debrodt & Bässler, 1989), it was not possible to discriminate single motor units in the EMG recordings of the flexor tibiae muscle. However, intracellular recordings verified that the muscle potentials with the largest amplitude could be attributed to the fast (fFlex) MNs, while spike activity of the slow (sFlex) MNs produced muscle potentials with smaller amplitude. Potentials of semifast (sfFlex) MNs of the flexor tibiae could not always be distinguished from potentials of slow or fast motor units by amplitude.

In some experiments, an EMG from the levator trochanteris muscle was recorded by inserting wires dorsally into the coxa. Also, hook electrodes were used to extracellularly record the action potentials of protractor coxae MNs from the nerve n12 and retractor coxae MNs from n15 proximal to the site where they had been crushed. All extracellular recordings were amplified and band-pass filtered (50Hz-10kHz).

2.3.2. Intracellular recordings

Intracellular recordings of MNs were made from their arborizations in the neuropil of the mesothoracic ganglion. Glass micropipettes (GB100-TF8P, SCIENCE PRODUCTS, Hofheim, Germany) were pulled on a P-97 filament puller (SUTTER INSTRUMENTS, Novato, USA) and filled with 3M KAc/0,05M KCl tip solution (electrode resistance 15-

25MO). The signals were amplified with a SEC-10L intracellular amplifier (NPI ELECTRONICS, Tamm, Germany) in bridge, discontinuous current-clamp (DCC) or discontinuous single-electrode voltage-clamp (SEVC) mode. During recordings in switched mode (DCC, SEVC), switching frequency of >12 kHz were used and electrode potential was monitored on an oscilloscope. MNs were identified by leg movements evoked by firing of action potentials upon injection of depolarizing current and by correlation with muscle potentials in the EMG recordings. In case of the flexor tibiae, slow, fast and semifast MNs differed in the amplitude of flexion of the FT-joint during injection of depolarizing current. Each action potential in an fFlex-MN evoked a clearly visible twitching movement, while a single spike in a sfFlex-MN and a sFlex-MN caused a barely detectable movement. In these neurons, a train of action potentials at high frequency caused a smooth flexion of the FT-joint that was always faster in case of the sfFlex-MN. Also in the sfFlex-MNs, a clearly visible leg movement was evoked at lower spike frequencies than in the sFlex-MNs. Similarly, extensor, depressor and levator motoneurons were identified. Because nl2 and nl5 had been crushed, there was no leg movement upon action potential firing in pro- and retractor MNs. In this case, the correlation of action potential firing with an extracellularly recorded action potential in the nerves nl2 or nl5 was used for identification.

Recordings where no stable resting membrane potential was reached were discarded. A total of 25 flexor MNs, 17 extensor MNs, 10 depressor MNs, 7 levator MNs, 2 retractor MNs and 3 protractor MNs were recorded in 54 animals.

2.4. Data recording and evaluation

The electrophysiological data and the voltage output of the treadmill tachometer were digitized with a MICRO1401 A/D converter and recorded with SPIKE2 software (both CAMBRIDGE ELECTRONIC DESIGN, Cambridge, UK) on a personal computer. The other DC-motor of the treadmill was connected to the voltage-current converter, and a SPIKE2 sequencer program was written to apply a continuous current to the motor (**Fig.1b**). For further data evaluation custom SPIKE2 script programs were written. In order to estimate the gross activity of the flexor muscle at a certain time the EMG data were rectified and smoothed (first order low-pass filter, time constant 20ms). The area under this smoothed rectified EMG (SR-EMG) was used as a measure of the work performed by the flexor muscle (Lippold, 1952; Winter, 1990). For averaging of the membrane potential of Flex- and Ext-MNs the

spikes were eliminated from the intracellular recordings by substitution with a straight line (maximal 5ms before to 5ms after peak of action potential).

2.5. Statistics

Mean values were compared using a t-test. Means and samples were regarded as significantly different at $P < 0.05$. Likewise in a regression analysis, a correlation was assumed at $P < 0.05$. The following symbols show the level of statistical significance: (-) not significant; (*) $0.01 < P < 0.05$; (**) $0.001 < P < 0.01$; (***) $P = 0.001$. In the text, N gives the number of experiments or animals while n gives the sample size. Values are shown as mean \pm standard deviation (SD).

3. Results

3.1. Basic description of walking movements and motor pattern

3.1.1. Leg anatomy

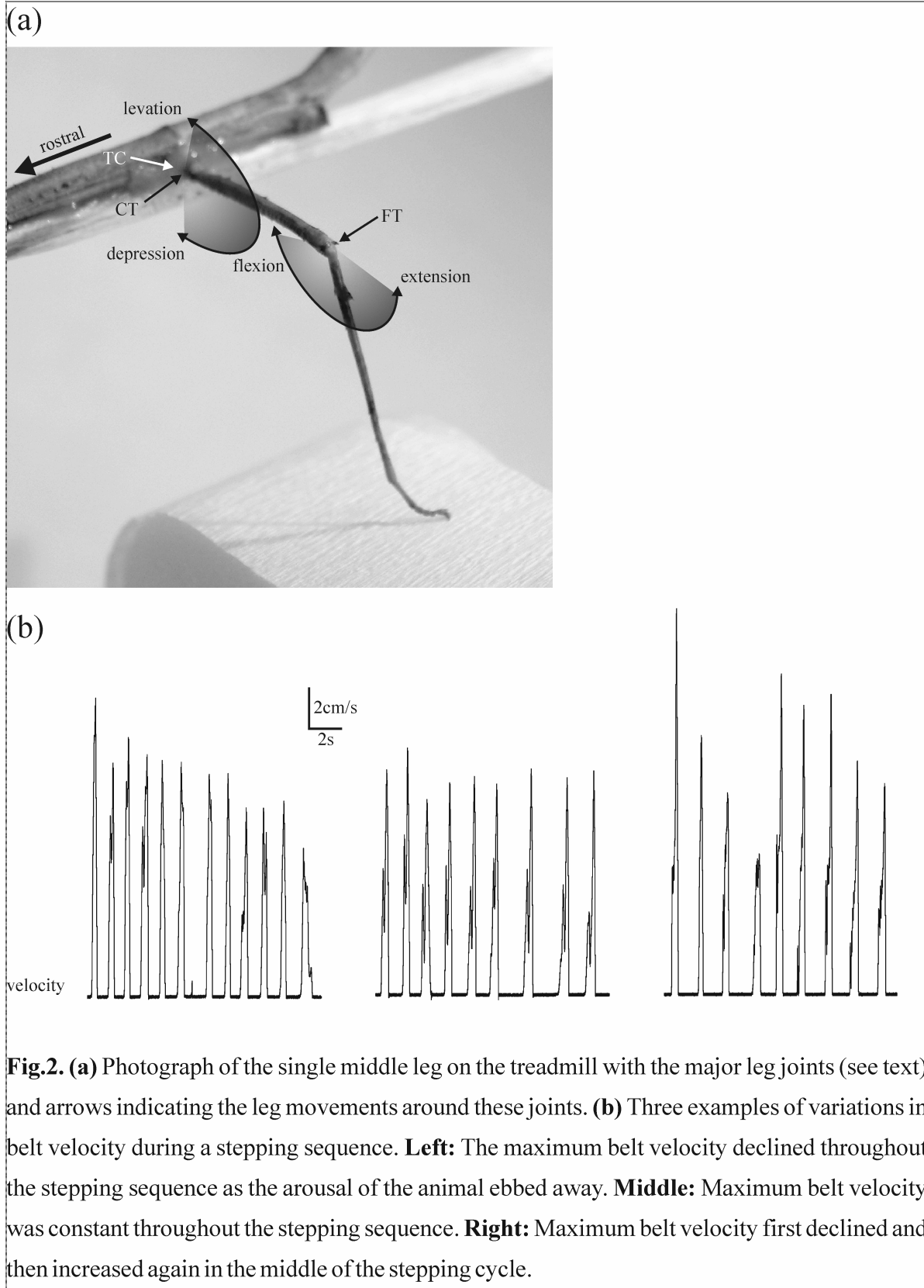
A photograph of the middle leg is shown in **Fig.2a** with arrows symbolizing the movement around the major leg joints. These are

- the **femur-tibia (FT-)** joint, where the tibia was flexed and extended by contraction of the flexor and extensor tibiae (**Flex/Ext**) muscles.
- the **coxa-trochanter (CT-)** joint, where the trochantero-femur was moved up- and downward by contraction of the levator and depressor trochanteris (**Lev/DepTr**) muscles.
- the **thorax-coxa (TC-)** joint where in the freely moving animal the coxa and thus the whole leg is pro- and retracted by contraction of the pro- and retractor coxae (**Pro/RetCx**) muscles. In the present experiments, this joint was deafferented, fixed with glue (see Materials & Methods) and thus unable to move.

3.1.2. Walking movements

When the animal was glued to the holder and positioned above the treadmill after the dissection, it was usually resting. A brief puff of air or tactile stimulation with a soft paint brush of the abdomen or antennae was applied to elicit walking episodes (see also Bässler, 1983). Upon stimulation, the animal started to perform walking and/or tapping movements with the middle leg and showed other signs of arousal (searching movements of the antennae, bending of the abdomen). After walking movements were initiated, the stimulation was terminated. Walking episodes typically consisted of three to ten steps, after long recording sessions sometimes only single steps could be elicited even upon strong tactile stimulation. The longest walking episode that was recorded consisted of 39 consecutive steps. In most cases the arousal of the animal slowly ebbed away after stimulation, and both maximum and mean belt velocity decreased toward the end of a stepping sequence while cycle period

increased (**Fig.2b, left**). In other instances the animal walked with a fairly constant maximum belt velocity over a long time (**Fig.2b, middle**) or increased the motor output during the sequence (**Fig.2b, right**). A more detailed and quantitative description of the velocity of walking movements will be given in chapter 3.4.



3.1.3. Motor pattern

The activity of motoneurons (MNs) innervating the major leg muscles was recorded extracellularly from the lateral motor nerves carrying their axons or by EMG recordings from the muscles. During walking, there was alternating activity in antagonistic MN pools that is described in more detail below. In all figures, if present, grey bars mark the resting state of the animal. Within a stepping sequence, horizontal black bars mark the duration of the stance phase, while white bars indicate the swing phase. Tapping movements or uncoordinated muscle activities (co-contraction, erratic activity) are labeled with asterisks.

FT-joint

The flexor and extensor muscles were recorded by EMG wires inserted into the flexor (**Fig.3a**). Due to the vicinity of the extensor, potentials from this muscle could be recorded simultaneously and distinguished by their smaller, more stereotypic amplitude and the time of occurrence. In **Fig.3a** and some of the following, the EMG recording from the flexor muscle is drawn twice with the enlarged trace showing the extensor muscle potentials more clearly (arrows in Fig.3a; see Materials & Methods, chapter 2.3.1).

During stance the belt was moved by flexion of the tibia. Stance phase was defined as the time of flexor tibiae (flexor) motoneuron (MN) activity recorded with the EMG. It should be noted that the onset of EMG activity occurred on average 126 ± 151 ms (mean \pm SD; N=4; n=282) before the contraction force of the flexor muscle was strong enough to move the belt (**Fig.3b**). Swing phase was defined as the rest of the step cycle. During swing, the tibia was extended. Extensor tibiae (extensor) MN activity started at the beginning of swing phase. Sometimes there was a short pause between the last extensor action potential and the beginning of the next stance phase (Fischer et al., 2001; see below).

CT-joint

EMG recordings from the levator (**Figs.3a; 4**) show that in this specific experiment the muscle was starting to contract at the transition from stance to swing phase and was lifting the leg when it was returned to the starting position for a new stance phase. The pattern of activity of levator and depressor showed considerable variation between preparations. Probably due to small differences in treadmill height, leg geometry or because of intrinsic variability, in 4 of 7 animals the levator was starting to contract early in stance phase (cf. **Fig.16**).

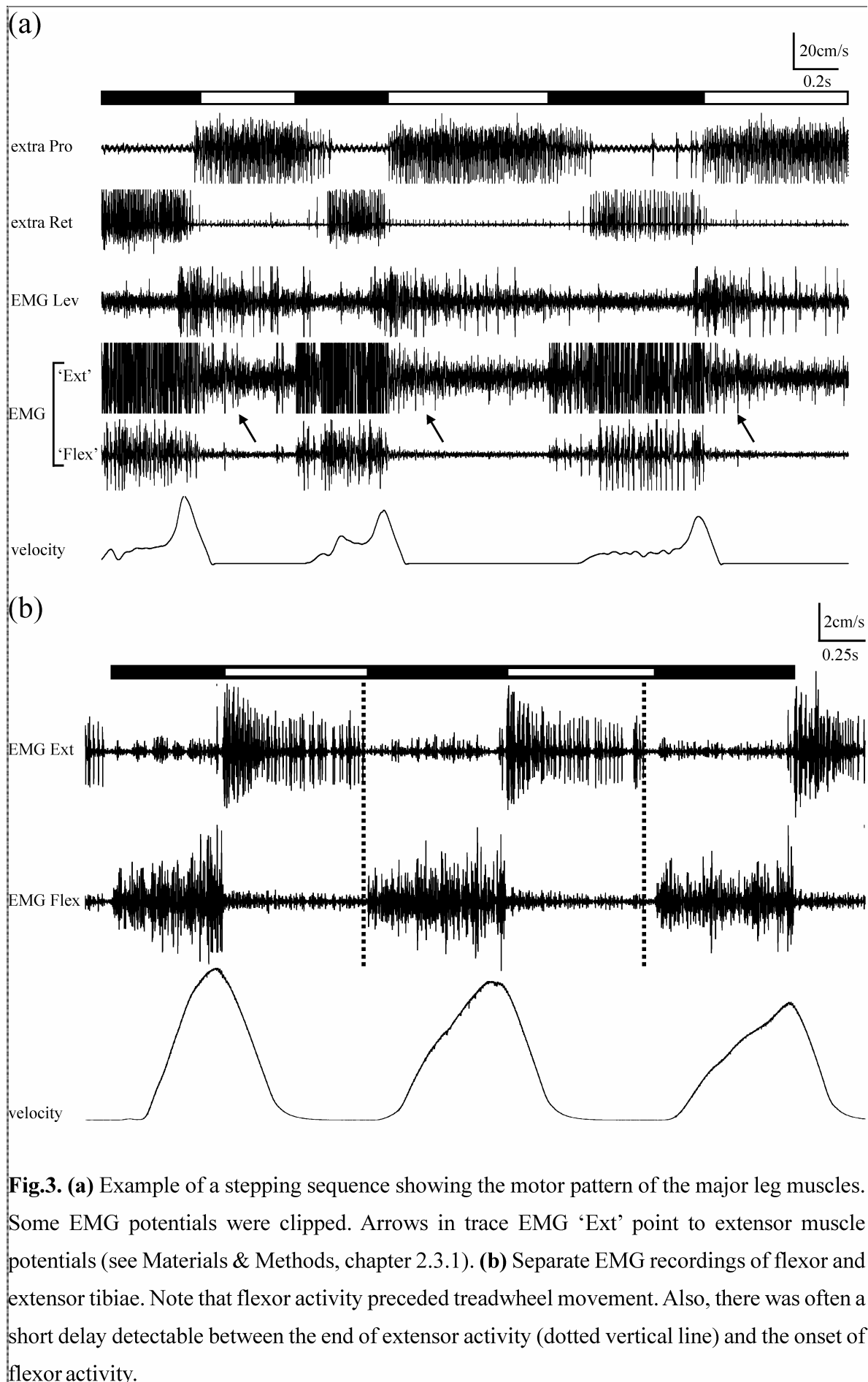


Fig.3. (a) Example of a stepping sequence showing the motor pattern of the major leg muscles. Some EMG potentials were clipped. Arrows in trace EMG 'Ext' point to extensor muscle potentials (see Materials & Methods, chapter 2.3.1). **(b)** Separate EMG recordings of flexor and extensor tibiae. Note that flexor activity preceded treadmill movement. Also, there was often a short delay detectable between the end of extensor activity (dotted vertical line) and the onset of flexor activity.

The antagonistic depressor tibiae MNs were recorded only intracellularly (see chapter 3.2) and showed antiphasic activity with respect to levator MNs.

TC-joint

Protractor and retractor MNs were recorded with extracellular hook electrodes from the lateral nerves nl2 and nl5, respectively (**Fig.4**). Although the TC-joint was immobilized and deafferented (for details see Materials & Methods, chapter 2.1), there was alternating activity in protractor and retractor MNs (Akay et al., 2004). Furthermore, like in intact walking animals, the motor pattern in this joint was coupled to that of the more distal leg joints. After tactile stimulation of the abdomen, retractor MNs were active during stance phase (**Figs.3a; 4a**). This resembles the situation in a freely moving animal, where in the stance phase of the middle leg during forward walking the propulsion is mainly generated by retraction of the leg around the TC-joint (Cruse, 1976). Interestingly, after tactile stimulation of the antennae, protractor MNs were active during stance, resembling the situation in a freely moving animal walking backward (**Fig.4b**). These results show that, albeit the somewhat artificial walking situation of the single middle leg on the treadmill, the interjoint coordination of the motor pattern generated bears similarities to the situation in the intact animal.

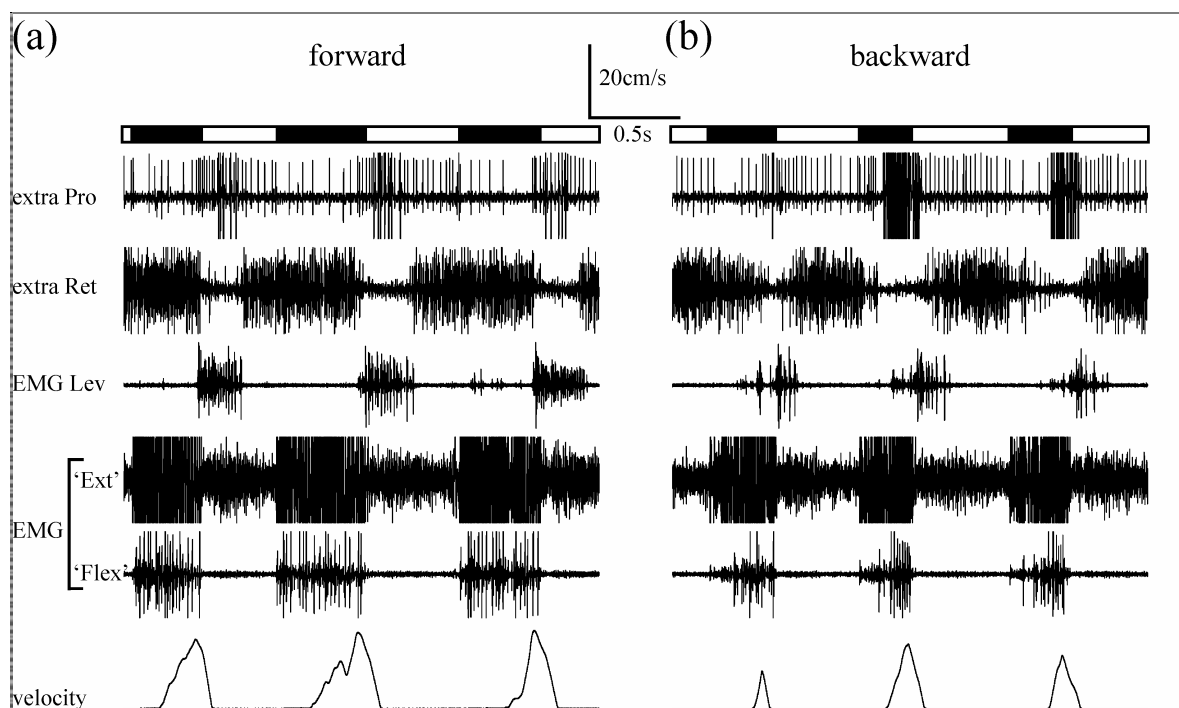


Fig.4. Motor pattern corresponding to forward and backward walking. Some EMG potentials were clipped. **(a)** Tactile stimulation was applied to the abdomen. The retractor was active during stance, resembling forward walking. **(b)** Tactile stimulation was applied to the antennae. The protractor was active during stance, resembling backward walking.

3.2. Synaptic drive to flexor tibiae MNs

An analysis of the inputs to MNs can give insights into the role of the premotor elements (CPG, sense organs). Intracellular recordings of MNs (TC-joint: pro- and retractor coxae MNs; CT-joint: levator and depressor trochanteris MNs; FT-joint: flexor and extensor tibiae MNs) were performed to elucidate the nature of the synaptic drive they receive from premotor sources. Different protocols for current injection were applied that will be described below in more detail. Most recordings were performed from flexor MNs, and in the first part of this chapter only flexor MNs will be discussed. Later in this chapter the results from other MNs will be presented.

3.2.1. Modulation of membrane potential during stepping

A total of 25 flexor MNs (14 slow, 4 semifast, 7 fast) were recorded. The activity of a semifast flexor MN during a stepping sequence is shown in **Fig.5a (left)**. When a stepping sequence was induced by stimulation of the animal (arrow in **Fig.5a, left** and following), the membrane potential of flexor MNs depolarized (N=25). Shortly after the stimulation there was a brief tapping movement visible that consisted of a weak flexion and extension of the tibia that was not accompanied by belt movement; another tapping movement occurred at the end of the stepping sequence (asterisks in **Fig.5a, left** and following).

Phasic modulation

During the flexion phase of the steps (i.e. stance phase) and tapping movements the neuron depolarized, while it repolarized throughout the extension (swing) phase, causing rhythmic membrane potential modulations of $17.9 \pm 4.2\text{mV}$ (peak to trough; range: 8.1 to 27.7mV; N=11, n=263) that correlated with the step cycles (**Fig.5a, left**). Of 25 recorded flexor MNs, 15 MNs (60%; 11 of 14 slow MNs; 2 of 4 semifast MNs, 3 of 7 fast MNs) were depolarized above threshold and fired action potentials during stance. Especially during slow steps in 10 of 25 flexor MNs (40%; 3 of 14 slow MNs, 2 of 4 semifast MNs, 4 of 7 fast MNs) no action potentials were generated during stance (**Fig.5a, right**).

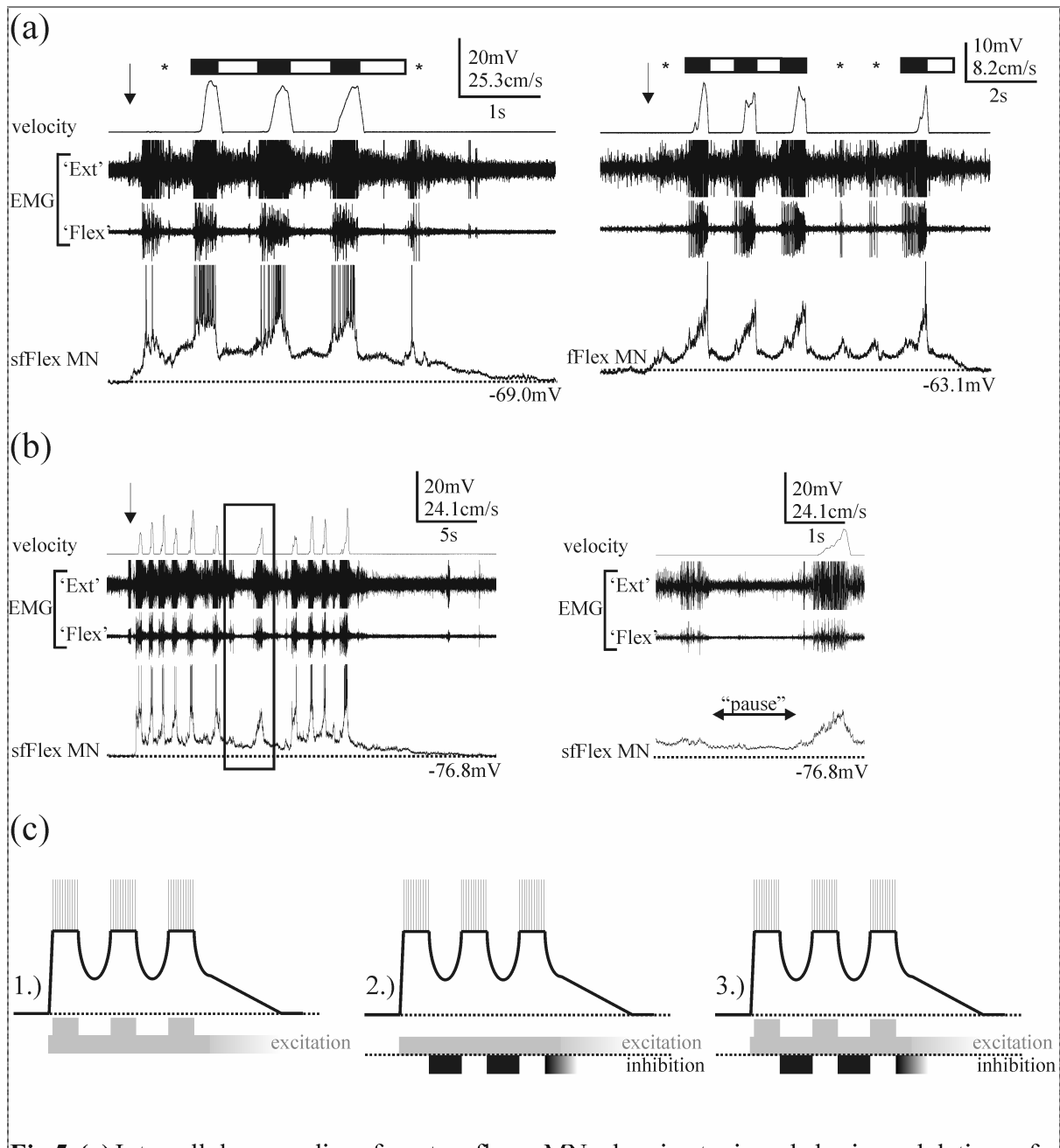


Fig.5. (a) Intracellular recordings from two flexor MNs showing tonic and phasic modulations of membrane potential. **Left:** Action potentials were generated during stance, while the neuron was silent during swing. **Right:** In some flexor MNs, no action potentials were generated during slow or small steps. **(b)** Intracellular recording of a semifast flexor MN. **Left:** During a short pause within a stepping cycle (box), there was no activity in flexor and extensor tibiae and thus supposedly no phasic synaptic inputs, making it possible to measure the tonic depolarization alone. **Right:** Pause drawn on an enlarged timescale. Action potentials and EMG potentials were clipped in (a) and (b). **(c)** Schematic drawing of how the observed membrane potential modulations may be caused by different forms of synaptic input.

Tonic depolarization

Throughout the stepping sequence, the membrane potential remained more depolarized than during rest in 18 of 25 MNs (72%), revealing a tonic depolarization (**Fig.5a,b**). In detail, 9 of 14 slow MNs (64%), 3 of 4 semifast MNs (75%) and 6 of 7 fast MNs (86%) were tonically depolarized. During stepping, the concurrent phasic modulation complicated the measurement of the amplitude of the tonic depolarization alone. **Fig.5b** shows a recording of a flexor MN during a stepping cycle that included a short pause between two steps (box in **Fig.5b, left**). This pause is displayed in **Fig.5b (right)** on an enlarged timescale, showing that there was no activity visible in the flexor and extensor tibiae EMG and thus supposedly no contamination by phasic inputs acting on the flexor MN. During this time, the amplitude of the tonic depolarization was $3.9 \pm 2.2\text{mV}$ (range: 1.3 to 9.5mV; N=18, n=28).

Hypothetical synaptic drive

In theory, there are different types of synaptic drive that could lead to the observed modulation (**Fig.5c**):

1. In addition to a tonic excitation that lasted throughout the stepping sequence, there could have been a phasic excitation during stance that ceased during swing, repolarizing the neuron.
2. A tonic excitation could have been shaped by phasic inhibitory inputs (Büschges, 1998; Büschges et al., 2004) that repolarized the neuron during swing.
3. Both a phasic excitation during stance and a phasic inhibition during swing could have been superimposed on a tonic excitation.

In addition, intrinsic cellular properties of the motoneurons like plateau potentials or postinhibitory rebound could play a role in generating the membrane potential modulations of the flexor MNs.

3.2.2. Input resistance shows synaptic drive

Method

When a MN receives synaptic inputs, ion channels in the membrane open, causing a decrease in membrane resistance. Membrane resistance of a MN, the so-called input resistance, can be measured by injection of short hyperpolarizing current pulses (e.g. -0.5 to -1.5nA, 50-150ms duration) through the intracellular microelectrode. According to Ohm's law ($U = R \cdot I$), the amplitude of the voltage deflection (U) upon current (I) injection is a measure of the

membrane resistance (R). In the bridge or current-clamp mode of the intracellular amplifier this means that if input resistance decreases because synaptic inputs (excitatory or inhibitory) cause an opening of ion channels, the voltage deflection upon injection of current pulses decreases (**Fig.6a**). Since not every synaptic input leads to a modulation of membrane potential (e.g. de- and hyperpolarizing inputs that cancel each other out or an ionic conductance with a reversal potential that is equal to the membrane potential at a given time), an analysis of the input resistance is valuable for determining the occurrence and strength of synaptic inputs. Also it can help to determine for example whether a depolarization of a neuron is due to a synaptic excitation or a release from inhibition.

Phasic conductance(s)

Hyperpolarizing current pulses were injected into an fFlex MN (**Fig.6b, left**). The voltage deflection that was a response to the current pulse, and thus the input resistance of the neuron, was greatest during rest prior to stimulation. The amplitude of the voltage deflection that was caused by the current pulses decreased during stance as well as during swing. In **Fig.6b (right)**, ten individual responses are shown in grey together with the averaged response (black). Input resistance was $4.6 \pm 0.3\text{M}\Omega$ during rest (range: 4.1 to $5.2\text{M}\Omega$, $N=1$, $n=18$). Because of strong fluctuations of the membrane potential during stance and swing, only the averaged trace of 18 individual current pulses could be used to calculate input resistance, which was $2.6\text{M}\Omega$ during stance and $1.4\text{M}\Omega$ during swing. In all 8 flexor MNs where hyperpolarizing current pulses were injected, a qualitative analysis showed that input resistance decreased during stance and even more during swing compared to rest. The smaller input resistance shows that there were conductances due to synaptic inputs during both stance and swing phase and that the conductance was largest during swing. This infers that the observed membrane potential modulations were not caused by a combination of a tonic excitation throughout the stepping sequence and a phasic excitation during stance (hypothesis 1; **Fig.5c**), because in this case input resistance during swing would have been larger than during stance.

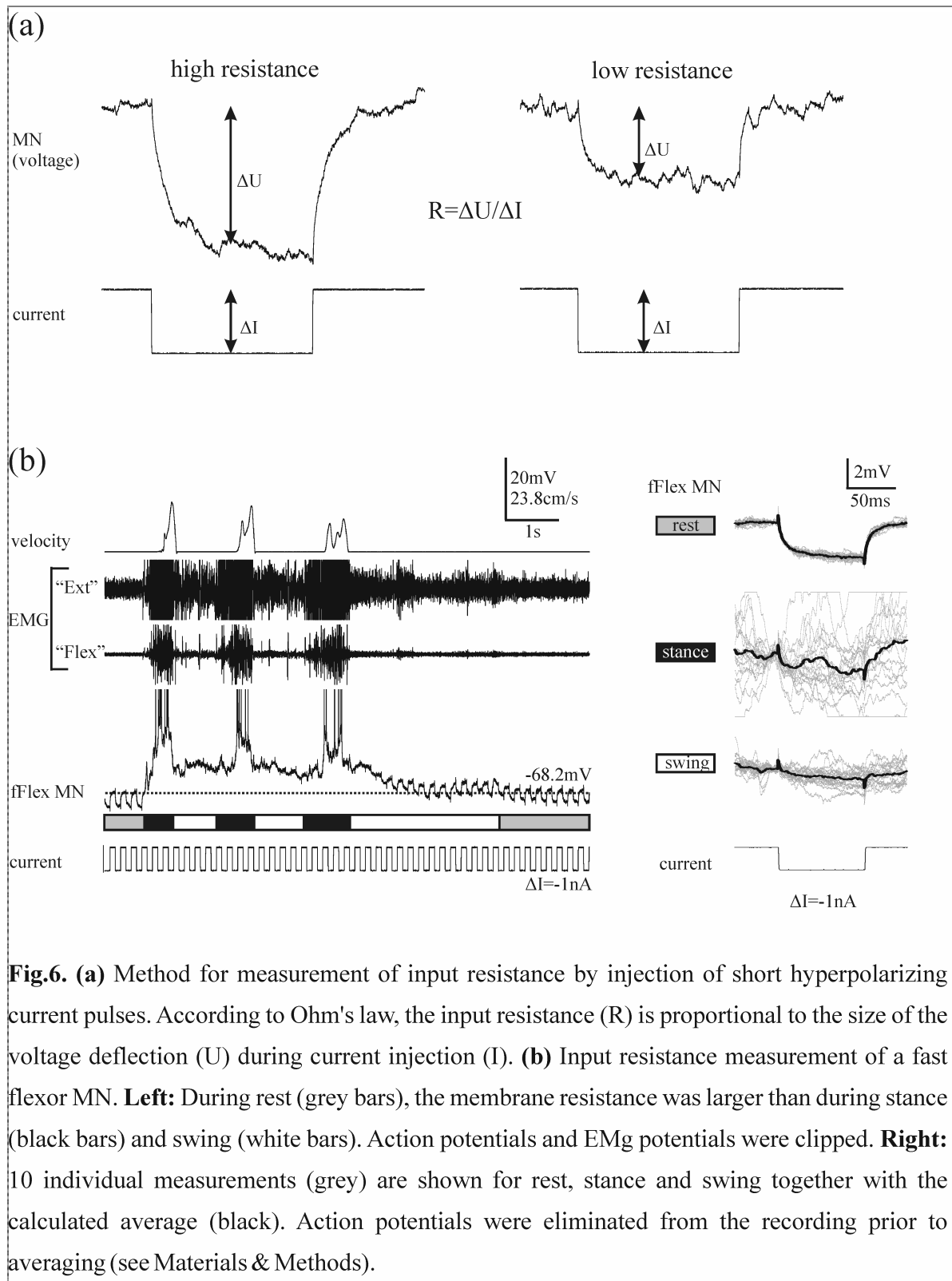
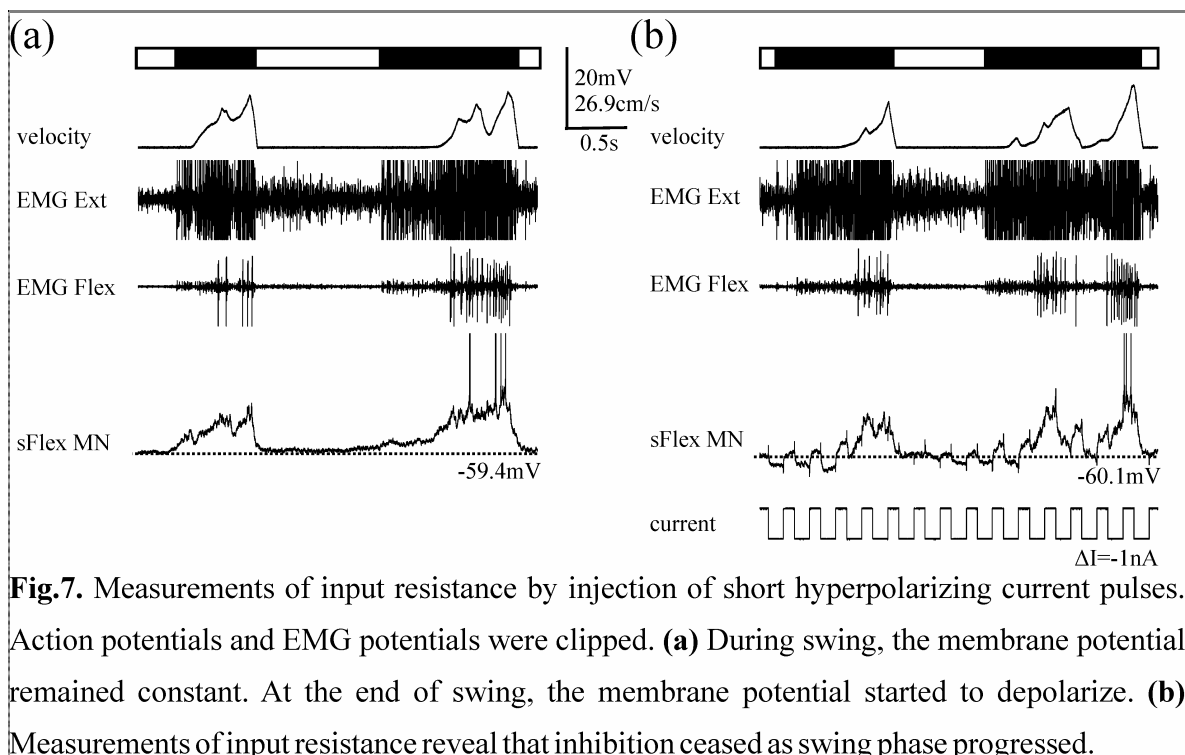


Fig.6. (a) Method for measurement of input resistance by injection of short hyperpolarizing current pulses. According to Ohm's law, the input resistance (R) is proportional to the size of the voltage deflection (U) during current injection (I). **(b)** Input resistance measurement of a fast flexor MN. **Left:** During rest (grey bars), the membrane resistance was larger than during stance (black bars) and swing (white bars). Action potentials and EMG potentials were clipped. **Right:** 10 individual measurements (grey) are shown for rest, stance and swing together with the calculated average (black). Action potentials were eliminated from the recording prior to averaging (see Materials & Methods).

The depolarization of flexor MNs started at the end of swing phase (**Fig.7a**). A close observation of the membrane resistance during swing revealed that the inhibitory conductance was large during the beginning of swing phase and then ebbed, because the voltage deflection became larger as swing phase proceeds (**Fig.7b**). While the inhibition ceased, the membrane potential depolarized only slightly, suggesting that

1. The reversal potential of the inhibition was close to the membrane potential during swing, so that both a strong and a weak inhibition brought the membrane potential to similar values.
2. Phasic inhibition was strongest during the first 30% of swing. At the end of swing, the amplitude of the tonic depolarization could be estimated, because the phasic inhibition was weak while the phasic excitation had not started yet. This was consistent with the extracellular data that showed that there was a short pause between extensor and flexor activity at the transition from swing to stance (**Fig.3b**).
3. The phasic depolarization of flexor MNs during stance was not entirely caused by a release from inhibition that allowed an underlying tonic excitation to depolarize the neuron (hypothesis 2; **Fig.5c**), because in this case there should have been a strong depolarization of the membrane potential during the time when the inhibition became weaker.

In conclusion, there must act both a phasic excitation during stance and a phasic inhibition during swing on the flexor MNs that caused the rhythmic membrane potential modulations.



Tonic depolarization

In addition to the phasic modulation, in 18 of 25 flexor MNs (72%) a tonic depolarization throughout the stepping sequence was observed that ebbed after the last step (**Fig.8a**). This tonic depolarization was also accompanied by an increase in membrane conductance. After activity in the tibial muscles had ceased (vertical dotted line), the membrane potential slowly hyperpolarized toward the resting value. Simultaneously with the ebbing depolarizing input, the membrane resistance significantly ($P=0.0013$) increased from $7.7 \pm 5.2\text{M}\Omega$ (range 3.4 to $22.8\text{M}\Omega$) to $8.8 \pm 6.1\text{M}\Omega$ (range 3.8 to $27.1\text{M}\Omega$) ($N=8$, $n=15$), which corresponded to a conductance increase of 26% due to the tonic depolarization (**Fig.8b**).

Conclusion

Measurements of input resistance showed that the membrane potential modulations of flexor MNs during stepping were caused by phasic excitatory and inhibitory synaptic inputs that were superimposed on an underlying tonic depolarization (**Fig.9**).

3.2.3. Current injection shows reversal potentials

In previous experiments in the stick insect by Ludwar et al. (2005b) as well, a tonic depolarization of MNs in the deafferented mesothoracic ganglion was observed during front leg walking. Their data show a reversal potential of the tonic depolarization of -47 to -32mV for different leg MNs (-39mV and -38mV for flexor MNs in the ipsi- and contralateral mesothoracic ganglion, respectively). The present study aimed at determining whether similar observations could be made in the single middle leg preparation, when the segmental networks for locomotion were operating.

Method

Injection of constant de- or hyperpolarizing current changes the membrane potential of a neuron to a different value that is either closer or further away from the reversal potential of an excitatory or inhibitory current elicited e.g. by synaptic inputs (**Fig.10**). Because this changes the electromotive force (EMF) that acts on the participating ions (the EMF is proportional to the difference between the membrane potential and the reversal potential), the amplitude of the voltage deflection during the phase of excitatory or inhibitory synaptic inputs will also change.

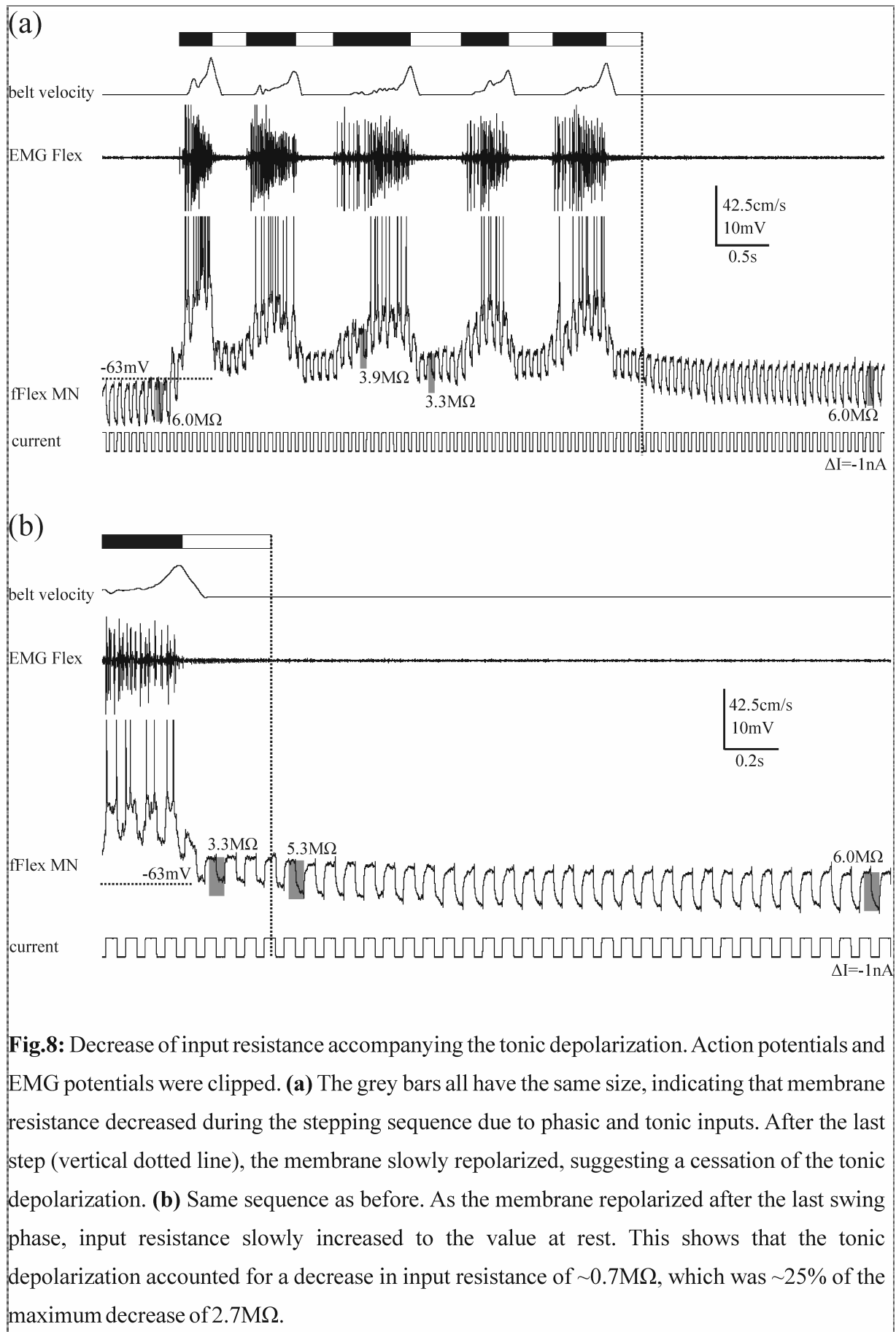


Fig.8: Decrease of input resistance accompanying the tonic depolarization. Action potentials and EMG potentials were clipped. **(a)** The grey bars all have the same size, indicating that membrane resistance decreased during the stepping sequence due to phasic and tonic inputs. After the last step (vertical dotted line), the membrane slowly repolarized, suggesting a cessation of the tonic depolarization. **(b)** Same sequence as before. As the membrane repolarized after the last swing phase, input resistance slowly increased to the value at rest. This shows that the tonic depolarization accounted for a decrease in input resistance of $\sim 0.7 \text{ M}\Omega$, which was $\sim 25\%$ of the maximum decrease of $2.7 \text{ M}\Omega$.

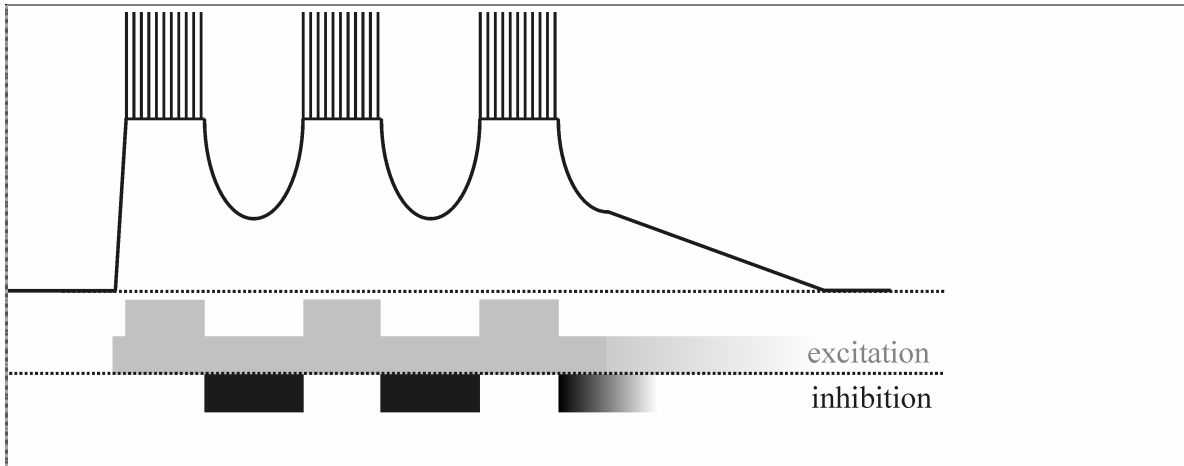


Fig.9. Schematic drawing of synaptic inputs to flexor MNs during walking movements. The experimental findings are consistent with the hypothesis that flexor MNs receive a tonic depolarization throughout the stepping sequence and additional phasic excitation and inhibition during stance and swing, respectively.

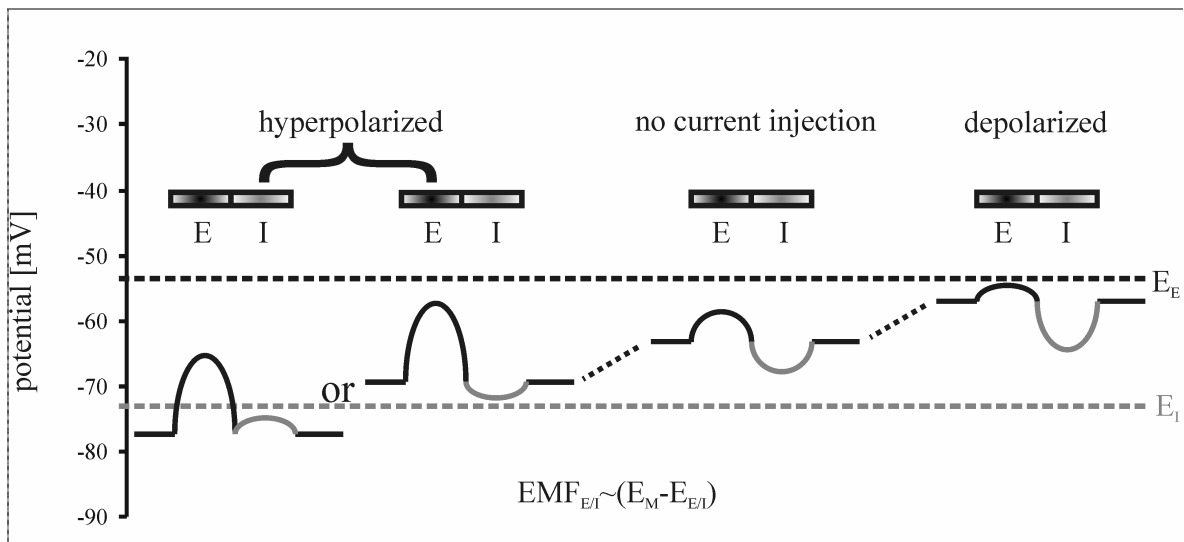


Fig. 10. Schematic drawing of the influence of intracellular current injection on the amplitude of membrane potential modulations. Without current injection, the membrane potential of a neuron depolarizes during an excitation (E, black trace) and hyperpolarizes during an inhibition (I, grey trace). The electromotive force (EMF) that acts upon the ions that are involved is proportional to the difference between the membrane potential E_M and the reversal potential of the excitatory or inhibitory current (E_E and E_I , respectively). Injection of constant depolarizing or hyperpolarizing changes the membrane potential and thus also the EMF and the amplitude (and sign) of the membrane potential modulation during excitation and inhibition.

An excitatory current is either caused by an inflow of Na^+ -ions into the cell or by a mixed $\text{Na}^+/\text{K}^+[\text{Ca}^{2+}]$ -current, both of which currents have a reversal potential that is more depolarized than the resting membrane potential. If the neuron is depolarized, the voltage deflection will be smaller because the imposed membrane potential is closer to the reversal potential of the excitation. Reversely, if the neuron is hyperpolarized, the excitatory current will cause a larger voltage deflection than at rest, because the imposed membrane potential is further away from the reversal potential of the excitation. An excitation can also be caused by cessation of a persistent outward current. In this case the input resistance will increase, which has however never been observed.

An inhibitory current is either caused by an inflow of Cl^- -ions into the cell or by an outflow of K^+ -ions; the reversal potential of both of these currents is more hyperpolarized than the resting potential. If the neuron is depolarized, the voltage deflection will be larger because the imposed membrane potential is further away from the reversal potential of the inhibition. Reversely, if the neuron is hyperpolarized, the inhibitory current will cause a smaller voltage deflection than at rest, because the imposed membrane potential is closer to the reversal potential of the inhibition. If the neuron is hyperpolarized to a value that is more negative than the reversal potential of the inhibitory current, the inhibition will switch sign. An inhibition can also be caused by cessation of a persistent inward current. In this case the input resistance will increase, which has however never been observed.

Thus, by constantly de- or hyperpolarizing the neuron, conclusions about the nature and the reversal potential of synaptic currents can be drawn.

Hypothetical considerations

Through injection of constant de- or hyperpolarizing current, a different membrane potential can be imposed (see above). **Fig.11a** shows a schematic drawing of the activity of a flexor MN during a series of steps. The bar labelled A_1 symbolizes the amplitude of the tonic depolarization, while the bar labelled A_2 symbolizes the amplitude of the phasic modulation. If the tonic modulation A_1 were caused by an excitation with a reversal potential slightly more depolarized than the resting membrane potential, the difference between the reversal potential and the imposed new resting potential would be larger when the neuron is hyperpolarized (left). In this case, A_1 would become larger. Correspondingly when the neuron is depolarized, the imposed new resting potential would be closer to (and maybe more depolarized than) the reversal potential, so the amplitude A_1 of the tonic depolarization would become smaller or switch sign and turn into a tonic hyperpolarization (see above). While the amplitude of the

tonic depolarization would vary when the neuron is de- or hyperpolarized by current injection, the amplitude of the phasic modulation (A_2), which is caused by a transition between phasic excitation and inhibition should remain more constant, because the opposite influences of the current injection on the modulation during excitation and inhibition would cancel each other out.

Tonic depolarization

The amplitude of the tonic depolarization could be estimated from the membrane potential at the end of swing phase, because here the phasic inputs were small (see chapter 3.2.2) or during short pauses within a stepping cycle (**Fig.5b**). In a fast flexor MN with a resting membrane potential of -68.3mV, the membrane potential at the end of swing phase was -65mV, so the amplitude of the tonic depolarization was approximately 3-4mV without current injection (**Fig.11b, middle**). During injection of constant hyperpolarizing current the membrane potential during rest changed to -92.9mV and the amplitude of the tonic depolarization increased to 13-14mV (**Fig.11b, left**). This is due to the fact that the imposed resting potential of the neuron was further away from the reversal potential of the tonic depolarization. During injection of constant depolarizing current the membrane potential during rest changed to -50.4mV (**Fig.11b, right**). There was no tonic depolarization visible, suggesting that the reversal potential of the tonic conductance in the neuron shown in **Fig.11** was \sim -50mV. The amplitude of the tonic modulation measured in 5 flexor MNs (2 slow, 2 semifast, 1 fast) during intracellular injection of de- and hyperpolarizing current is shown in **Fig.11c**. The data points can be fitted with a regression line ($P < 0.0001$; $N=5$, $n=27$) that gives a reversal potential of -49.0mV.

Phasic excitation

During injection of depolarizing current, the phasic depolarization was clearly visible while the tonic depolarization was not (**Fig.11b, right**). This shows that the reversal potential of the phasic excitatory current in this neuron was more depolarized than that of the tonic depolarization. The amplitude of the phasic excitation was measured in 5 flexor MNs (2 slow, 2 semifast, 1 fast) during intracellular injection of de- and hyperpolarizing current (**Fig.11d**). The amplitude of the tonic excitation decreased when the neuron was depolarized ($P=0.0002$; $N=5$, $n=90$). Even at the most depolarized membrane potential values around -20mV, the tonic excitation did not change sign. The variability of the data does not allow a calculation of

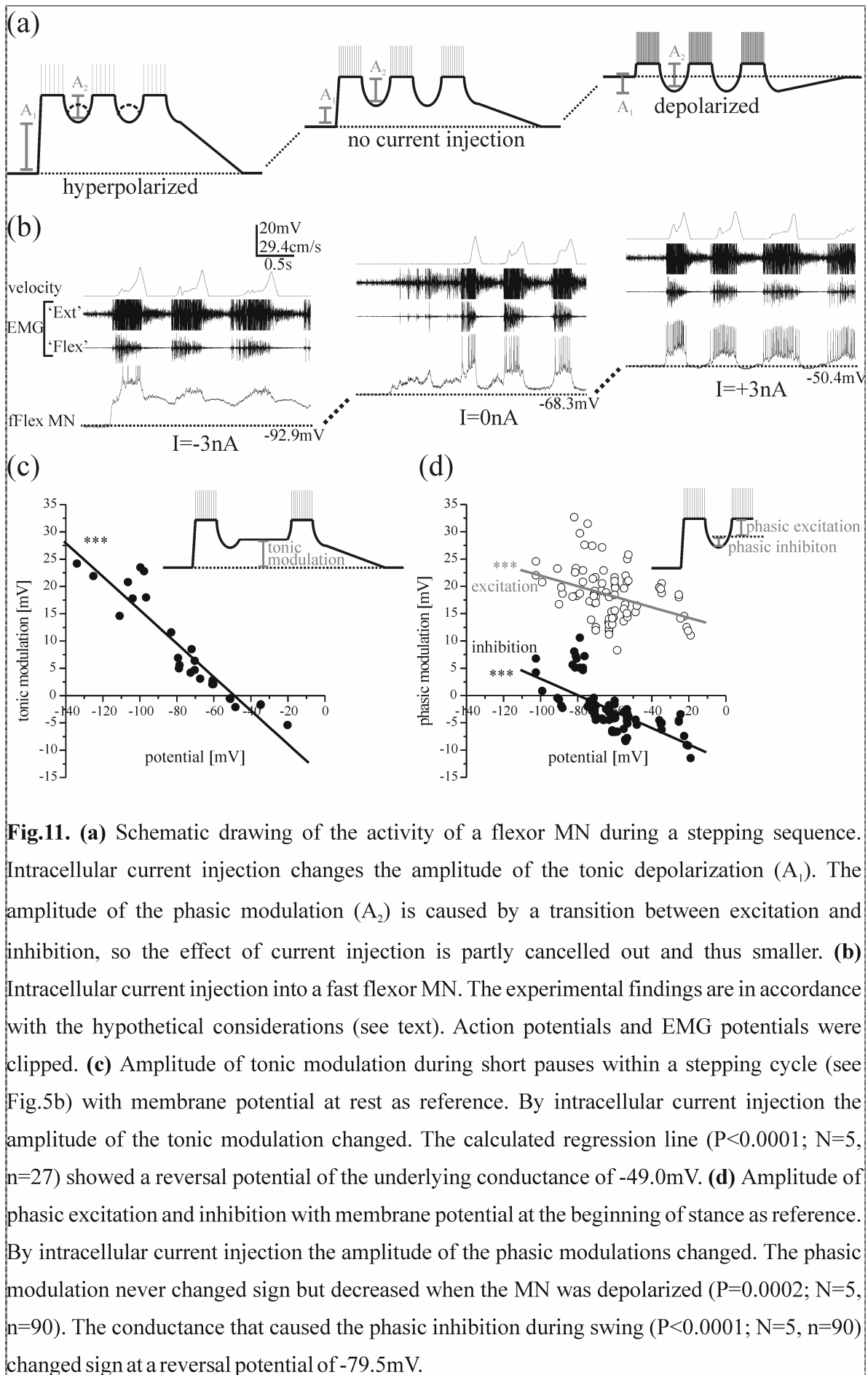


Fig.11. (a) Schematic drawing of the activity of a flexor MN during a stepping sequence. Intracellular current injection changes the amplitude of the tonic depolarization (A_1). The amplitude of the phasic modulation (A_2) is caused by a transition between excitation and inhibition, so the effect of current injection is partly cancelled out and thus smaller. **(b)** Intracellular current injection into a fast flexor MN. The experimental findings are in accordance with the hypothetical considerations (see text). Action potentials and EMG potentials were clipped. **(c)** Amplitude of tonic modulation during short pauses within a stepping cycle (see Fig.5b) with membrane potential at rest as reference. By intracellular current injection the amplitude of the tonic modulation changed. The calculated regression line ($P < 0.0001$; $N = 5$, $n = 27$) showed a reversal potential of the underlying conductance of -49.0mV . **(d)** Amplitude of phasic excitation and inhibition with membrane potential at the beginning of stance as reference. By intracellular current injection the amplitude of the phasic modulations changed. The phasic modulation never changed sign but decreased when the MN was depolarized ($P = 0.0002$; $N = 5$, $n = 90$). The conductance that caused the phasic inhibition during swing ($P < 0.0001$; $N = 5$, $n = 90$) changed sign at a reversal potential of -79.5mV .

the reversal potential. It is likely to be caused by the fact that the peak potential of flexor MNs varies with belt velocity (see chapter 3.4). Also, every action potential creates a shunt across the membrane that especially at high action potential frequencies may have opposed further depolarizations.

Phasic inhibition

The phasic inhibition was strongest during the first 30% of swing (see **Fig.7b**). In a fast flexor MN, the membrane potential during this time was approximately -65mV when no current was injected (**Fig.11b, middle**). By injection of constant current through the micropipette into the cell the amplitude and sign of the phasic inhibition could be influenced. When the neuron was hyperpolarized by current injection, the phasic inhibition switched sign and became a depolarizing ‘hump’ with a peak around -75mV (**Fig.11b, left**), indicating that the reversal potential of the phasic inhibition in this neuron lay between -65 and -75mV.

The amplitude of the phasic inhibition was measured in 5 flexor MNs (2 slow, 2 semifast, 1 fast) during intracellular injection of de- and hyperpolarizing current (**Fig.11d**). The data points can be fitted with a regression line ($P < 0.0001$; $N=5$, $n=90$) that gives a reversal potential of -79.5mV.

The phasic inhibition was mediated by inhibitory postsynaptic potentials (IPSPs) that could be detected in the intracellular recordings during swing (**Fig.12a**). Under the assumption that the majority of the membrane potential fluctuations during swing were caused by IPSPs, the amplitude of this “jitter” allows predictions about IPSP amplitude. To determine the amplitude of the jitter, the intracellular recording of a flexor MN was high-pass filtered (frequency 71Hz) in order to eliminate slow modulations and the root mean square value (RMS) of the filtered trace was determined (**Fig.12b**). When no current was passed through the electrode, the membrane potential during swing hyperpolarized to a potential of -66.0mV and the RMS value of a 0.25s time interval during swing was 0.31mV (**Fig.12b, middle**). When the neuron was hyperpolarized, the membrane potential during swing depolarized to a potential of -71.8mV and the RMS value was 0.25mV (**Fig.12b, left**). When the neuron was depolarized, the membrane potential during swing strongly hyperpolarized to a potential of -31.5mV and the RMS value was 0.49mV (**Fig.12b, right**). This again shows that the reversal potential of the phasic inhibitory current in this neuron was between -66.0 and -71.8mV and was closer to -71.8mV, because the RMS value was smaller at this potential.

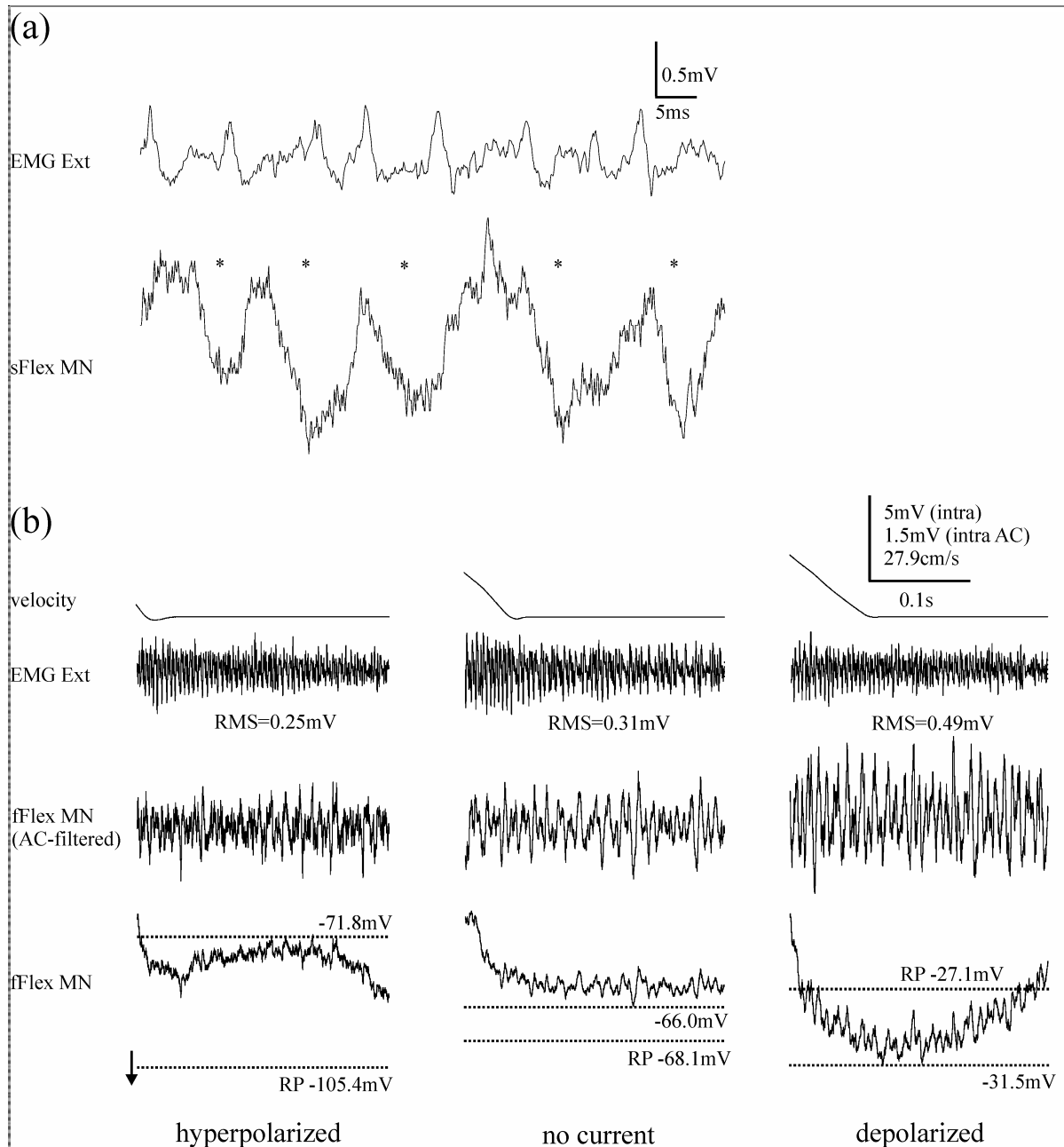


Fig.12. (a) Intracellular recording of a slow flexor MN. During swing, individual IPSPs could be detected (asterisks). **(b)** Analysis of IPSP amplitude during intracellular current injection into a fast flexor MN. Flexor recordings were AC-filtered and the root mean square (RMS) value was calculated. The RMS value was greatest when the neuron was depolarized, suggesting that the individual IPSPs had the largest amplitude because of a large difference between membrane potential and reversal potential of the inhibition. The RMS value was smallest when the neuron was hyperpolarized, suggesting that the individual IPSPs had the smallest amplitude because the membrane potential was close to the reversal potential of the inhibition.

Conclusions

The experiments involving current injection show that

1. The tonic depolarization was caused by a conductance with a reversal potential of -49mV . This would be expected from a mixed Na^+/K^+ -current (Ludwar et al. 2005b).
2. The phasic excitation was caused by a conductance with a reversal potential that was more depolarized than -20mV . This would be expected from a Na^+ - or a mixed Na^+/Ca^+ -current.
3. The phasic inhibition was caused by a conductance with a reversal potential of -79.5mV , which is consistent with both a K^+ - and a Cl^- -current.

3.2.4. Voltage-clamp recordings

Method

When analyzing bridge- or current-clamp data, voltage-dependent membrane properties have to be considered. For example, due to a voltage-gated opening and closing of ion channels cell membranes do not have a linear current-voltage (I-V) relationship over the whole potential range, causing an error in measurements of input resistance when the potential changes. Also, when the membrane potential has reached the reversal potential of a given conductance, there is no more voltage change detectable although the channels are still open.

In order to circumvent these problems, measurements were performed in the discontinuous single-electrode voltage-clamp mode (dSEVC, short: VC) of the amplifier. However, due to the large membrane area of the dendritic tree, the whole neuron could not be clamped to the holding potential, i.e. no space-clamp could be obtained (Spruston et al., 1993). Thus, often action potentials were still generated, presumably because the membrane potential at the spike generating zone was not equal to the holding potential. This problem has to be kept in mind when analyzing data from VC recordings.

Analogously to the current-clamp recordings, measurements of membrane resistance were performed in voltage-clamp mode by analyzing the current that flows across the membrane as a response to an imposed short hyperpolarizing voltage step. Also, the cell membrane could be clamped at different holding potentials, allowing conclusions about the reversal potentials of the underlying ionic currents.

Tonic depolarization

Measurements of input resistance were performed in voltage-clamp mode (**Fig.13a**), showing that when the tonic depolarization ebbed the input resistance in this slow flexor MN increased from $28.2 \pm 3.77\text{M}\Omega$ to $36.6 \pm 2.54\text{M}\Omega$ (N=1, n=18).

Phasic modulation

The VC recordings were well suited to reveal the underlying synaptic drive to MNs. In **Fig13b**, the membrane potential of a semifast flexor MN showed little modulation during swing in the CC recording (**left**); probably because the value of -56 to -57mV was close to the reversal potential of the inhibitory conductance in this neuron. In the VC recording at a depolarized holding potential (**middle**), an outward current was visible during swing (arrow). This suggests that the reversal potential of the inhibitory conductance in this neuron was more hyperpolarized than the holding potential of -42.3mV. At a slightly hyperpolarized holding potential (**right**), an inward current during swing was visible (arrow). The current switched sign between -42.3 and -65.3mV, suggesting that the reversal potential of the inhibitory conductance in this neuron was more depolarized than -65.3mV.

Together, these examples show that the data obtained from voltage clamp recordings qualitatively substantiate the results from current-clamp experiments.

3.2.5. Functional significance of the tonic depolarization

Susceptibility to other inputs

The role of a depolarizing current in a MN is usually to bring the membrane potential above spike threshold or closer to the threshold in order to cause spiking or facilitate spiking upon a different excitatory input. It has to be kept in mind however, that if a large depolarizing conductance has a reversal potential below spike threshold, there is a shunt across the membrane that makes the neuron insensitive for other inputs. In general, the shunting effect and the depolarizing effect of the conductance compete, and the reversal potential of the tonic conductance determines which influence prevails (Brizzi et al., 2004).

In case of the leg MNs recorded in the stick insect, the reversal potential (-49mV, see above) was more depolarized than the resting potential (-62 to -67mV, see chapter 3.4) and very close to spike threshold (-50 to -51mV, see chapter 3.4). Thus, theoretically the shunting effect could impair spike generation. This was tested by injection of short, depolarizing current pulses into a slow flexor MN that were just sub-threshold prior to tactile

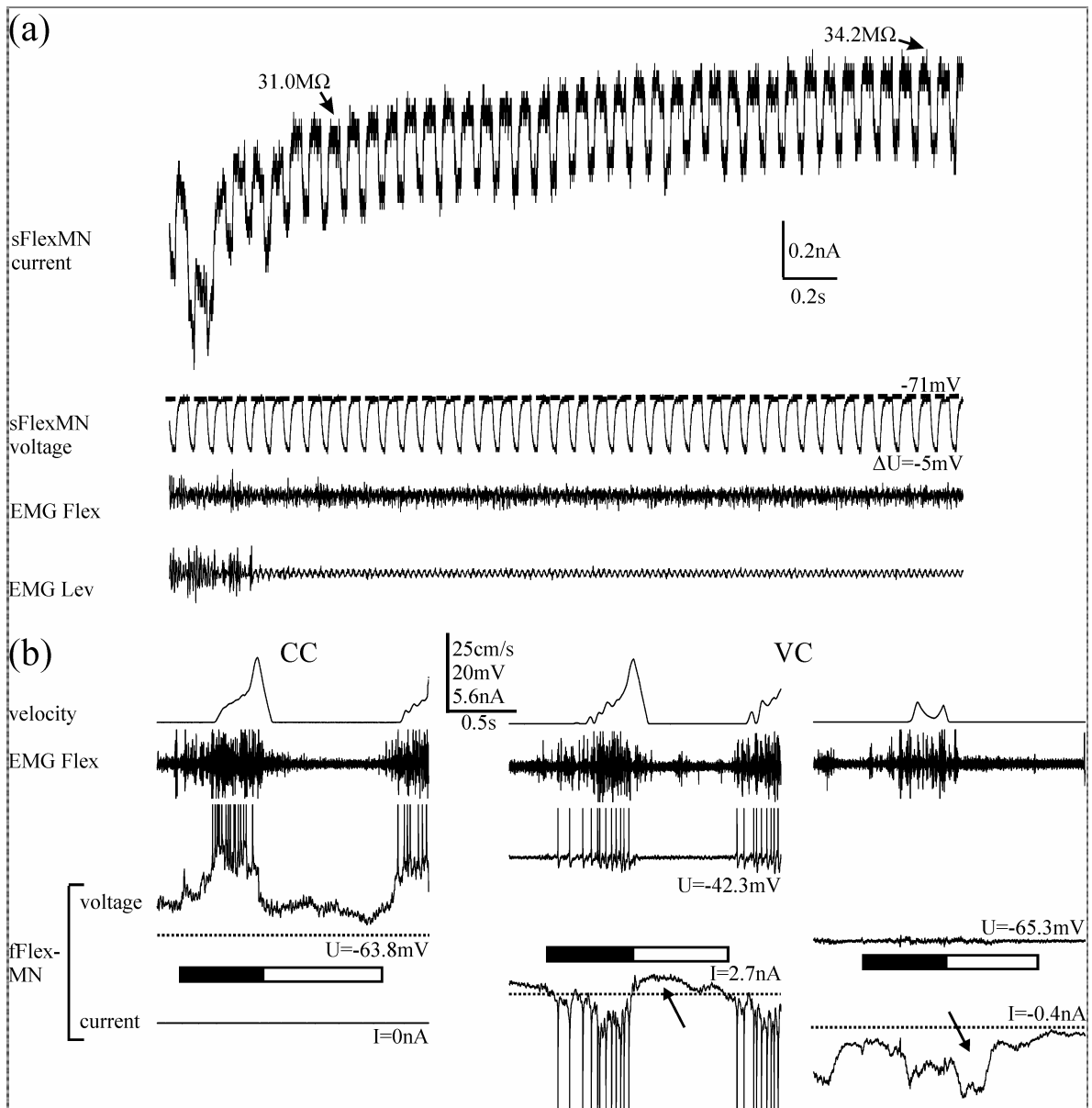


Fig. 13. (a) Measurement of input resistance of a slow flexor MN. Recordings in VC mode also show that the tonic depolarization was associated with an increased conductance that faded after the last step. **(b)** Intracellular recording of a semifast flexor MN in current-clamp (CC) and voltage-clamp (VC) mode. In CC (**left**), the membrane potential showed little modulation during swing. This suggests that the membrane potential during swing (-56 to -57 mV in this neuron) corresponded to the reversal potential of the inhibitory conductance. In the VC recording at a depolarized holding potential (-42.3 mV, **middle**), an outward current during swing (arrow) became visible suggesting a reversal potential of the inhibitory conductance that is more hyperpolarized than the holding potential. At a slightly hyperpolarized holding potential (-65.3 mV, **right**) during swing there is an inward current (arrow), suggesting a reversal potential of the inhibitory conductance that is more depolarized than the holding potential. Dotted lines in (b) and (c) show the current measured while the animal was resting. Action potentials, EMG potentials and current trace were clipped.

stimulation of the animal. After leg movements had stopped, in 4 of 6 flexor MNs the pulses were sufficient to elicit spike activity in the MN (**Fig.14a**). This suggests that the tonic depolarization acted to make the neuron more susceptible to excitatory inputs.

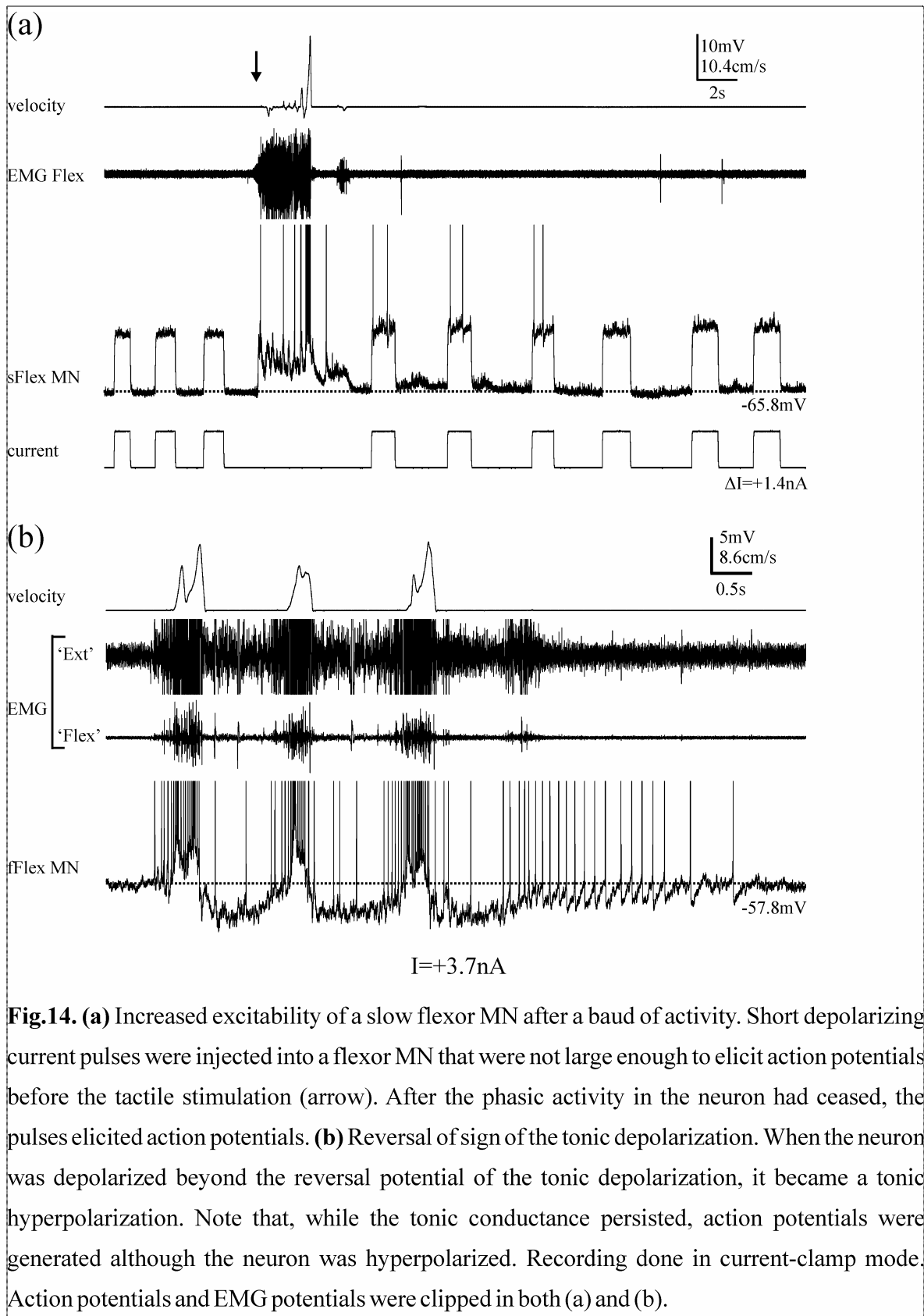


Fig.14. (a) Increased excitability of a slow flexor MN after a burst of activity. Short depolarizing current pulses were injected into a flexor MN that were not large enough to elicit action potentials before the tactile stimulation (arrow). After the phasic activity in the neuron had ceased, the pulses elicited action potentials. **(b)** Reversal of sign of the tonic depolarization. When the neuron was depolarized beyond the reversal potential of the tonic depolarization, it became a tonic hyperpolarization. Note that, while the tonic conductance persisted, action potentials were generated although the neuron was hyperpolarized. Recording done in current-clamp mode. Action potentials and EMG potentials were clipped in both (a) and (b).

Reversal potential

When a neuron was held at a depolarized value by current injection, the tonic conductance produced a hyperpolarization (**Figs.11d; 14b**). Interestingly, while the tonic hyperpolarization was ebbing in **Fig.14b**, the neuron was firing action potentials although it was more hyperpolarized than at rest. This suggests that depolarization is not the only mechanism through which the tonic conductance increased the neuron's excitability, but that second messenger pathways might be involved (Trimmer, 1994; Heinrich et al., 2001). This idea is also consistent with the slow time-course of decay of the tonic depolarization, which lasted up to several seconds (**Figs.5b; 6b**).

3.2.6. Other leg motoneurons

Extensor MNs

A total of 17 extensor MNs were recorded, in 7 of which (41%) a tonic depolarization could be observed without current injection. **Fig.15** shows an example of the activity of a fast extensor MN (FETi) during a stepping sequence. The extensor MN depolarized and was firing action potentials during swing and repolarized during stance. This caused a phasic modulation of the membrane potential, but in this case no tonic depolarization was visible.

Hyperpolarizing current pulses were injected into a FETi MN (**Fig.15b, left**). As in case of the flexor neurons, the voltage deflection that was a response to the current pulse (as a measure of the input resistance) was greatest prior to stimulation during rest. The amplitude of the voltage deflection that was caused by the current pulses decreased during stance as well as during swing. In **Fig.15b (right)**, 24 individual responses are shown in grey together with the average (black). The input resistance was $3.6 \pm 0.44\text{M}\Omega$ at rest (range 2.9 to 4.5 $\text{M}\Omega$; N=1, n=24). Because of strong fluctuations of the membrane potential during stance and swing, only the averaged trace of 24 individual current pulses could be used to calculate input resistance, which was 1.9 $\text{M}\Omega$ during stance and 2.0 $\text{M}\Omega$ during swing. The smaller input resistance compared to rest shows that there were conductances due to synaptic inputs during both stance and swing phase.

In a slow extensor MN, there was no tonic depolarization visible without current injection at a resting potential of -54.8mV, while the amplitude of the phasic modulation was 15-19mV (**Fig.15c, middle**). During injection of constant hyperpolarizing current (**Fig.15c, left**) the membrane potential during rest changed to -90.3mV. A tonic depolarization became visible with an amplitude of 15mV while the amplitude of the phasic modulation slightly decreased

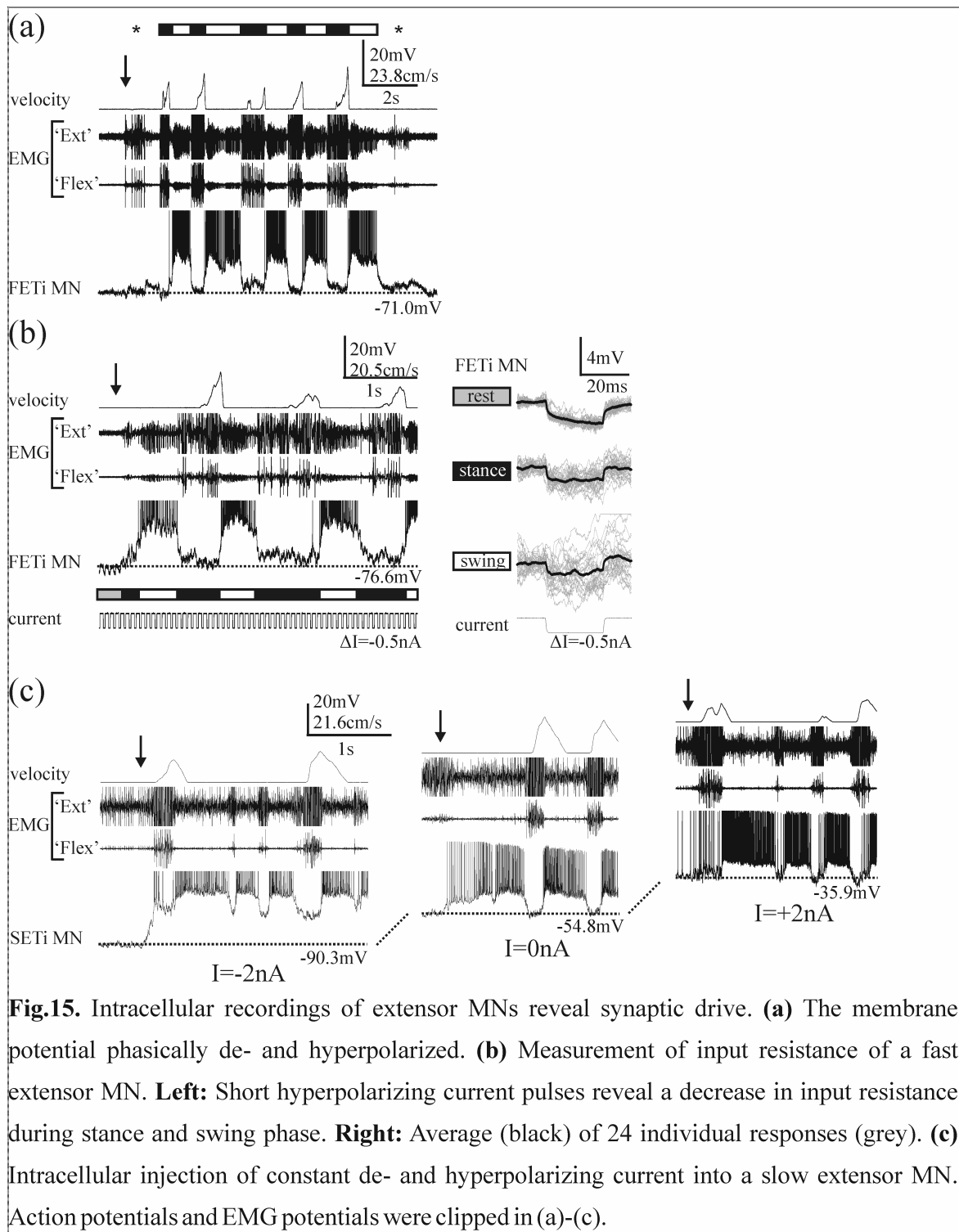


Fig.15. Intracellular recordings of extensor MNs reveal synaptic drive. **(a)** The membrane potential phasically de- and hyperpolarized. **(b)** Measurement of input resistance of a fast extensor MN. **Left:** Short hyperpolarizing current pulses reveal a decrease in input resistance during stance and swing phase. **Right:** Average (black) of 24 individual responses (grey). **(c)** Intracellular injection of constant de- and hyperpolarizing current into a slow extensor MN. Action potentials and EMG potentials were clipped in (a)-(c).

to 14-18mV. The hyperpolarization during stance did not reverse sign. During injection of constant depolarizing current (**Fig.15c, right**) the membrane potential during rest changed to -35.9mV. Again, there was no more tonic depolarization visible, suggesting that the reversal potential of the tonic depolarization was close to this value. The amplitude of the phasic modulation was 13-16mV. Also, during extensor activity the potential hyperpolarized below the altered resting potential, indicating an active inhibition during swing instead of a cessation of excitation.

Levator MNs

A total of 7 levator MNs were recorded, in 3 of which (43%) a tonic depolarization could be observed without current injection. **Fig.16** shows a recording of a fast levator motoneuron during a sequence of steps that is interrupted by two tapping movements (asterisks). The variability of levator activity has been discussed before (chapter 3.1.3). In this example, the levator was phasically depolarized and firing action potentials throughout stance phase and the initial part of swing phase. After that, the neuron repolarized. Throughout the stepping sequence, a tonic depolarization of 6-7mV was visible.

In the same levator MN, a tonic depolarization of 5-6mV was visible without current injection at a resting potential of -63.8mV, while the amplitude of the phasic modulation was 7-13mV (**Fig.16b, middle**). During injection of constant hyperpolarizing current (**Fig.16b, left**) the membrane potential during rest changed to -96.7mV. The amplitude of the tonic depolarization increased to 9-10mV while the amplitude of the phasic modulation was 9-12mV. The hyperpolarization during stance did not reverse sign. During injection of constant depolarizing current (**Fig.16b, right**) the membrane potential during rest changed to -25.0mV. Again, there was no more tonic depolarization visible. The amplitude of the phasic modulation was 9-15mV. Also, probably during activity of the antagonistic depressor MNs the potential hyperpolarized below the altered resting potential, indicating an active inhibition instead of a cessation of excitation.

Depressor MNs

A total of 10 depressor MNs were recorded, in 8 of which (80%) a tonic depolarization could be observed without current injection. The activity of a slow depressor MN (sDepr MN) during a series of steps is shown in **Fig.17**. A comparison of the depressor activity with the levator EMG showed that fast levator potentials (large units in EMG Lev) never occur during sDepr firing, indicating the antagonistic nature of levator and depressor MNs. Sometimes, small units in the levator EMG were co-active with low-frequency spikes in the depressor, which was hyperpolarized by a few millivolts during this episode of co-contraction (dotted boxes in **Fig.17**).

In a slow depressor MN, there was a tonic depolarization of ~2mV visible without current injection at a resting potential of -62.1mV, while the amplitude of the phasic modulation was ~9mV (**Fig.17b, middle**). During injection of constant hyperpolarizing current (**Fig.17b, left**) the membrane potential during rest changed to -76.6mV. The tonic depolarization increased to an amplitude of ~7mV while the amplitude of the phasic modulation increased to 13-16mV.

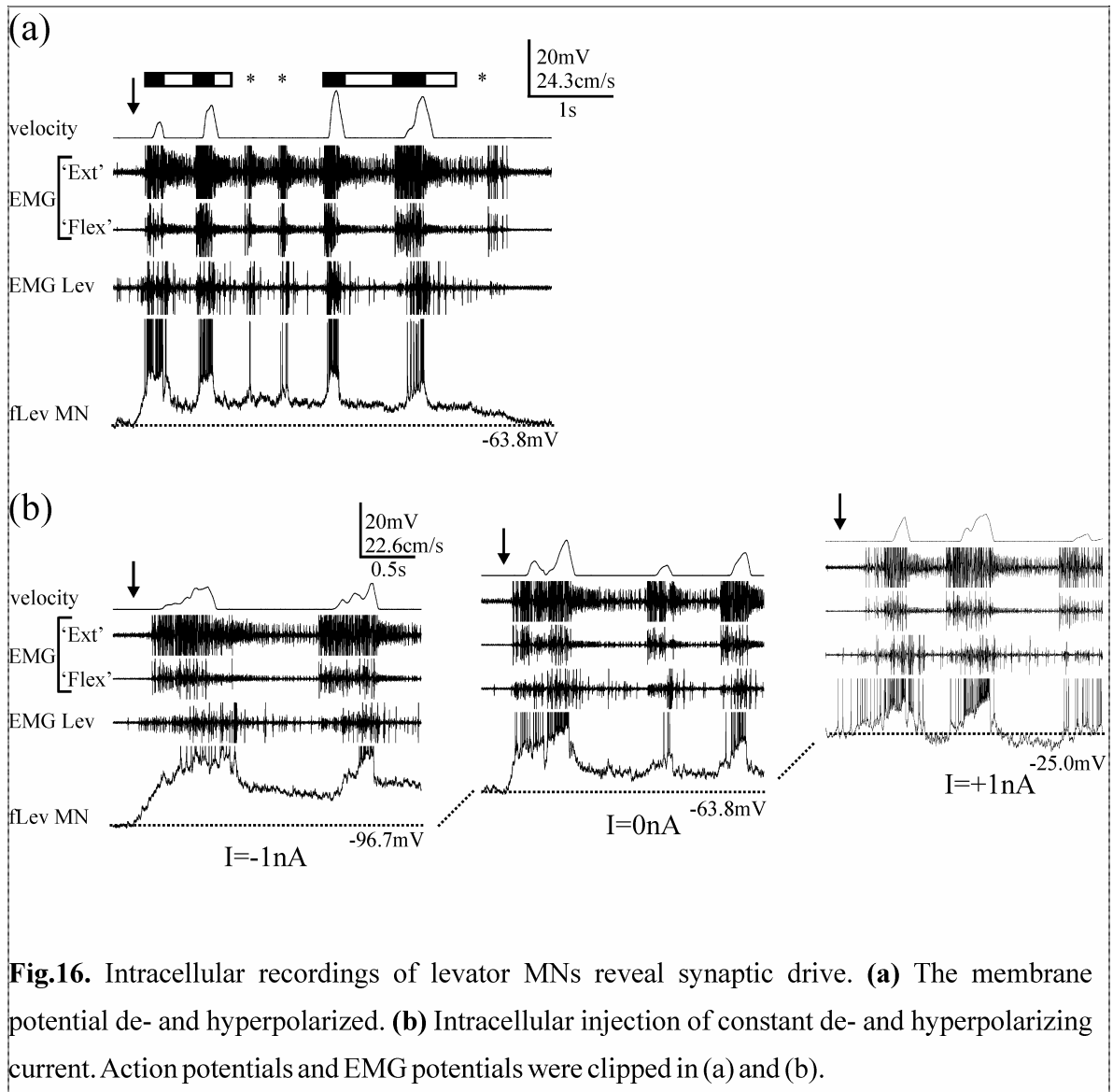


Fig.16. Intracellular recordings of levator MNs reveal synaptic drive. **(a)** The membrane potential de- and hyperpolarized. **(b)** Intracellular injection of constant de- and hyperpolarizing current. Action potentials and EMG potentials were clipped in (a) and (b).

The hyperpolarization during early swing did not reverse sign. During injection of constant depolarizing current (**Fig.17b, right**) the membrane potential during rest changed to -55.3mV . There was no more tonic depolarization visible. The amplitude of the phasic modulation was $\sim 16\text{mV}$. Also, during levator activity the potential hyperpolarized below the altered resting potential, indicating an active inhibition instead of a cessation of excitation.

Protractor MNs

A total of 3 protractor MNs were recorded, in 2 of which (67%) a tonic depolarization could be observed without current injection. An intracellular recording of a protractor MN is shown in **Fig.18a**. As in a freely moving animal walking forward, there was protractor activity during swing phase (Akay et al., 2004). A large tonic depolarization of 9-13mV was visible that slowly decayed after the stepping sequence.

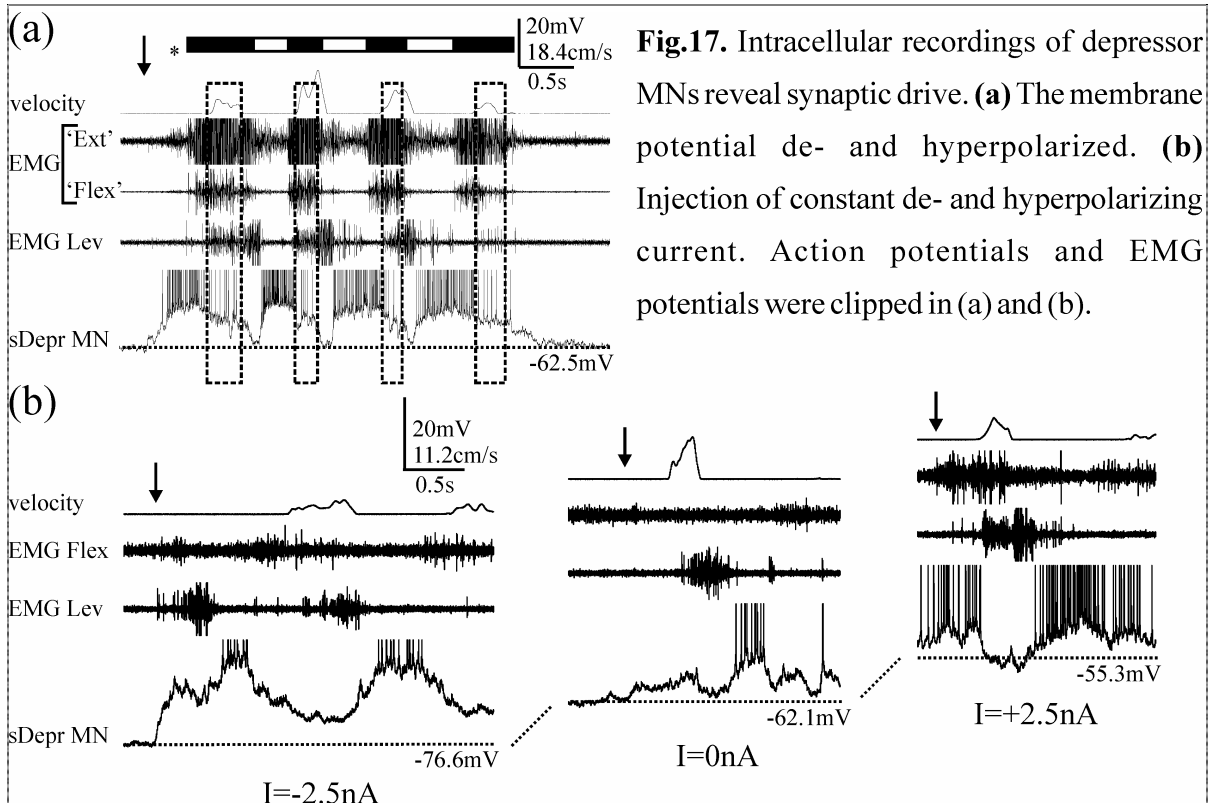


Fig.17. Intracellular recordings of depressor MNs reveal synaptic drive. **(a)** The membrane potential de- and hyperpolarized. **(b)** Injection of constant de- and hyperpolarizing current. Action potentials and EMG potentials were clipped in (a) and (b).

Retractor MNs

A total of 2 retractor MNs were recorded, in 1 of which a tonic depolarization could be observed without current injection. **Fig.18b** shows a recording of a retractor MN that was active during stance, resembling forward walking.

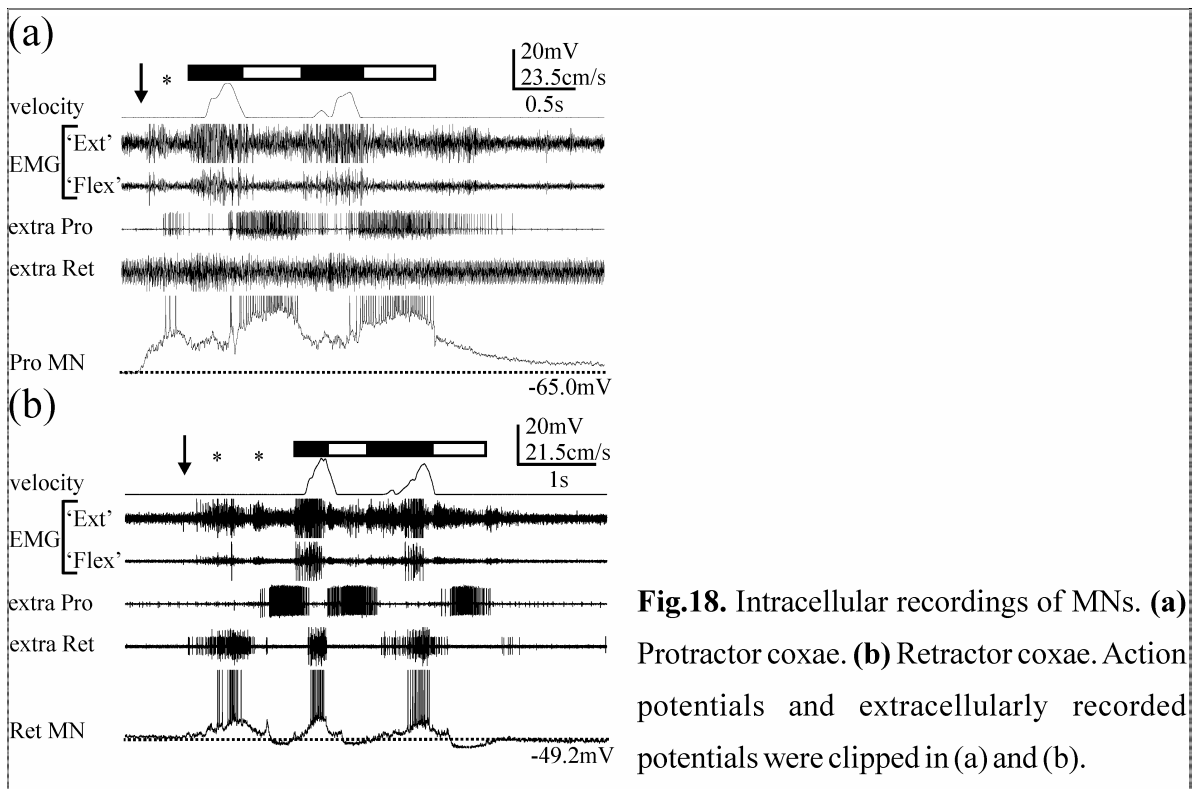


Fig.18. Intracellular recordings of MNs. **(a)** Protractor coxae. **(b)** Retractor coxae. Action potentials and extracellularly recorded potentials were clipped in (a) and (b).

3.2.7. Summary

A tonic excitation and phasic excitation and inhibition were shown for flexor MNs (**Figs.6b; 9; 11b**). Experiments involving measurements of input resistance and current injection showed that the same was true for extensor MNs (**Fig.15**).

For levator and depressor MNs, no measurements of input resistance were performed. In both neuron populations a tonic depolarization could be observed, although in some cases only during injection of constant hyperpolarizing current (**Figs.16a;17a**). A phasic inhibition could be shown by the fact that during activity of the respective antagonist the membrane potential hyperpolarized below resting value during injection of depolarizing current (**Figs.16b, right; 17b, right**). Although it could not be ruled out that the synaptic drive to levator and depressor MNs was caused by a combination of tonic excitation and phasic inhibition (**Fig.5c, middle**), the similarity of the activity pattern during walking with flexor and extensor MNs suggested that there also was a phasic excitation.

Due to a small number of recorded cells, no experiments involving current injections or measurements of input resistance were performed on protractor and retractor MNs. However, the general pattern of synaptic drive appeared to be similar in protractor and retractor MNs as for the other MNs.

3.3. Recruitment of slow and fast flexor MNs

3.3.1. Muscle structure

In most insect skeletal muscles, the muscle fibers can be classified in slow, intermediate and fast types that differ in their metabolism and contractile properties. Correspondingly, there are slow, intermediate and fast MNs that differ for example in the amount of transmitter that is released at the neuromuscular junction (Rathmayer, 1996) or their axon diameter (Gewecke, 1995). Each of these neurons can innervate muscle fibers with different properties, and individual muscle fibers are mostly innervated by MNs with different properties (Bässler et al., 1996; Sasaki & Burrows, 1998). Thus, MNs can generate fast twitches or slow continuous muscle contractions. Many insect muscles do not have a homogenous fiber type distribution. For example, the stick insect extensor tibiae muscle (Bässler & Storrer, 1980; Bässler et al., 1996; Bässler & Stein, 1996) and the flexor tibiae muscle of the locust (Theophilidis & Burns, 1983; Sasaki & Burrows, 1998) have a proximal part that is innervated almost exclusively by fast MNs and a distal part that is innervated mostly by slow MNs.

The flexor tibiae is one of the most complexly innervated muscles in the stick insect and in invertebrates in general. In the phylogenetically close species *Carausius morosus*, it is innervated by at least 14 excitatory MNs with slow, fast and intermediate characteristics (Debrodt & Bässler 1989; Storrer et al., 1986). In EMG recordings, muscle potentials from different fibers can be distinguished by amplitude; fast MNs produce large muscle potentials and slow MNs produce small muscle potentials (Cruse & Pflüger, 1981). However, because the amplitude of the recorded muscle potentials also depends on parameters like the distance of the fiber from the recording site, intracellular recordings are required to be certain about the identity of the MNs.

3.3.2. Functional requirements

As in any other muscle contraction, for contractions during walking it is required that the neurons in a motor pool are recruited in an orderly fashion, i.e. muscle fibers that generate small forces must be activated earlier than those generating large forces. It has been shown in the previous chapter that the basic features of the synaptic drive from premotor elements are similar for both the MNs within a motor pool and within different motor pools. In case of the flexor tibiae, this leads to the question of whether there is a recruitment order from slow to

fast MNs during walking and (if so) what the mechanisms are that are responsible for this recruitment.

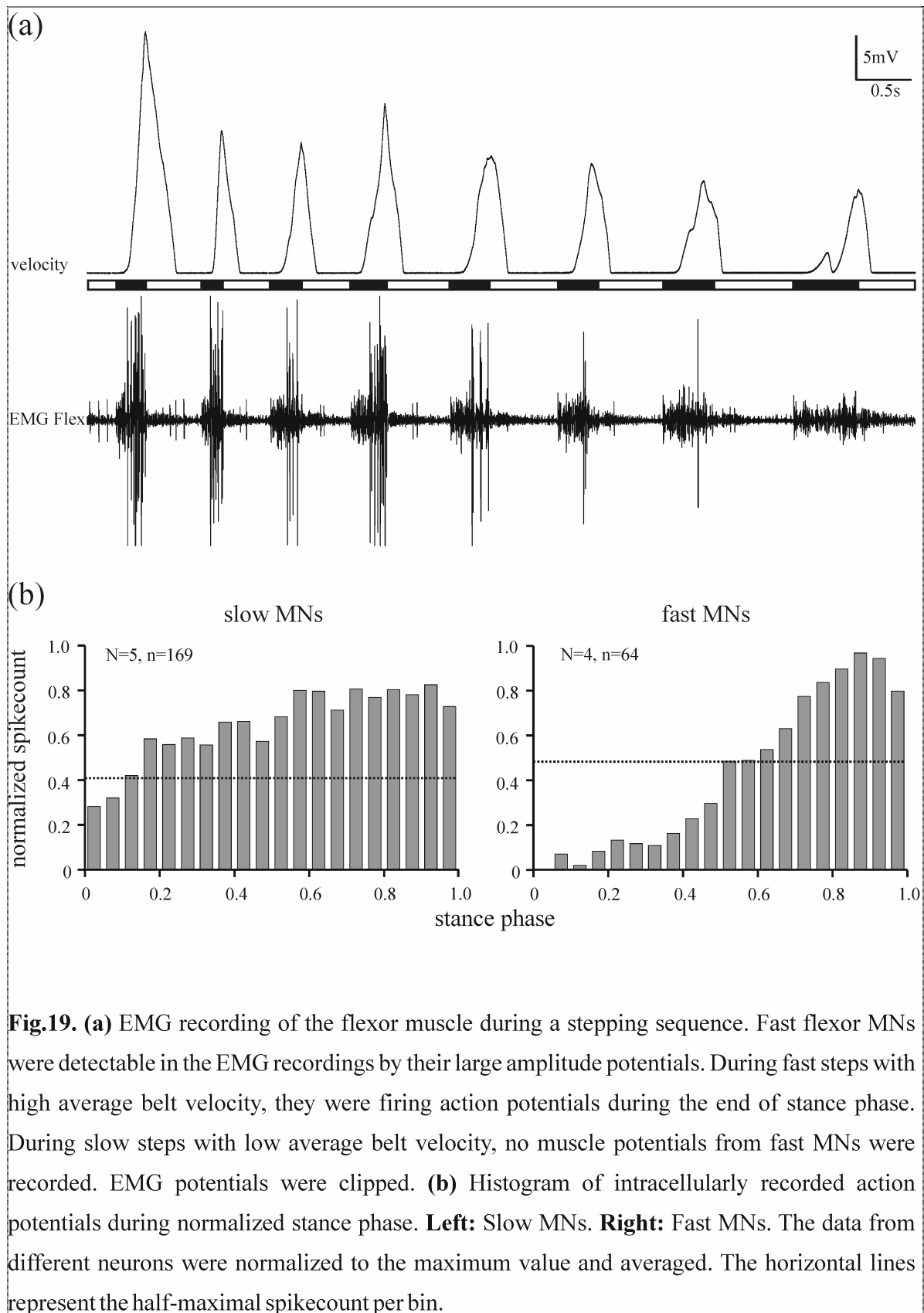
3.3.3. Consecutive recruitment

As a first step it was investigated how fast and slow motor units of the flexor tibiae muscle were activated during the stance phase of the single leg preparation. An example of an EMG recording of the flexor tibiae during a typical series of steps on the treadmill is given in **Fig.19a**. The muscle potentials with large amplitudes, attributable to activity of the fFlex-MNs, occurred 0.40 ± 0.26 s (N=3, n=63) after the first small amplitude muscle potentials, which were evoked by activity of the sFlex-MNs. Once active, fFlex-MNs fired action potentials until the end of stance phase. However during slower (smaller maximum and mean belt velocity) or smaller steps (smaller step width), no fast motor units were activated.

To describe the distribution of action potentials of fFlex and sFlex-MNs during steps on the light treadmill, the stance phase was normalized with respect to its duration and divided into 20 bins. The number of intracellularly recorded action potentials in each bin was normalized to the maximum value and the mean value for all investigated fast and slow neurons (N=4 and 5, respectively) was calculated (**Fig.19b**). It became evident that spike frequency rose more rapidly and earlier during stance phase in sFlex-MNs compared to fFlex-MNs. The half-maximal spike frequency (slow: normalized spike count = 0.41, fast: 0.48) was reached after 10 to 15% of stance phase for the sFlex-MNs, while for the fFlex-MNs it was reached as late as after 50 to 60% of stance phase.

3.3.4. Membrane potential depolarization in slow and fast flexor motoneurons

In order to find out whether the different firing pattern of the MNs resulted from a different time course of membrane potential during stance phase, intracellular recordings of fast and slow MNs were compared (**Fig.20a**). In both sFlex- and fFlex-MNs the membrane potential depolarization started with the beginning of stance phase. The slow MN fired action potentials throughout the whole stance phase. In the fast MN the membrane potential steadily depolarized beginning at the start of the stance phase on and reached the threshold for the initiation of action potentials later during stance phase. Please note the more hyperpolarized membrane potential of the fast MN.



Intracellular recordings from fast and slow flexor MNs were averaged during the normalized stance phase after the action potentials had been eliminated from the intracellular recording (**Fig.20b**, see Materials & Methods, chapter 2.4). In addition to the mean values the most

depolarized and the most hyperpolarized MNs analyzed were also included in the figure. It became evident that fast and slow MNs were constantly depolarized throughout the whole stance phase with a similar time course. The membrane potential of fFlex-MNs was relatively more hyperpolarized than that of sFlex-MNs.

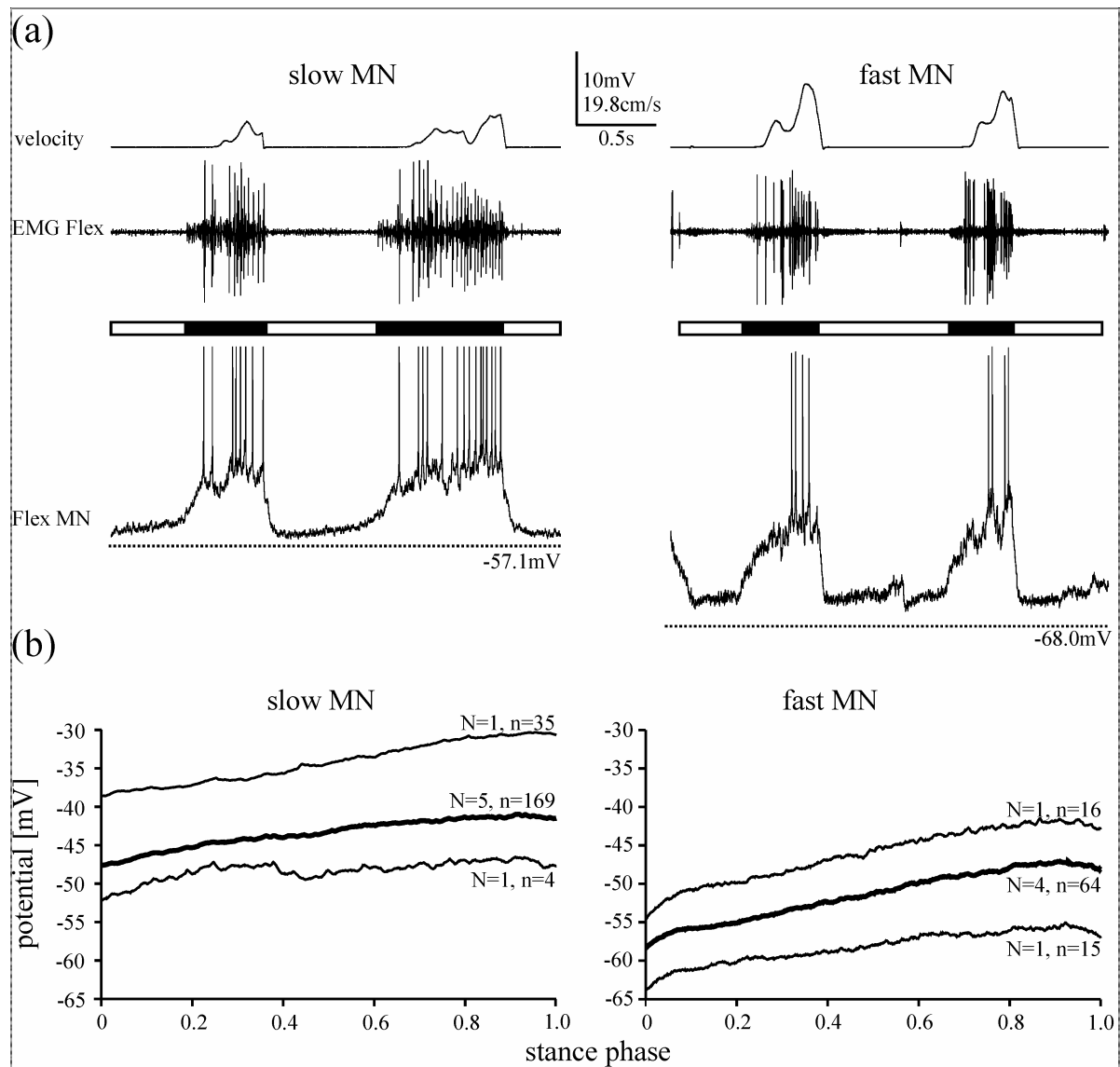


Fig.20. Membrane potential depolarization of fast and slow flexor MNs during stance. **(a)** Both slow and fast flexor MNs depolarized throughout stance phase. The slow MN fired action potentials throughout stance phase, while the fast MN was recruited late during stance. Action potentials and EMG potentials were clipped. **(b)** Average time-course of membrane potential depolarization during stance in slow and fast MNs. The average (thick trace) is shown together with the most depolarized and the most hyperpolarized neuron analyzed.

3.3.5. Common synaptic inputs

Despite the difference in the pattern of spike activity both types of MNs received similar activation patterns from their premotor network. I investigated this by comparing the time course of membrane potential of fast flexor MNs during steps with no fast MN activity with the EMG activity of the whole flexor muscle, which was described by rectifying and low-pass filtering of the EMG recording (Lippold, 1952) with a time constant of 20ms (see Materials & Methods, chapter 2.4). The value of this smoothed rectified EMG (SR-EMG) was used as an approximation of the overall EMG activity at the recording site (**Fig.21**). In all cells investigated (N=7), the time course of the SR-EMG resembled the membrane potential fluctuations in the recorded fFlex-MN very closely. The observation that the membrane potential of individual fFlex-MNs that were not firing action potentials was modulated in the same way as the activity of the subpopulation of sFlex-MNs that was recruited during the steps indicated that both MN populations were driven by similar, if not common, synaptic inputs.

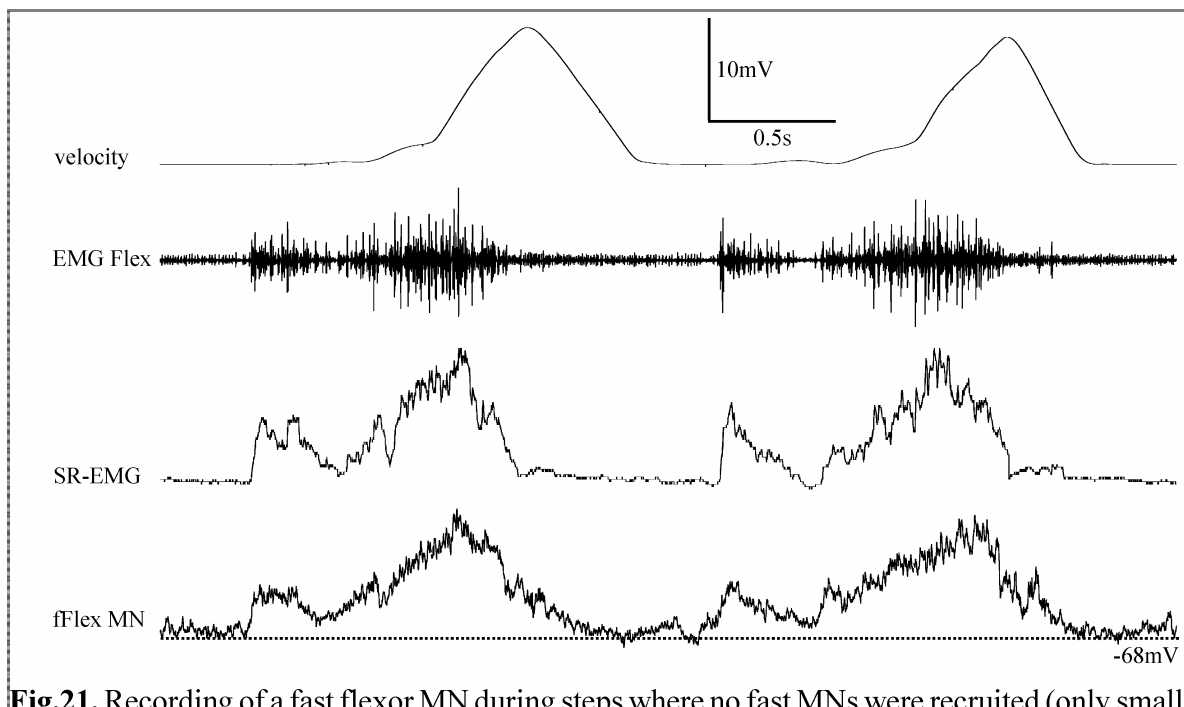


Fig.21. Recording of a fast flexor MN during steps where no fast MNs were recruited (only small amplitude units in EMG). The flexor EMG was rectified and smoothed (SR-EMG) in order to more clearly show the overall muscle activity. The membrane potential fluctuations in the flexor neuron very closely resembled the SR-EMG, suggesting common synaptic inputs to the flexor MN pool.

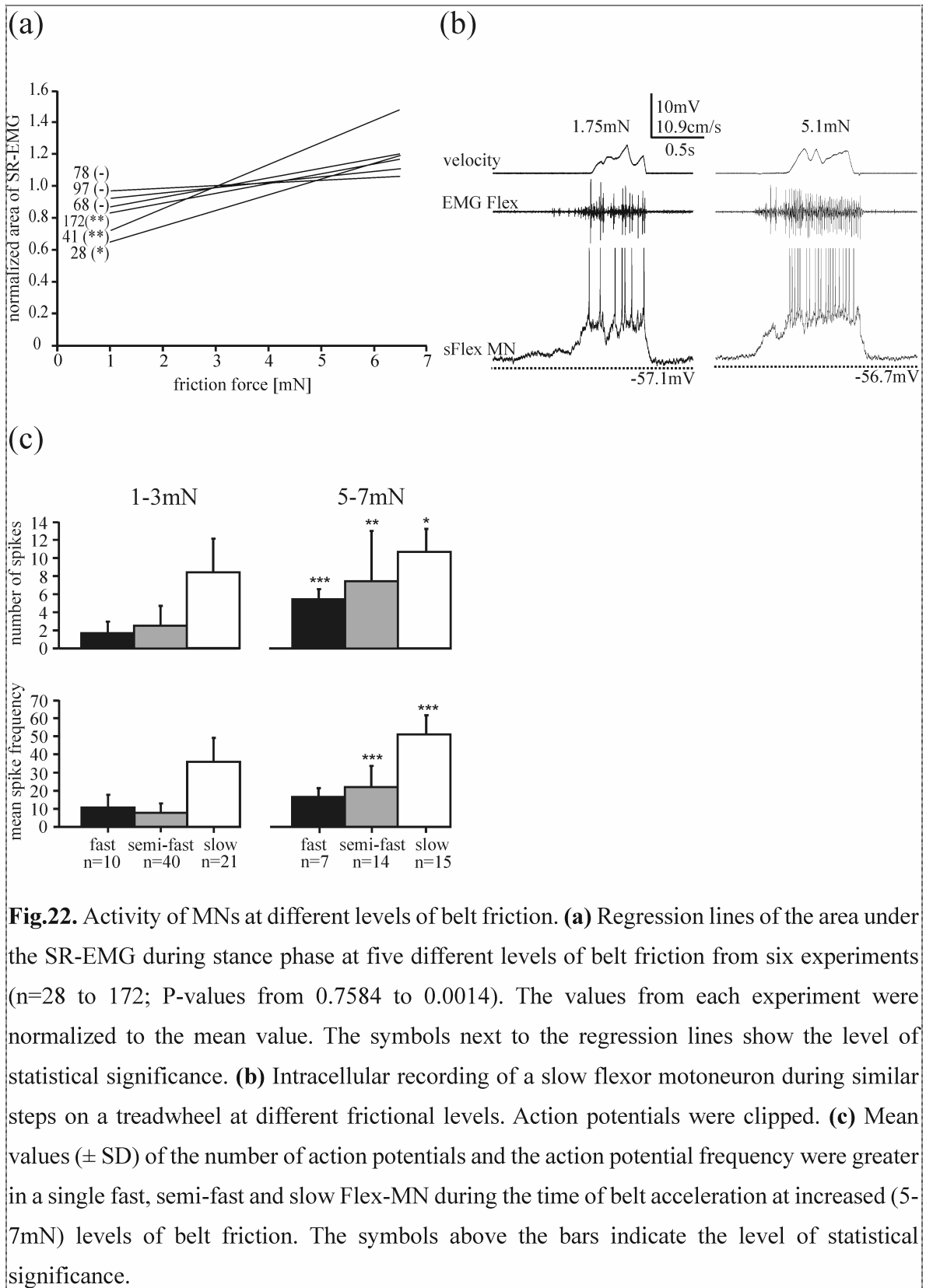
3.3.6. Activity at different frictional levels

Finally, I was interested in the question how the activity of the flexor tibiae muscle and its MNs during stance phase was adapted to different load situations mimicked by a variation in belt friction. In order to answer this question I induced stepping sequences and varied belt friction of the treadmill from reduced to enlarged values compared to control while recording flexor muscle and MN activity. The area under the SR-EMG during stance phase was used as a measure of the activity of the flexor muscle (Lippold, 1952; Winter, 1990). For all animals tested the normalized area under the SR-EMG increased with belt friction. The regression lines for the relationship between belt friction and the area under the SR-EMG for six different animals are shown in **Fig.22a**. The regression lines for the relationship between belt friction and the area under the SR-EMG showed a positive slope in all six cases examined, with the relationship being statistically significant ($P < 0.05$) in three out of six cases.

The question arises whether both slow and fast MN activity was altered with changing load conditions. Therefore, the activity, i.e. the number of action potentials generated in individual flexor MNs and the mean action potential frequency during stance phase, was evaluated under conditions of varying belt friction (**Fig.22b**). A quantitative analysis showed a common change in activity in slow, semifast and fast MNs of the flexor tibiae under conditions of modified belt friction (**Fig.22c**). This means that not only recruitment of flexor MNs adapts to load conditions, but also each individual MN was contributing to flexor force under varying conditions.

3.3.7. Resting membrane potential and spike threshold

The resting membrane potential of slow and fast flexor MNs prior to tactile stimulation and the value of the membrane potential threshold at which action potentials were initiated was determined (**Fig.23a**). The average resting membrane potentials of the slow and the fast flexor MN populations were significantly different ($P = 0.0262$). While it was $-61.8 \pm 7.5\text{mV}$ for the sFlex-MNs ($N = 20$) it was $-67.2 \pm 4.3\text{mV}$ for the fFlex-MNs ($N = 13$). [The higher sample size compared to other experiments was due to the fact that intracellular recordings from older experiments with a heavier treadmill were included.] In both subsets of MNs the membrane potential for action potential generation was not significantly different ($-51.2 \pm 7.2\text{mV}$ for the slow flexor MNs and $-50.1 \pm 3.9\text{mV}$ for the fast flexor MNs; $P = 0.6485$). Thus the threshold depolarization (the difference between resting membrane potential and spike threshold) was significantly different in slow and fast MNs $10.6 \pm 5.0\text{mV}$ and $17.0 \pm 3.8\text{mV}$, respectively; $P = 0.0004$).



3.3.8. Conclusions

Both fast and slow flexor MNs depolarized throughout stance phase with a similar time course, suggesting that they received substantial common synaptic excitation. Fast flexor MNs had a more hyperpolarized resting membrane potential. During slow steps, the depolarization of fast flexor MNs was not large enough to reach spike threshold (**Fig.23b, left**). During faster steps fast MNs were recruited, with the more negative resting membrane potential at least partly responsible for their late recruitment during stance (**Fig.23b, right**).

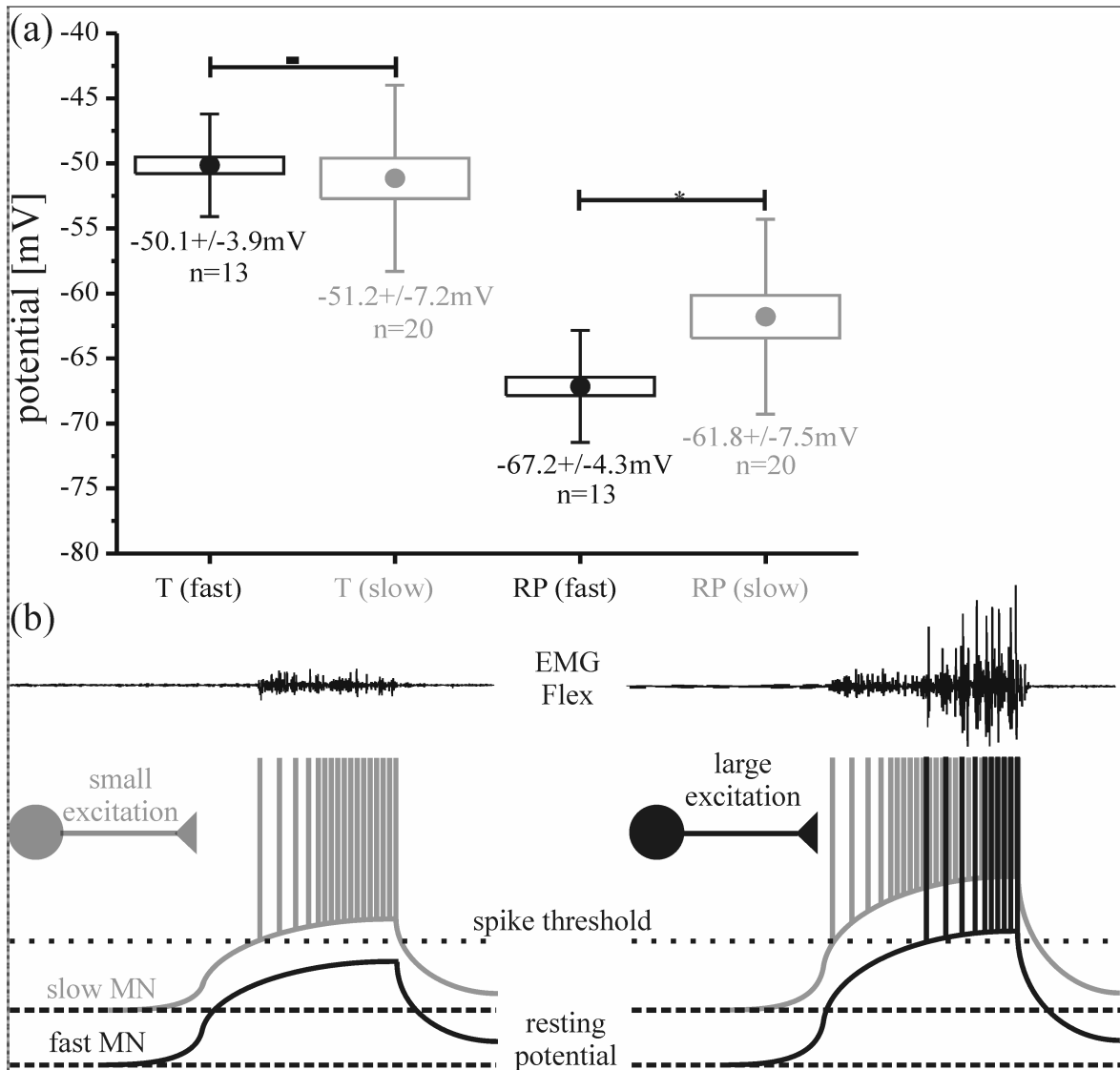


Fig.23. (a) Values of spike threshold and resting membrane potential in slow and fast flexor MNs. The spike threshold (T) was not significantly different, while the resting membrane potential (RP) was significantly more hyperpolarized in fast flexor MNs. **(b)** Schematic drawing of the membrane potential depolarization of slow and fast flexor MNs during stance. **Left:** During small steps, fast flexor MNs are not recruited because of their more hyperpolarized resting membrane potential. **Right:** During fast steps, fast MNs require a longer depolarization to reach spike threshold and are recruited later than slow MNs.

3.4. Control of stepping velocity

3.4.1. Correlation of cycle period and belt velocity

A section of a stepping sequence that consisted of a total of 12 steps is shown in **Fig.24a**. The activity of the flexor muscle during stance is visible from the EMG and the intracellular recording of a fast flexor (fFlex) MN. During long stepping sequences, cycle period often increased while mean and maximum belt velocity decreased (**Fig.24b**). In other cases, belt velocity did not decline but also increased within a sequence (cf. **Fig.2b**). In general there was a negative correlation between cycle period and mean belt velocity (**Fig.24c**). Both a short cycle period and a high mean belt velocity, i.e. a stronger and faster phase stance muscle contraction, would in freely walking animals contribute to a high walking velocity. Therefore, steps with short cycle period and high mean belt velocity will be called ‘fast’ steps, while steps with long cycle period and low mean belt velocity will be called ‘slow’ steps.

3.4.2. Amplitude of membrane potential modulation and spike frequency

As shown in chapter 3.2, in the stick insect the membrane potential modulations of flexor MNs during stepping were generated by phasic excitatory and inhibitory synaptic inputs. In addition, leg MNs were depolarized tonically throughout stepping sequences (see also Büschges et al., 2004; Ludwar et al., 2005b). During stance, flexor MNs were excited and their suprathreshold activity was responsible for the belt movement, while they were inactivated by inhibition during swing. Thus, the maximal depolarization (peak potential) in flexor MNs occurred during stance and the minimal (trough potential) during swing. When comparing steps of different velocity it was obvious that more flexor MNs were recruited during faster steps (e.g. **Fig.27b**) and that activation of flexor MNs increased (**Fig.25a**). Flexor MNs had a more depolarized peak potential and were firing more action potentials during fast steps than during slow steps (**Figs.25a,b**). The values of peak potentials showed the same modulation as both, maximum and mean belt velocity throughout the stepping sequence. Trough potential was not modulated and appeared to be independent of variations in mean belt velocity (**Fig.25b**). This was true for all recorded flexor MNs (N=25).

The membrane potential of extensor MNs reached a peak during swing and a trough during stance. Contrary to the flexor MNs, the activity of extensor MNs was independent of mean belt velocity during the previous stance phase (**Fig.25c**). Neither peak potential nor trough

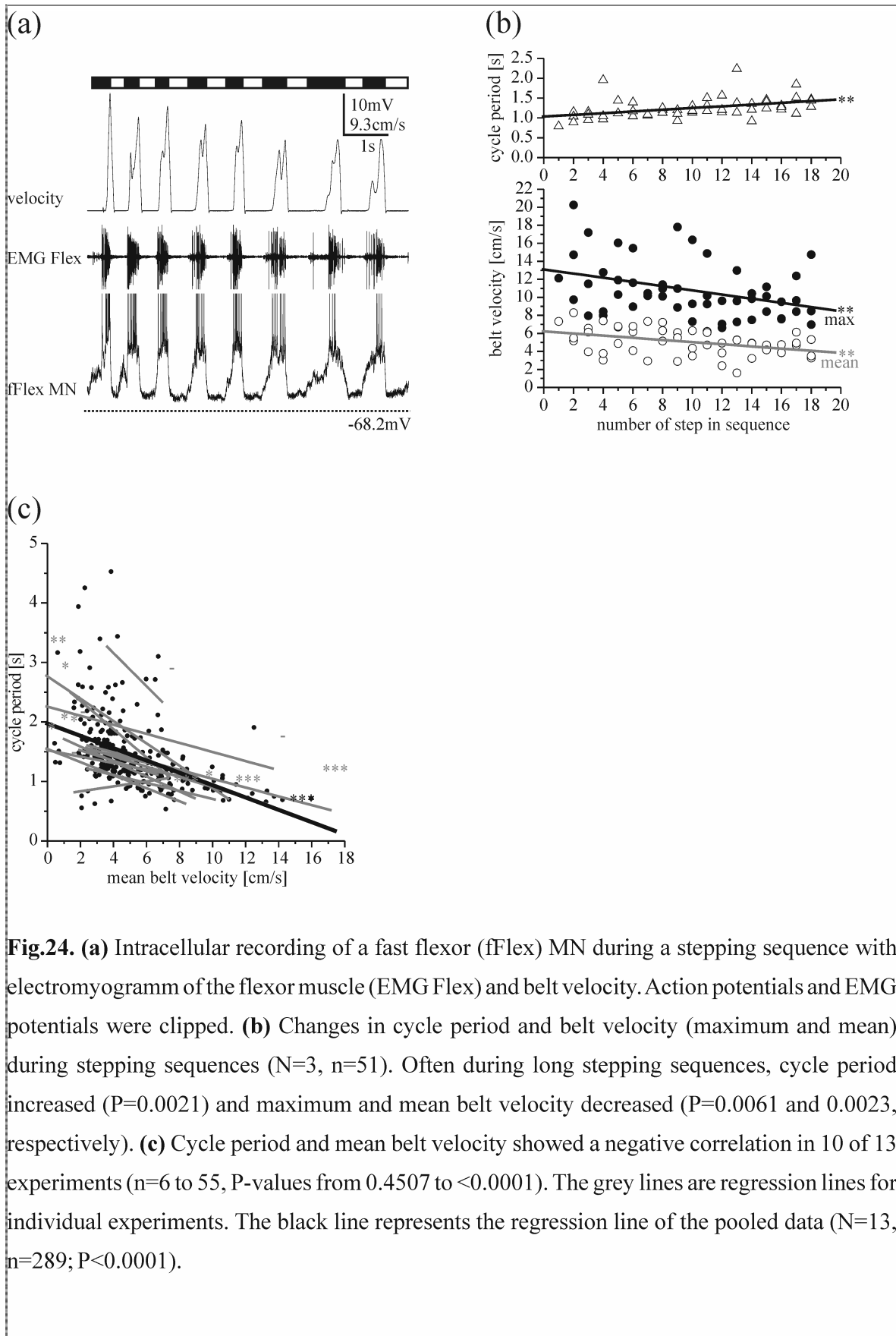


Fig.24. (a) Intracellular recording of a fast flexor (fFlex) MN during a stepping sequence with electromyogram of the flexor muscle (EMG Flex) and belt velocity. Action potentials and EMG potentials were clipped. **(b)** Changes in cycle period and belt velocity (maximum and mean) during stepping sequences (N=3, n=51). Often during long stepping sequences, cycle period increased (P=0.0021) and maximum and mean belt velocity decreased (P=0.0061 and 0.0023, respectively). **(c)** Cycle period and mean belt velocity showed a negative correlation in 10 of 13 experiments (n=6 to 55, P-values from 0.4507 to <0.0001). The grey lines are regression lines for individual experiments. The black line represents the regression line of the pooled data (N=13, n=289; P<0.0001).

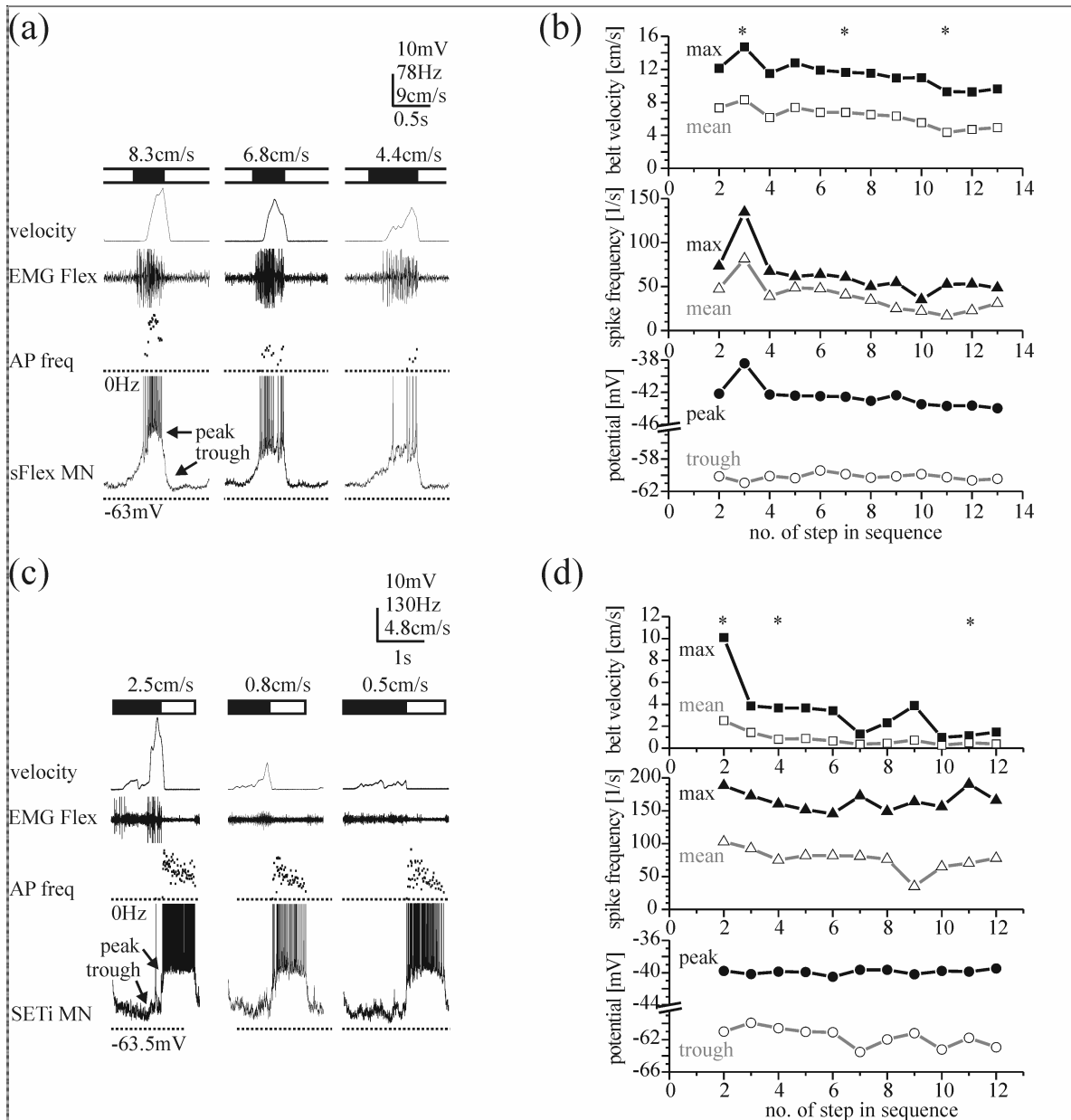


Fig.25. (a) Example of three steps with different mean belt velocities (8.3 to 4.4cm/s) recorded within a stepping sequence from a slow flexor MN. During the stance phase of fast steps, the neuron showed a larger depolarization and was firing more action potentials than during slow steps. Action potentials and EMG potentials were clipped. **(b)** Quantification of peak and trough potential, spike frequency and belt velocity during the stepping sequence from (a); asterisks mark steps shown there. Along with maximum and mean belt velocity, maximum and mean spike frequency decreased during this stepping sequence, as did the peak membrane potential during stance. The trough membrane potential during swing remained constant. **(c)** Example of three steps with different mean belt velocities (2.5 to 0.5cm/s) recorded within a stepping sequence in a slow extensor MN. The depolarization and action potential activity was similar during all steps. Action potentials and EMG potentials were clipped. **(d)** Quantification of peak and trough

potential, spike frequency and belt velocity during the stepping sequence from (c); asterisks mark steps shown there. Maximum and mean belt velocity decreased during this stepping sequence, while maximum and mean spike frequency changed only slightly. Neither peak nor trough potential showed the same variation as belt velocity.

potential showed systematic changes in parallel to maximum and mean belt velocity during the stepping sequence (**Fig.25d**). The same was true in all recorded extensor MNs.

The relationship between mean belt velocity and peak and trough potential in flexor MNs is drawn in **Fig.26a**. Recordings from four slow flexor MNs were selected that included a large number of steps over a large mean belt velocity range. There was a positive correlation between peak potential of flexor MNs and mean belt velocity, while trough potential was correlated with mean belt velocity only in 1 of 4 neurons. In addition, maximum and mean action potential frequency of flexor MNs was correlated with mean belt velocity (**Fig.26b**). This was observed in all 25 recorded flexor MNs; no difference between slow, semifast and fast MNs was detected.

In nearly all recordings, stepping sequences started with a stance phase and ended with a swing phase (not shown). I compared the activity of extensor MNs to the mean belt velocity of the previous stance phase. Four recordings from extensor MNs (2 SETi, 2 FETi) were selected that included a large number of steps, 3 of which included steps that covered a large mean belt velocity range. There was no consistent correlation of peak or trough potential (**Fig.26c**) with mean belt velocity. This was observed in all 15 recorded extensor MNs; no difference between SETi and FETi MNs was detected. In addition, maximum and mean action potential frequency during swing was not correlated with mean belt velocity during the previous stance phase (**Fig.26d**). This is supported by 15 FETi recordings in the closely related stick insect species *Carausius morosus* (v. Uckermann, 2004).

In walking, flexor and extensor MNs receive phasic inhibition during the activity of their respective antagonistic MNs (see chapter 3.2). As stated above, there was no correlation of trough potential of extensor MNs with mean belt velocity and therefore not with flexor activity (**Fig.26c**). Only in one neuron where steps with exceptionally high flexor activity were compared to ones with very low flexor activity could I observe that the strength of inhibition of extensor MNs during stance, as concluded from the level of hyperpolarization, was somewhat correlated to the level of flexor activity (**Fig.26e**).

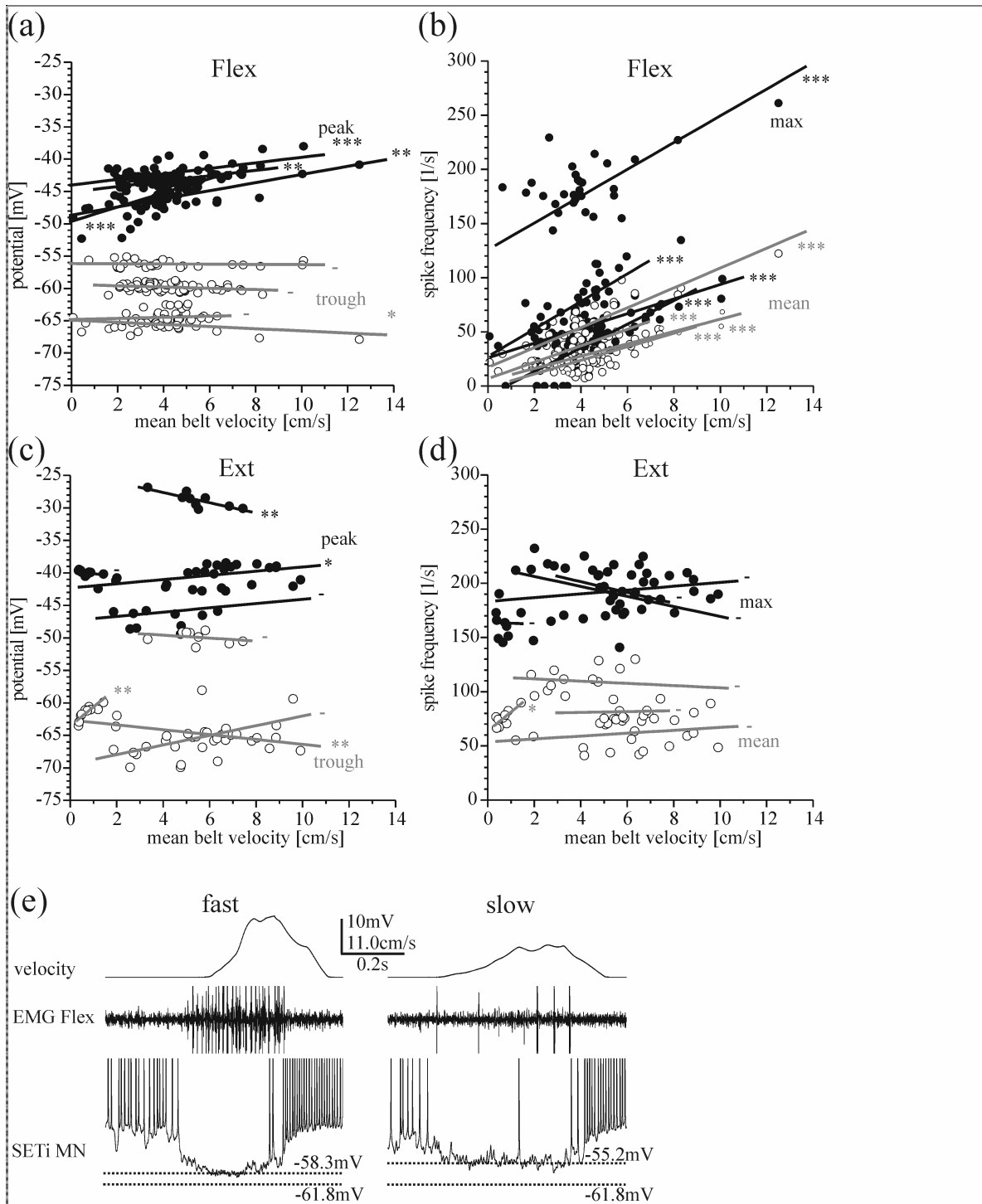


Fig.26. (a) Peak and trough membrane potential of 4 flexor MNs at different mean belt velocities (n=27 to 56). 4 slow (sFlex) MNs were evaluated. The peak potential showed a positive correlation in 4 neurons (P-values from 0.0017 to 0.0006), while the trough potential showed a negative correlation in 1 neuron (P=0.0464). **(b)** Maximum and mean spike frequency during stance of the neurons shown in (a). The maximum and mean spike frequency showed a positive correlation in 4 neurons (P-values from 0.0004 to <0.0001 and 0.0002 to <0.0001, respectively). **(c)** Peak and trough membrane potential of 4 extensor MNs at different mean belt velocities

(n=12 to 16). 2 slow (SETi) and 2 fast (FETi) MNs were evaluated. The peak potential showed a positive correlation in 1 neuron (P-value: 0.0324) and a negative correlation in 1 neuron (P-value 0.0099). The trough potential showed a positive correlation in 1 neuron (P-value: 0.0023) and a negative correlation in 1 neuron (P-value 0.0015). **(d)** Maximum and mean spike frequency during swing of the extensor MNs from (c). The maximum spike frequency showed no correlation in 4 of 4 neurons (P-values from 0.9494 to 0.1905), while the mean spike frequency shows a positive correlation in 1 of 4 neurons (P=0.0107). **(e)** Intracellular recording of a SETi MN. During steps with very high flexor activity the neuron was more strongly hyperpolarized than during steps with very weak flexor activity. Action potentials and EMG potentials were clipped.

3.4.3. Time course of membrane potential modulation in flexor motoneurons

The activity of a flexor MN during a walking sequence with steps of varying velocity is shown in **Fig.27a**. In order to analyze the changes in time course of membrane potential modulation that accompanied variations in belt velocity I compared steps with high mean belt velocity (**Fig.27b, left**) to those with low velocity (**Fig.27b, right**). When the intracellular traces were aligned at the time of the beginning of flexor EMG activity (**Fig.27c**) it became apparent that flexor MNs depolarized in a similar way at the beginning of stance during both slow and fast steps (see arrows in **Fig.27b-d**). After this initial depolarization the membrane potential quickly depolarized to its maximal value during fast steps, while the depolarization ebbed before a second depolarization to the maximal value could be observed during slow steps. The same was true when comparing the average membrane potentials recorded during the ten steps with the highest mean belt velocity with those that showed the lowest mean belt velocity for a given recording (**Fig.27c, bottom left**). At the end of flexor EMG activity (i.e. the transition from stance to swing phase) the membrane potential rapidly hyperpolarized both in fast and slow steps (**Fig.27c, top right; averages bottom right**). Please note that the depolarization at the transition from swing to stance was in general slower than the hyperpolarization at the transition from stance to swing. The results described above were true for all flexor MN recordings.

The depolarization at the beginning of stance phase was further analyzed by averaging the membrane potential of flexor MNs during steps with intermediate mean belt velocity. In all cases, the time course of the initial depolarization was similar, while its amplitude appeared to be slightly smaller during slow steps as compared to faster steps (~3.3mV compared to

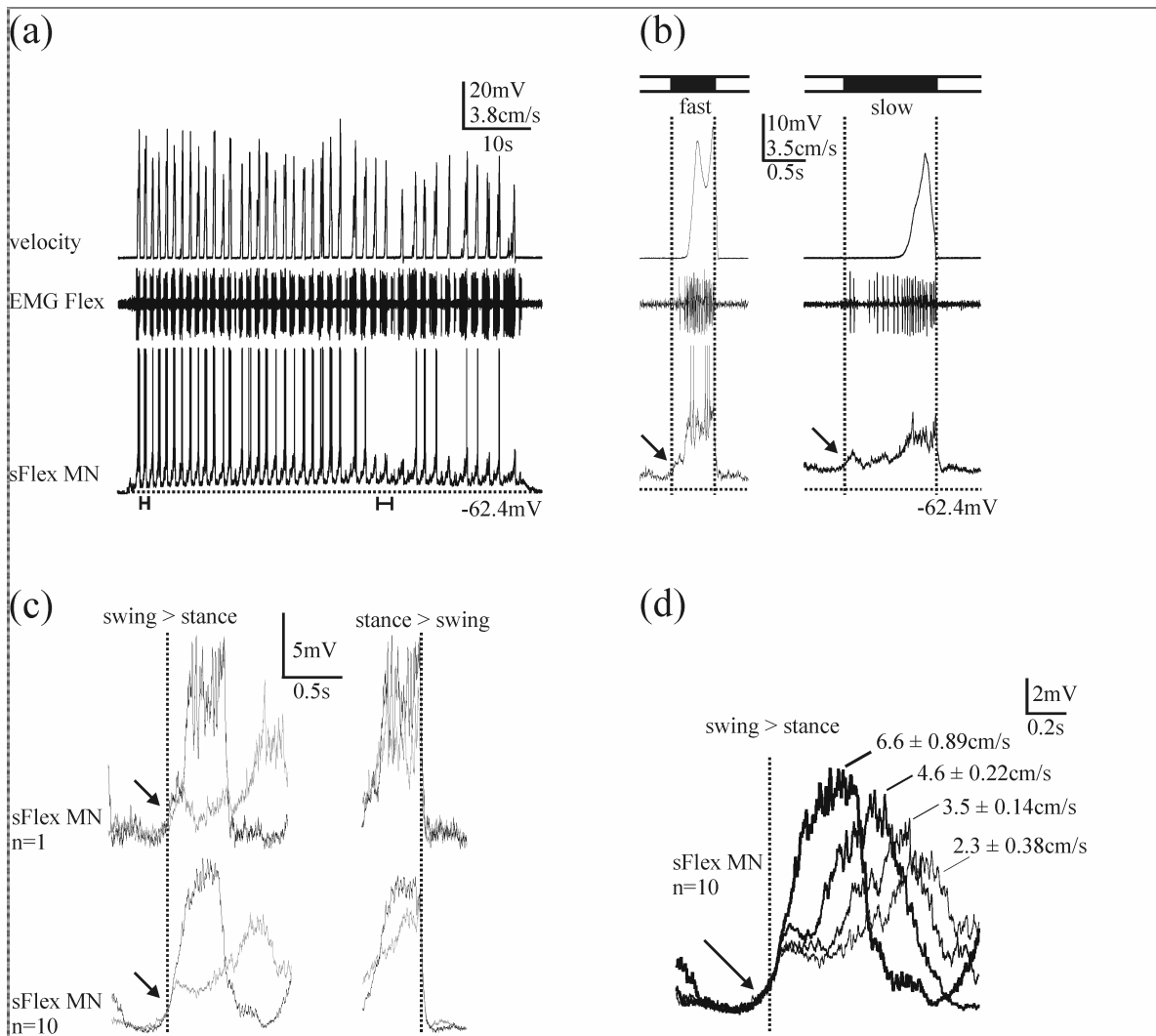


Fig.27. (a) Intracellular recording of a sFlex MN during a stepping sequence with variable cycle period and belt velocity. The lines mark the sequences shown in (b). **(b)** Episodes from (a) with fast and slow steps. Action potentials were clipped in (a) and (b). Arrows in (b)-(d) mark the initial depolarization at the beginning of stance. **(c) Top:** Intracellular recordings from (b) aligned at the time of phase transitions and superimposed; spikes had been eliminated from the recording. Note that the initial depolarization at the transition from swing to stance was similar in the recording from the fast step (black trace; mean belt velocity 9.8cm/s) and slow step (grey trace; mean belt velocity 3.4cm/s). After the initial depolarization, the neuron depolarized rapidly and with large amplitude in case of the fast step and more slowly in case of the slow step. At the transition from stance to swing, the neuron rapidly hyperpolarized during both fast and slow steps. **Bottom:** Averaged membrane potential of the neuron shown in (a) during the 10 fastest steps (black trace; $6.6 \pm 0.89\text{cm/s}$) and 10 slowest steps recorded (grey trace; $2.4 \pm 0.38\text{cm/s}$) aligned at the time of phase transitions and superimposed; spikes had been eliminated. **(d)** From the same neuron, in addition to the 10 fastest and 10 slowest steps recorded, 10 steps with above-average mean belt

velocity ($4.6 \pm 0.22\text{cm/s}$) and 10 steps with below-average mean belt velocity ($3.4 \pm 0.14\text{cm/s}$) were selected. The membrane potential recorded during these steps was averaged and aligned around the beginning of stance phase after spikes had been eliminated. At the swing-stance transition, the initial depolarization was similar in all averaged traces. During the slowest steps, the initial depolarization had the smallest amplitude (approximately 3.3mV). Around 350ms after the initiation of stance, there was another slow depolarization of around 3.3mV . The faster the steps were, the larger was the amplitude of the initial depolarization and the sooner (and more rapidly) the second depolarization occurred. During the fastest steps, the initial depolarization had the largest amplitude (approximately 3.9mV). Around 60ms after the initiation of stance, there was a depolarization of around 11.7mV .

3.9mV). During slow steps, the second depolarization to the maximal value appeared late ($\sim 0.35\text{s}$ after the beginning of stance) and with a slow time course and smaller amplitude ($\sim 7.6\text{mV}$). It appeared sooner ($\sim 0.06\text{s}$ after the beginning of stance phase) and had a faster time course and larger amplitude ($\sim 11.7\text{mV}$) during fast steps (**Fig.27d**).

As mentioned before, flexor MNs are tonically depolarized throughout stepping (Ludwar et al., 2005b; see above) and phasically inhibited during swing (see chapter 3.2). I was interested to know whether the initial depolarization could be the result of the termination of this inhibition. In **Fig.28a**, an intracellular recording of a flexor MN is shown together with the extensor EMG (see materials and methods, same recording as in Fig.8b). Please note that extensor activity was highest during the first half of swing and then slowly decreased. The membrane potential of the flexor MN showed little modulation during swing. Injection of short hyperpolarizing current pulses revealed that while extensor activity decreased the input resistance of flexor MNs increased ($N=13$). **Fig.28b** shows quantitatively that the voltage deflections as a response to hyperpolarizing current pulses (a measure for the input resistance, see above) steadily increased during the end of swing and the beginning of stance phase. The solid vertical line marks the beginning of the initial depolarization ($0.07 \pm 0.061\text{s}$ before the beginning of stance; $N=4$, $n=128$), the dashed vertical line marks the standard deviation. The stereotypic initial depolarization occurs during an increase in input resistance, indicating that a release from inhibition may be involved in its generation. This assumption is supported by the fact that the amplitude of the underlying tonic depolarization ($3.9 \pm 2.2\text{mV}$; range: 1.3 to 9.5mV ; observed in $N=18$ of 25 MNs, $n=28$) was also stereotypic and not correlated with mean belt velocity (**Figs.24b; 25a; 27a**).

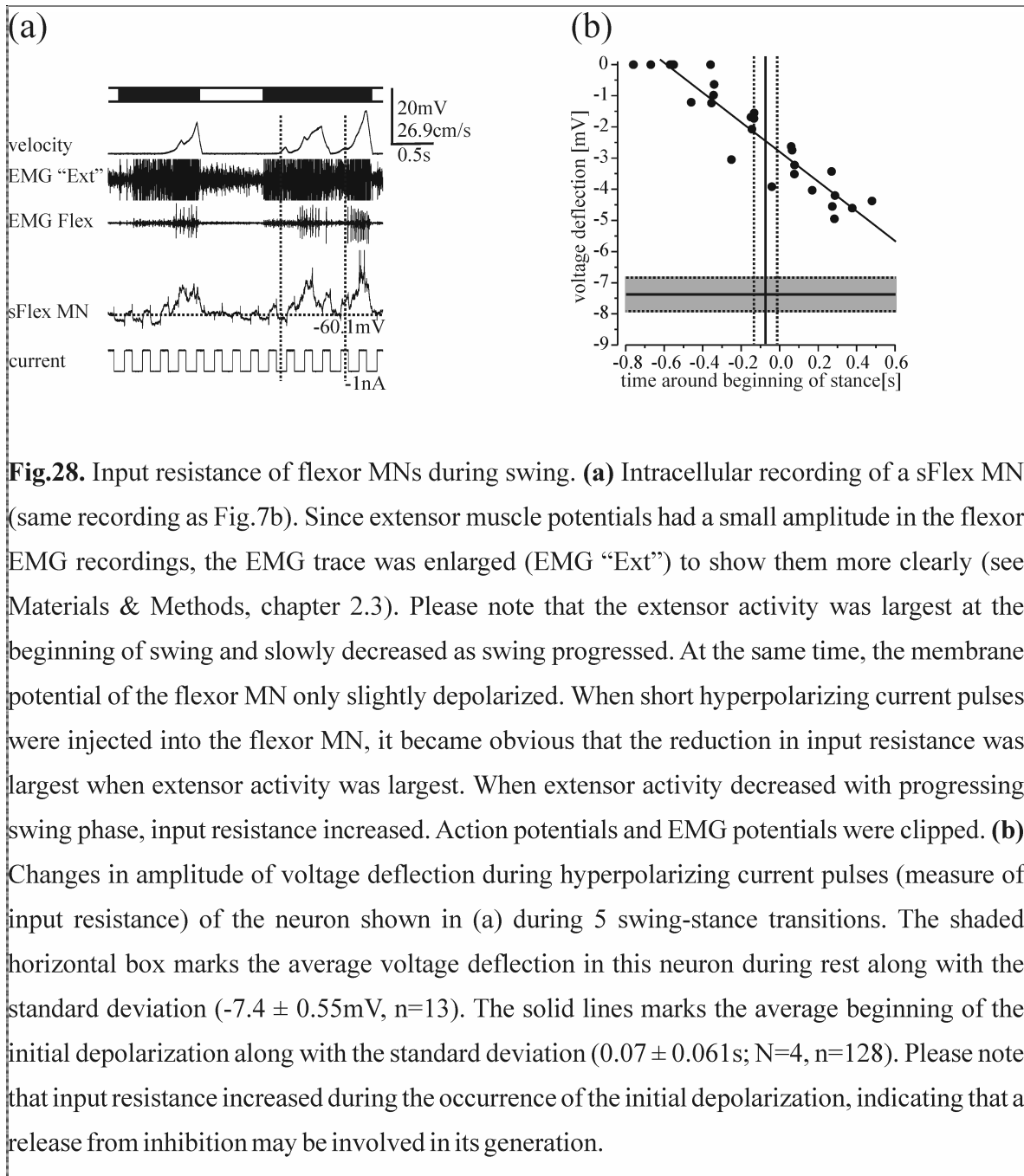


Fig.28. Input resistance of flexor MNs during swing. **(a)** Intracellular recording of a sFlex MN (same recording as Fig.7b). Since extensor muscle potentials had a small amplitude in the flexor EMG recordings, the EMG trace was enlarged (EMG "Ext") to show them more clearly (see Materials & Methods, chapter 2.3). Please note that the extensor activity was largest at the beginning of swing and slowly decreased as swing progressed. At the same time, the membrane potential of the flexor MN only slightly depolarized. When short hyperpolarizing current pulses were injected into the flexor MN, it became obvious that the reduction in input resistance was largest when extensor activity was largest. When extensor activity decreased with progressing swing phase, input resistance increased. Action potentials and EMG potentials were clipped. **(b)** Changes in amplitude of voltage deflection during hyperpolarizing current pulses (measure of input resistance) of the neuron shown in (a) during 5 swing-stance transitions. The shaded horizontal box marks the average voltage deflection in this neuron during rest along with the standard deviation ($-7.4 \pm 0.55\text{mV}$, $n=13$). The solid lines marks the average beginning of the initial depolarization along with the standard deviation ($0.07 \pm 0.061\text{s}$; $N=4$, $n=128$). Please note that input resistance increased during the occurrence of the initial depolarization, indicating that a release from inhibition may be involved in its generation.

3.4.4. Time course of membrane potential modulation in extensor motoneurons

All 17 recorded extensor MNs rapidly depolarized at the transition from stance to swing phase and fired action potentials within 5-30ms (**Fig.29a,b**). The membrane potential modulation recorded during steps with high mean belt velocity (**Fig.29b, left**) was compared to that during steps with low mean belt velocity (**Fig.29b, right**). Both the hyperpolarization at the beginning of stance and the depolarization at the beginning of swing were similar during fast

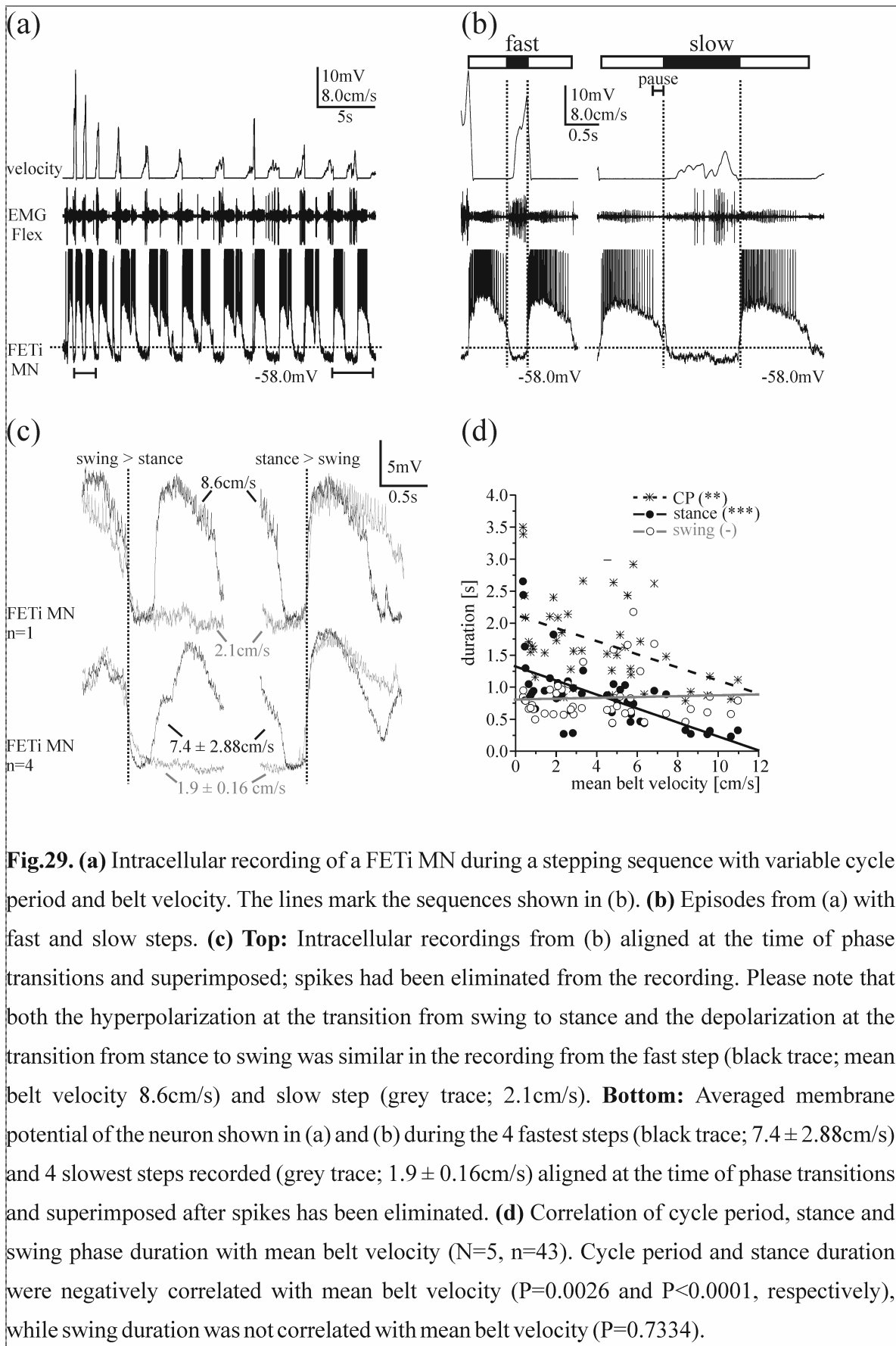


Fig.29. (a) Intracellular recording of a FETi MN during a stepping sequence with variable cycle period and belt velocity. The lines mark the sequences shown in (b). **(b)** Episodes from (a) with fast and slow steps. **(c) Top:** Intracellular recordings from (b) aligned at the time of phase transitions and superimposed; spikes had been eliminated from the recording. Please note that both the hyperpolarization at the transition from swing to stance and the depolarization at the transition from stance to swing was similar in the recording from the fast step (black trace; mean belt velocity 8.6cm/s) and slow step (grey trace; 2.1cm/s). **Bottom:** Averaged membrane potential of the neuron shown in (a) and (b) during the 4 fastest steps (black trace; 7.4 ± 2.88 cm/s) and 4 slowest steps recorded (grey trace; 1.9 ± 0.16 cm/s) aligned at the time of phase transitions and superimposed after spikes has been eliminated. **(d)** Correlation of cycle period, stance and swing phase duration with mean belt velocity (N=5, n=43). Cycle period and stance duration were negatively correlated with mean belt velocity ($P=0.0026$ and $P<0.0001$, respectively), while swing duration was not correlated with mean belt velocity ($P=0.7334$).

and slow steps (**Fig.29c, top**), with the hyperpolarization being slower than the depolarization. The averaged membrane potential modulation during the four steps with the highest mean belt velocity and the four steps with the lowest mean belt velocity recorded from this neuron (**Fig.29c, bottom**) confirm this finding. The results described above were true for all extensor MN recordings.

In 50% of the steps at the end of swing phase there was a pause between the last extensor spike and the onset of flexor activity during which the neuron remained depolarized (**Fig.29b**; duration 0.42 ± 0.360 s; 33 of 66 steps recorded in 6 animals). The duration of stance phase (i.e. flexor activity) and swing phase (i.e. the phase of extensor depolarization which lasted from the first extensor spike until the next flexor activity) was evaluated more closely (**Fig.29d**). As shown before in **Fig.24c**, cycle period was negatively correlated with mean belt velocity. While the duration of the stance phase also showed a negative correlation, the duration of swing phase was independent of mean belt velocity, which shows that extensor activity was more stereotypic than flexor activity in respect to both magnitude and duration.

4. Discussion

4.1. Synaptic drive to leg MNs

The synaptic drive to leg MNs (evaluated in detail in flexor MNs) consists of a tonic depolarization in combination with phasic excitatory and inhibitory inputs. This was investigated in experiments involving measurements of input resistance (**Figs.6; 8**) and intracellular current injection (**Fig.11**). In a previous study on the nature of the synaptic drive to MNs in the single leg preparation (Schmidt et al., 2001), no tonic depolarization of MNs has been reported. This is probably due to the more depolarized average resting membrane potential of flexor MNs (-47 to -61mV) reported by Schmidt et al. (2001). Therefore, the resting membrane potential was closer to the reversal potential of the tonic depolarization, such that it could only be observed when hyperpolarizing current was injected intracellularly (Schmidt et al., 2001; their Fig.4A). In general, the tonic depolarization was greatest when the neuron had a comparably hyperpolarized resting membrane potential. This is consistent with the finding that a tonic depolarization could be observed without current injection only in 64% of the investigated slow MNs but in 86% of the fast MNs recorded from (see chapter 3.2.1), because the latter ones have a more hyperpolarized resting membrane potential (see chapter 3.3.7).

In many other animal model systems has a combination of a tonic depolarization and alternating phasic de- and hyperpolarization of motoneurons been shown to underlie rhythmic MN activity (locust flight: Hedwig & Pearson, 1984; lamprey: Wallén et al., 1985, 1993; tadpole: Soffe & Roberts, 1982; Roberts et al., 1985, 1986; rat: Cazalets et al., 1996; cat: Perreault, 2002). The results also complement earlier experiments investigating the synaptic drive to MNs in other (reduced) preparations of the stick insect (see below).

4.1.1. Tonic depolarization

In the single middle leg preparation of the stick insect, a tonic depolarization was effective in all recorded MN types (**Figs.5; 15-18**). The tonic depolarization began when walking

movements were initiated and ebbed away <1s to >10s after the last step was completed (**Fig.8**). In some cases no tonic depolarization could be observed at rest, while it became apparent when hyperpolarizing current was injected intracellularly. Without current injection, the amplitude of the tonic depolarization in flexor MNs was $3.9\text{mV} \pm 2.2\text{ mV}$ (range:1.3 to 9.5mV; N=18, n=28). The reversal potential of the tonic depolarization in flexor MNs was -49mV and thus more negative than the value of -47 to -32mV reported previously by Ludwar et al. (2005b) for the intersegmental preparation. It was associated with a decrease in input resistance by 26% (N=8, n=15). The value of the reversal potential suggests a mixed Na^+/K^+ -conductance as the ionic basis of the tonic depolarization. The same was suggested by Ludwar et al (2005b), who found a more depolarized reversal potential of -47 to -32mV in mesothoracic MNs during front leg walking. Both the values of the present study and those of Ludwar et al. (2005b) show that the reversal potential of the tonic depolarization is slightly more depolarized than the spike threshold of flexor MNs (-51.2 to -50.1mV, **Fig.23a**). Therefore, the likely role of the tonic depolarization is primarily to depolarize the membrane potential in order to bring the neuron closer to spike threshold and thus increase its excitability for excitatory inputs (**Fig.14a**, see also Ludwar et al., 2005b). Metabotropic effects may be responsible for increasing neuronal excitability, which is supported by the slow time course of decay of the tonic depolarization (up to >10s). Preliminary results by S. Westmark (personal communication) suggest a role of metabotropic acetylcholine receptors. This receptor type is involved in increasing MN excitability in MNs e.g. of the tobacco hornworm *Manduca sexta* (Trimmer & Weeks, 1993; Trimmer, 1994). Three sets of experiments suggest that the tonic depolarization of MNs does not originate from sensory organs but is an ubiquitous centrally generated mechanism to increase neuronal excitability: (i) In experiments where parts of the locomotor network were activated by topical application of the muscarinic agonist pilocarpine (Büschges et al., 1995; Büschges, 1998), a tonic depolarization of MNs that was sculpted by phasic inhibition was responsible for the observed membrane potential modulations. It was discussed that the tonic depolarization was mediated either by muscarinic acetylcholine receptors on the motoneurons (Bai & Sattelle, 1994; Büschges, 1998) or excitatory nonspiking interneurons, which also have been shown to be tonically depolarized during stepping, albeit with a small amplitude (Büschges, 1995; Ludwar et al., 2005b). (ii) In the deafferented thoracic nervous system, switching between antagonistic motoneuron pools can be elicited by tactile stimulation of head or abdomen (Büschges et al., 2004). Also in this preparation, a tonic depolarizing and phasic inhibitory drive are provided by central pattern generating networks (Büschges et al., 2004). (iii) In the previously

described experiments by Ludwar et al. (2005b), a tonic depolarization of flexor motoneurons (~4mV at rest) could be observed in the deafferented mesothoracic ganglion during front leg walking. In summary, these experiments suggest that the tonic depolarization is generated during arousal of the animal by central networks and mediated at least partly by nonspiking interneurons (Ludwar et al., 2005b).

4.1.2. Phasic modulation

In the experiments mentioned above, both a tonic depolarization and phasic inhibition was shown to originate from central pattern generating networks. A phasic excitation was never observed in deafferented (Büschges et al., 2004) or pharmacologically activated preparations (Büschges, 1998), suggesting that it may originate from other sources, e.g. local sensory signals and coordinating pathways from other segments. In my experiments, the amplitude of phasic excitation of flexor MNs increased with stepping velocity, which is indicative of a contribution of afferent feedback (**Figs.25a,b; 26a**). A phasic excitation of motoneurons by local sense organs has been shown previously in the stick insect for the femoral campaniform sensilla (Schmitz & Stein, 2000; Akay et al., 2001) and the femoral chordotonal organ (Bässler, 1988). These pathways act either directly (monosynaptically) or via intercalated (spiking or nonspiking) interneurons on the MNs (reviewed in Burrows, 1996; Bässler & Büschges 1998; Zill et al., 2004). A phasic modulation originating from intersegmental pathways has also been identified in experiments where MNs were recorded in the deafferented mesothoracic ganglion during front leg walking, however with much smaller amplitude (0.5 to 3 mV; Ludwar et al., 2005b). Since pharmacological activation of the prothoracic CPG by pilocarpine does not lead to coupled phasic modulations in mesothoracic MNs (Ludwar et al., 2005a), the intersegmental phasic excitation, just like the local phasic excitation, seems to depend on signaling from sense organs and not on the CPG networks. In case of the intersegmental afferent pathways, no monosynaptic connections to MNs have been identified in the stick insect, but intersegmental interneurons have been identified morphologically and physiologically that receive inputs from the femoral chordotonal organ (Brunn & Dean, 1994; Büschges, 1989; see discussion in Ludwar et al., 2005b).

4.2. Recruitment of slow and fast flexor MNs

In the single leg preparation of the stick insect *Cuniculina impigra* I studied the influence of friction of a treadmill on the activity of the flexor tibiae motoneurons. Under conditions of increased friction, the summed activity of the flexor tibiae muscle as well as the spike activity of individual slow, semifast and fast flexor motoneurons increased. Also, I collected evidence that motoneurons innervating the flexor tibiae muscle receive substantial common synaptic inputs from premotor interneurons during the walking-like movements investigated.

4.2.1. Activity control in slow and fast Flex-MNs during stance

Intracellular and electromyographic recordings show that fast motoneurons of the flexor tibiae were recruited later during stance phase than sFlex-MNs (**Figs.19a,b; 20a**). Albeit the delayed activation of the fFlex-MNs, individual intracellular recordings (**Fig.20a**) reveal that the membrane potential of both fast and slow motoneurons started to depolarize at the beginning of stance phase. The average membrane potential of fast and slow Flex-MNs during stance phase also shows a very similar time course (**Fig.20b**). This indicates that the two motoneuron populations were synchronously excited throughout stance phase, probably by common sources of synaptic drive. In the locust, common synaptic drive from premotor interneurons onto motoneurons has been shown during reflex movements as synchronized EPSPs in slow and fast motoneurons innervating the same muscle (Burrows & Horridge, 1974; Wilson, 1979). Further evidence derives from the similarity between the SR-EMG and the time course of the membrane potential of the fFlex-MNs (**Fig.21**). In the example shown, no action potentials from fFlex-MNs were detectable in the EMG recording. Therefore, it can be assumed that the value of the SR-EMG was determined solely by the activity of slow and probably semifast motoneurons. Thus, the fFlex-MN must share common inputs with the motoneuron population contributing to the muscle contraction.

Considering the similarity in membrane potential depolarization and the value of the spike threshold in fFlex and sFlex-MNs, the more negative resting membrane potential of the fFlex-MNs ($-67.2 \pm 4.3\text{mV}$ compared to $-61.8 \pm 7.5\text{mV}$; cf. Schmidt et al., 2001) is likely to contribute greatly to their delayed activation. In case of the fFlex-MNs, a stronger and longer lasting depolarization is required for the membrane potential to reach the threshold for the generation of action potentials. Thus, the difference in membrane potential provides a mechanism for successive recruitment of motoneurons in response to a common and

synchronous excitatory input due to a difference in intrinsic properties (cf. Burrows, 1996, pp. 65-66).

One cellular property known to influence the excitability of motoneurons in vertebrates as well as invertebrates is motoneuron size ('size principle'; cat: Henneman et al., 1965; reviewed in Pinter, 1990; lobster: Davis, 1971). Also in invertebrates, fast motoneurons are known to be larger in size than slow motoneurons. For example, they have a larger soma size and axonal diameter than slow motoneurons (e.g. stick insect: Storrer et al., 1986; locust: Burrows & Hoyle, 1973; Hoyle & Burrows, 1973; lobster: Davis, 1971). Fast motoneurons have larger conduction velocities than slow motoneurons (stick insect: Bässler, 1984; Hess & Büschges, 1997). Because of their larger size, fast motoneurons are less susceptible to excitation either by intracellular current injection or natural synaptic input (stick insect: Debrodts & Bässler, 1990; locust: Burrows & Horridge, 1974; Burrows & Hoyle, 1973; Burrows, 1980; lobster: Davis, 1971; vertebrates: Henneman et al. 1965) than the slow motoneurons, which has been discussed as the primary reason for their delayed recruitment compared to slow motoneurons. The present data add to these differences a physiological factor that is capable of explaining the delay in activity of fast motoneurons. Future studies will have to deal with the intrinsic mechanisms underlying the different resting membrane potential.

4.2.2. Influence of belt friction

The activity of the flexor tibiae muscle as determined by the value of the SR-EMG increased under conditions of increased belt friction (**Fig.22a**). When motoneuron activity was compared during similar steps the elevated activity became most obvious (**Fig.22b**). An increase in the rate of action potentials in both slow and fast motoneurons of the flexor tibiae contributed to the elevated muscle activity (**Fig.22c**). In summary, under all conditions tested the motor output of the leg was adjusted to belt friction. The major factor appears to be alterations in the magnitude of synaptic drive to the whole population of flexor motoneurons investigated in the present study. Although individual premotor neurons are known in insects that make specific connections with only subset of motoneurons innervating a given leg muscle (e.g. locust: Burrows, 1980), such differential premotor innervation does not seem to result in differing synaptic drive to leg motoneurons during the execution of active leg movements (cf. deductions of Burrows & Hoyle, 1973). Consequently it currently appears that a large proportion of synaptic drive is shared by the whole population of flexor

motoneurons with intrinsic cellular properties being responsible for their differential, i.e. progressive recruitment.

This uniformity of synaptic inputs to slow and fast motoneurons may be state-dependent. In the stick insect two distinct behavioral states can be distinguished ('active' and 'inactive' animal; Bässler, 1993). Debrodt and Bässler (1990) found that fast motoneurons of the flexor tibiae in *Extatosoma tiaratum* were preferentially excited by fast stimuli applied to the femoral chordotonal organ (fCO), while slow motoneurons showed a larger response to slow stimulus velocities. In contrast to my experimental situation, these experiments were conducted in 'inactive animals'. Pfeiffer (1991) found that flexor motoneurons showed different responses to stimuli applied to the fCO in the 'inactive' animal, while in the 'active' animal the responses of slow and fast motoneurons were very similar. These findings suggest that in the resting animal differential premotor innervation may play an important role, while during locomotion common synaptic inputs may prevail.

4.3. Control of stepping velocity

I analyzed the changes in step parameters and motoneuronal activity that occurred during variations in stepping velocity of the stick insect middle leg on a treadmill. As reported previously for the intact walking animal (Wendler, 1964; Graham, 1972), changes in stepping speed were accompanied by changes in cycle period, such that fast stepping velocities were correlated with short cycle periods. Intracellular recordings revealed that during fast steps flexor MNs showed a faster depolarization and stronger activation. Interestingly, alterations in time course of membrane potential related to changes in stepping velocity were almost exclusively limited to stance phase (i.e. flexor) MNs, while there were no systematic alterations detectable in swing phase (i.e. extensor) MNs. This indicates that stepping velocity is mediated by phasic neural mechanisms effective only during the generation of the stance phase motor output. Most importantly, I did not detect any evidence for both MN pools being affected in a similar way during changes in stepping velocity, for example by tonic background excitation that increases excitability of MNs during high motor output. It therefore appears that the mechanisms responsible for generating changes in stepping velocity specifically affect the neural subsystem generating stance phase motor output, but not (or only subtly) the part of the premotor network which generates the swing phase in the single middle leg.

4.3.1. Cycle period of single leg stepping movements and varying stepping velocity

During steps with high mean belt velocity, both the cycle period (**Figs.24c; 29d**) and the duration of flexor MN activity (i.e. stance) was short, while the duration of extensor activity (i.e. swing) remained unchanged (**Fig.29d**). Also in freely moving stick insects a short cycle period contributes to high walking speeds, and the decrease in cycle period is mainly due to a decrease in stance duration (Wendler, 1964; Graham, 1972).

I have shown that swing duration did not correlate with mean belt velocity. As I have furthermore shown that mean belt velocity in the single middle leg correlates with cycle period, the data imply that swing phase duration is independent of cycle period. This result differs from Fischer et al (2001) who concluded on the basis of EMG recordings only that the duration of both stance phase and swing phase depended on cycle period (their Fig.3D). In a model calculation, Cruse (1983) discussed similar findings that were obtained on crustacean

walking. A model was put forward wherein the seemingly discrepant results were explained by differences in walking conditions. Under small load, swing duration in the model was proportional to cycle period. Under high load, a parameter called *central excitation* was high, such that the swing phase muscle activity saturated and swing duration was independent of cycle period (Cruse, 1983). However, the treadmill used in my investigation had a lower inertia than the one used by Fischer et al. (2001), so the independence of swing duration that I found cannot be explained with differences in load alone. A comparison of the results is further complicated by the fact that Fischer et al. (2001) did not monitor belt velocity. Since it has been shown that slower steps are generated on high inertia treadmills (Gabriel et al., 2003) it is probable that belt velocities were shifted towards lower values in their investigation.

4.3.2. Time course of membrane potential modulation of flexor motoneurons

My analysis proceeded to determine constant and variable features in the time course of membrane potential modulation of flexor during walking movements. In all flexor MNs recorded the membrane potential depolarization as well as mean and maximum spike frequency was correlated with mean belt velocity (**Fig.26a,b**). This indicates that during stance flexor MNs receive common synaptic drive (cf. chapter 3.3.5) and (if they are activated above spike threshold) thereby contribute to the control of stepping velocity during stance phase. In this, the results are similar to the flexor MN activity under conditions of varying load (**Fig.22**).

Interestingly, there appear to be two distinct phases of depolarization in the activation of flexor MNs during stance phase, i.e. an initial depolarization at the beginning of flexor activity and a subsequent fast and large depolarization that changes with stance velocity (**Fig.27c,d**). All flexor MNs recorded showed a similar initial depolarization, which for some MNs (i.e. the slow flexor MNs due to their earlier recruitment; see chapter 3.3) was sufficient to bring them above action potential threshold and initialized the flexor burst. For individual MNs the time course of this depolarization at the beginning of stance was similar during slow and fast steps. I could show that it occurred well after the maximal conductance in the flexor MNs during swing (**Fig.28a,b**). This maximal conductance is generated by inhibitory synaptic inputs (chapter 3.2). In this phase the input resistance in flexor MNs was still increasing (**Fig.28b**). On one hand excitatory synaptic inputs are conceivable that are related to touch

down of the leg, e.g. from tarsal receptors (Laurent & Hustert, 1988) or campaniform sensilla on the leg (Newland & Emptage, 1996; Akay et al., 2001). On the other hand however, some arguments point towards a different origin. I believe that the initial depolarization is the result of an interplay between a release from the inhibition that was active during leg swing, and the state-dependent tonic depolarization in leg MNs which persists during stepping activity (Büschges et al. 2004; Ludwar et al. 2005b; see chapter 3.2) for the following reasons. (i) The initial depolarization developed comparably slowly and, like the tonic depolarization, was independent of stance velocity (**Figs.24a; 25a; 27a**). (ii) It occurred although the input resistance of flexor MNs was still increasing from its minimal values during leg swing, indicating that it was not likely generated by an additional phasic synaptic conductance. Even though I do not know the cause of the initial depolarization of flexor MNs at the beginning of leg stance, the fact that it is independent of stepping velocity has important implications for the control of stance velocity. It indicates that at this time during the step cycle no neural inputs to the flexor MNs were active that caused a differentiation towards slow or fast stance phases.

The second depolarization of flexor MNs varied with stepping velocity, i.e. it occurred earlier and was larger for fast steps compared to slower steps (**Fig.27d**). It was this depolarization by which fast flexor MNs were activated above action potential threshold and that therefore contributed mostly to alterations of stepping velocity. There are different possibilities for how this second depolarization is generated. Previous investigations show that sensory signals from strain and movement sensors reinforce flexor MN activation during voluntary and locomotor movements (Bässler, 1986, 1988; Schmitz et al., 1995; Akay et al., 2001; summary in Bässler & Büschges, 1998), as has been shown in a variety of walking systems (for summary see Pearson, 1993; Büschges & El Manira, 1998). At present it is not known what other sources of synaptic inputs are contributing to the control of flexor MN activity. No evidence exists for a contribution of phasic excitatory synaptic drive from central pattern generating networks of the FT-joint. On the contrary, only phasic inhibitory synaptic inputs from central sources are known that could contribute to patterning of MN activity (Büschges, 1998; Büschges et al., 2004). Given that some of the synaptic drive that controls flexor MN activation arises from sense organs, it is quite conceivable that changes in the effectiveness of these pathways may alter rate and amplitude of activation in flexor MNs. Such alterations will occur automatically with changes in stance velocity, e.g. by faster flexion of the joint or greater forces generated by the flexor muscle. A mechanism would still be needed, however, through which the leg muscle control system can control the effectiveness or gain of these

sensory feedback pathways in order to achieve a stronger motor output. For changing cycle period in walking, similar solutions via sensory feedback from the limb have recently been discussed for the cat (Yakovenko et al., 2005). One possible mechanism is presynaptic inhibition of sensory afferents, which has been investigated in great detail with respect to its putative function in gain control (Burrows & Matheson, 1994; Sauer et al., 1997; for summary see Büschges & El Manira, 1998; Clarac et al., 2000; Nusbaum et al., 1997). It is conceivable that by a reduction in presynaptic inhibition the gain of the reinforcing sensory pathways during stance increases and larger, more rapid depolarizations of flexor MNs are generated. Further experiments involving recordings from the major sensory afferents, i.e. those of the campaniform sensilla and the femoral chordotonal organ, will be necessary for an unequivocal conclusion. In summary, my results strongly suggest that those synaptic inputs to leg motoneurons that determine the stance phase motor output and thereby the stepping velocity are only activated during an already ongoing stance phase motor output.

4.3.3. Antagonistic synaptic drive to flexor and extensor MNs and organization of the leg muscle control system for the single leg

During the transition of step phases, particular antagonistic features were observed in the membrane potential modulations of flexor and extensor MNs (**Fig.30**). At the transition from stance to swing phase, the membrane potential of both MN pools rapidly changed, i.e. flexor MNs were hyperpolarized and extensor MNs were depolarized rapidly. On the other hand, at the transition from swing to stance phase both the depolarization of flexor MNs and the hyperpolarization of extensor MNs was generally slower. Interestingly, in studies where vibration stimuli were applied to the femoral chordotonal organ in order to induce phase transitions, the latency for the transition from flexor to extensor activity was shorter than from extensor to flexor activity (Bässler et al., 2003). This suggests that neuronal mechanisms exist in the animal that facilitate a particularly fast transition from flexor to extensor activity, the functional meaning of which remains to be investigated.

There was no close correlation between mean belt velocity (which represents the level of flexor activity) and trough potential of extensor MNs during stance (**Fig.26c**). This may be due to the small difference of the membrane potential to the reversal potential of the inhibitory conductance (cf. flexor MNs in chapter 3.2.3). Therefore, both weak and strong inhibition could hyperpolarize the extensor MNs to the same value.

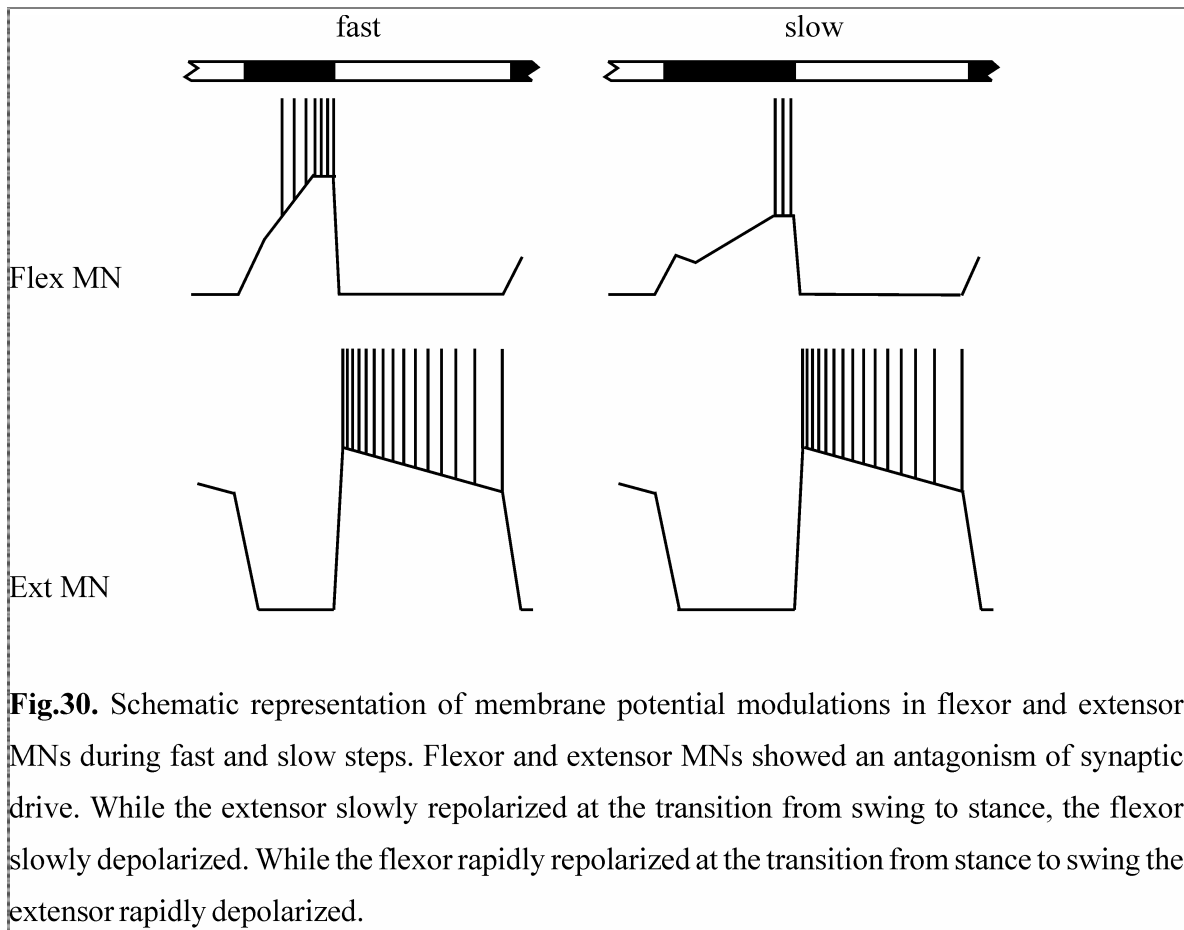


Fig.30. Schematic representation of membrane potential modulations in flexor and extensor MNs during fast and slow steps. Flexor and extensor MNs showed an antagonism of synaptic drive. While the extensor slowly repolarized at the transition from swing to stance, the flexor slowly depolarized. While the flexor rapidly repolarized at the transition from stance to swing the extensor rapidly depolarized.

The antagonistic nature of the synaptic drive to flexor and extensor MNs is supported by two observations: (i) For gross differences the flexor activation level during stance was correlated to some extent with the level of hyperpolarization of extensor MNs (**Fig.26e**). (ii) Measurements of input resistance qualitatively show that the level of inhibition of flexor MNs during swing was correlated with extensor activity (**Fig.28a**). Together, this raises the possibility that both antagonistic MN pools share common premotor elements that contribute to phase transitions. Indeed, in the stick insect mesothoracic ganglion local premotor nonspiking interneurons exist that provide excitatory drive to one pool of MNs, e.g. the extensor MNs and inhibitory synaptic drive to the antagonistic pool, i.e. the flexor MNs, and *vice versa* (Büschges, 1995; Büschges & Schmitz, 1991; Sauer et al., 1996). In another orthopteran insect (i.e. the locust), MNs of antagonistic pools have been shown to receive “mirror-image synaptic drive” from certain premotor interneurons (Burrows & Horridge, 1974; summary in Burrows, 1996). In a functional context this may be useful, because co-contractions of antagonistic muscles are both energetically unfavorable and potentially harmful for the animal (Cruse 2002). In order to further analyze the nature of the antagonistic

drive from premotor elements, paired recordings from flexor and extensor MNs will be necessary.

Despite the basic antagonistic nature of the synaptic drive to tibial MNs during the generation of stepping movements (see above), there appears to be no influence between stance and swing phase generation in such a way that the magnitude of motor output during stance would influence the subsequent swing phase. While flexor activation was strongly modulated with changing step velocity, no correlated alterations were found in the pattern of extensor MN activation. The time course of the transitions between the stepping phases was not affected by stance phase velocity either. A possible explanation for this has already been mentioned above: in a computational study Cruse (1983) proposed that due to high central excitation under conditions of high load swing phase motor output is always maximal, implying that MN activity is also saturated and independent of cycle period and thus to step velocity. I cannot rule out this possibility. However, the treadmill used in my study has a rather low moment of inertia (see Materials and Methods, chapter 2.2). Also, in the single leg preparation both fast and very slow steps are generated (**Fig.25a,c**). Thus, the parameter that corresponds to the central excitation (Cruse, 1983), which together with load determines both stance and swing duration in his model, appears not always to be maximal but to be rather variable. I therefore assume that the stereotypic nature of extensor MN activity during swing is not due to saturation effects.

The results are interesting also in the light of current conclusions concerning the organization of the stick insect walking system, as derived from behavioral studies on intact walking animals (e.g. Cruse & Müller, 1984; Schmitz et al., 2000; see also Cruse, 2002). It has been reported in the stick insect that, depending on the actual magnitude of motor output during stance, i.e. comparing uphill vs. downhill walking, the velocity of the subsequent swing phase was altered (Schmitz et al., 2000). This result corroborated considerations about a very close coupling of the neural networks in charge of generating stance and swing phase (Cruse, 2002). My intracellular analysis of leg motoneuron activity in single leg stepping indicates that such influence of the magnitude of motor output during stance and the subsequent swing phase may be not a property of the local pattern generating networks of a leg, but rather arise from intersegmental sources. Both phasic and tonic influences are known to act between the legs of a walking stick insect (Cruse et al., 1998; Ludwar et al., 2005a,b). Thus, it may well be that the influence of stance phase on the subsequent swing phase arises from the cooperative action of the neural networks coordinating the walking movements of the six legs.

Literature

- Akay T., Bässler U., Gerhartz P. and Büschges A. (2001). The role of sensory signals from the insect coxa-trochanteral joint in controlling motor activity of the femur-tibia joint. *J Neurophys* **85**:594-604.
- Akay T., Haehn S., Schmitz J. and Büschges A. (2004). Signals from load sensors underlie interjoint coordination during stepping movements of the stick insect leg. *J Neurophys* **92**:42-51.
- Altman JS. and Kien J. (1979) Suboesophageal neurons involved in head movements and feeding in locusts. *Proc R Soc Lond B* **205**:209-27.
- Angstadt JD., Grassmann JL., Theriault KM. and Levasseur SM. (2005). Mechanisms of postinhibitory rebound and its modulation by serotonin in excitatory swim motor neurons of the medicinal leech. *J Comp Physiol A* **191**:715-32.
- Arshavsky YI., Deliagina TG., Orlovsky GN., Panchin YV., Popova LB. and Sadreyev RI. (1998). Analysis of the central pattern generator for swimming in the mollusk *Clione*. *Ann N Y Acad Sci* **860**:51-69.
- Ayers JL. and Davis WJ. (1974). Neuronal control of locomotion in the lobster, *Homarus americanus*. I. Motor program for forward and backward walking. *J Comp Physiol* **115**: 1-27.
- Bässler U. (1983) Neural basis of elementary behavior in stick insects. Springer Verlag, Berlin, New York.
- Bässler U. (1984). A movement generated in the peripheral nervous system: rhythmic flexion by autotomized legs of the stick insect *Cuniculina impigra*. *J Exp Biol* **111**:191-99.
- Bässler U. (1986). Afferent control of walking movements in the stick insect *Cuniculina impigra*. II. Reflex reversal and the release of swing phase in the restrained foreleg. *J Comp Physiol A* **158**:351-62.
- Bässler U. (1988). Functional principles of pattern generation for walking movements of stick insect forelegs: the role of the femoral chordotonal organ afferences. *J Exp Biol* **136**:125-47.
- Bässler U. (1993). The walking- (and searching-) pattern generator of stick insects, a modular system composed of reflex chains and endogenous oscillators. *Biol Cybern* **69**:305-17.
- Bässler U. and Büschges A. (1998). Pattern generation for stick insect walking movements - multisensory control of a locomotor program. *Brain Res Rev* **27**:65-88.
- Bässler U. and Stein W. (1996). Contributions of structure and innervation pattern of the stick insect extensor tibiae muscle to the filter characteristics of the muscle-joint system. *J Exp Biol* **199**:2185-98.

- Bässler U. and Storrer J. (1980). The neural basis of the femur-tibia-control-system in the stick insect *Carausius morosus*. I: Motoneurons of the extensor tibiae muscle. *Biol Cybern* **38**:107-14.
- Bässler U. and Wegener U. (1983). Motor output of the denervated thoracic ventral nerve cord in the stick insect *Carausius morosus*. *J Exp Biol* **105**:127-45.
- Bässler U, Sauer AE. and Büschges A. (2003). Vibration signals from the FT joint can induce phase transitions in both directions in motoneuron pools of the stick insect walking system. *J Neurobiol* **56**:125-38.
- Bässler D., Büschges A., Meditz S. and Bässler U. (1996). Correlation between muscle structure and filter characteristics of the muscle-joint system in three orthopteran insect species. *J Exp Biol* **199**:2169-83.
- Bai D and Sattelle DB. (1994). Muscarinic acetylcholine receptors on an identified motor neurone in the cockroach, *Periplaneta americana*. *Neurosci Lett* **175**:161-5.
- Bal T., Nagy F. and Moulins M. (1988). The pyloric central pattern generator in crustacea: A set of conditional neuronal oscillators. *J Comp Physiol* **163**:715-27.
- Bentley D. (1977). Control of cricket song patterns by descending interneurons. *J Comp Physiol A* **116**:19-38
- Blickhan R. (1996). Motorische Systeme bei Vertebraten. In: *Neurowissenschaft*; Dudel J., Menzel R. and Schmidt RF. (eds). Springer Verlag; pp. 191-212.
- Brizzi L., Meunier C., Zytnicki D., Donnet M., Hansel D., Lamotte d'Incamps B. and van Vreeswijk C. (2004). How shunting inhibition affects the discharge of lumbar motoneurons: a dynamic clamp study in anaesthetized cats. *J Physiol* **558**:671-83.
- Brown TG. (1911). The intrinsic factors in the act of progression in the mammal. *Proc R Soc Lond B* **84**:308-319.
- Brunn J. and Dean J. (1994). Intersegmental and local interneurons in the metathorax of the stick insect *Carausius morosus* that monitor middle leg position. *J Neurophysiol* **72**:1208-19.
- Buchanan JT., Brodin L., Dale N. and Grillner S. (1987). Reticulospinal neurons activate excitatory amino acid receptors. *Brain Res* **408**:321-5.
- Bucher D., Akay T., DiCaprio RA. and Büschges A (2003). Interjoint coordination in the stick insect leg-control system: the role of positional signaling. *J Neurophysiol* **89**:1245-1255.
- Büschges A. (1989). Processing of sensory input from the femoral chordotonal organ by spiking interneurons of the stick insect. *J Exp Biol* **144**:81-111.
- Büschges A. (1998). Inhibitory synaptic drive patterns motoneuronal activity in rhythmic preparations of isolated thoracic ganglia in the stick insect. *Brain Res* **783**:262-71.

- Büschges A. (2005). Sensory control and organization of neural networks mediating coordination of multisegmental organs for locomotion. *J Neurophysiol* **93**:1127-35.
- Büschges A. and El Manira A. (1998). Sensory pathways and their modulation in the control of locomotion. *Curr Opin Neurobiol* **8**:733-9.
- Büschges A., Schmitz J. and Bässler U. (1995). Rhythmic patterns in the thoracic nerve cord of the stick insect induced by pilocarpine. *J Exp Biol* **198**:435-56.
- Büschges A., Ludwar BC., Bucher D., Schmidt, J. and DiCaprio, RA. (2004). Synaptic drive contributing to rhythmic activation of motoneurons in the deafferented stick insect walking system. *Eur J Neurosci* **19**:1856-62.
- Burns MD. (1973). The control of walking in Orthoptera. I. Leg movements in normal walking. *J Exp Biol* **58**:45-58.
- Burrows M. 1980. The control of sets of motoneurons by local interneurons in the locust. *J Physiol* **298**:213-33.
- Burrows M. (1996). *The neurobiology of an insect brain*. Oxford University Press, New York; pp 48-68.
- Burrows M. and Horridge GA. (1974). The organization of inputs to motoneurons of the locust metathoracic leg. *Phil Trans R Soc Lond B* **269**:49-94.
- Burrows M. and Hoyle G. (1973). Neural mechanisms underlying behavior in the locust *Schistocerca gregaria*. III. Topography of limb motoneurons in the metathoracic ganglion. *J Neurobiol* **4**:167-86.
- Burrows M. and Matheson T. (1994). A presynaptic gain control mechanism among sensory neurons of a locust leg proprioceptors. *J Neurosci* **14**:272-82.
- Buss RR. and Drapeau P. (2001). Synaptic drive to motoneurons during fictive swimming in the developing zebrafish. *J Neurophysiol* **86**:197-210.
- Cazalets J.-R., Borde M. and Clarac F. (1996). The synaptic drive from the spinal locomotor network to motoneurons in the newborn rat. *J Neurosci* **16**:298-306.
- Chrachri A. and Clarac F. (1990). Fictive locomotion in the fourth thoracic ganglion of the crayfish, *Procambarus clarkii*. *J Neurosci* **10**:709-19.
- Clarac F. and Chasserat C. (1986). Basic processes of locomotor coordination in the rock lobster. I. Statistical analysis of walking parameters. *Biol Cybern* **55**:159-70.
- Clarac F., Cattaert D. and Le Ray D. (2000). Central control components of a 'simple' stretch reflex. *Trends Neurosci* **23**:199-208.
- Clark JT. (1974). *Stick and Leaf Insects*. Barry Shurlock & Co. Ltd., Winchester, UK.

- Cooper RL. and Ruffner ME. (1998). Depression of Synaptic Efficacy at Intermolt in Crayfish Neuromuscular Junctions by 20-Hydroxyecdysone, a Molting Hormone. *J Neurophysiol* **79**:1931–41.
- Cruse H. (1976): On the function of the legs in the free walking stick insect *Carausius morosus*. *J Comp Physiol* **112**, 235-62.
- Cruse H. (1983). The influence of load and leg amputation upon coordination in walking crustaceans: A model calculation. *Biol Cybern* **49**:119-25.
- Cruse H. (1990). What mechanisms coordinate leg movement in walking arthropods? *Trends Neurosci* **13**:15-21.
- Cruse H. (2002). The functional sense of central oscillations in walking. *Biol Cybern* **86**:271-80.
- Cruse H. and Müller U. (1984). A new method measuring leg position of walking crustaceans shows that motor output during return stroke depends on load. *J Exp Biol* **110**:319-22.
- Cruse H. and Pflüger H.-J. (1981). Is the position of the femur-tibia joint under feedback control in the walking stick insect? II. Electrophysiological recordings. *J Exp Biol* **92**:97-107.
- Cruse H., Dürr V. and Schmitz J. (2003). Control of hexapod walking in biological systems. In: *Proceedings of the 2nd Int. Symposium on Adaptive Motion of Animals and Machines*, Kyoto 2003. Tsuchiya, Ishiguro, Osuka, Kimura (eds.).
- Cruse H., Bartling Ch., Cymbalyuk G., Dean, J. and Dreifert M. (1994) A neural net controller for a six-legged walking system. In: *From perception to action conference* Gaussier P. and Nicoud JD. (eds). IEEE Computer Society Press, Los Alamitos, CA; pp. 55-65.
- Cruse H., Kindermann T., Schumm M., Dean J. and Schmitz J. (1998). Walknet-a biologically inspired network to control six-legged walking. *Neural Netw* **11**:1435-47.
- Dale N. (1986). Excitatory synaptic drive for swimming mediated by amino acid receptors in the lamprey. *J Neurosci* **6**:2662-75.
- Davis WJ. 1971. Functional significance of motoneuron size and soma position in swimmeret system of the lobster. *J Neurophysiol* **34**:274-288.
- Debrodt B. and Bässler U. (1989). Motor neurones of the flexor tibiae muscle in phasmids. *Zool Jb Physiol* **93**:481-94.
- Debrodt B. and Bässler U. (1990). Responses of flexor motor neurons to stimulation of the femoral chordotonal organ of the phasmid *Extatosoma tiaratum*. *Zool Jb Physiol* **94**:101-19.
- Dürr V. Krause A., Schmitz J. and Cruse H. (2002). Neuroethological concepts and their transfer to walking machines. *Int J Robotics Res* **22**:151-67.

- Dürr V., Schmitz J. and Cruse H. (2004). Behaviour-based modelling of hexapod locomotion: linking biology and technical application. *Arth Struct Devel* **33**:237-50.
- Ekeberg Ö., Blümel M. and Büschges A. (2004):Dynamic simulation of insect walking. *Arth Struct Devel* **33**: 287-300.
- Fischer H., Schmidt J., Haas R. and Büschges A. (2001). Pattern generation for walking and searching movements of a stick insect leg. I. Coordination of motor activity. *J Neurophysiol* **85**:341-53.
- Friesen WO. (1994). Reciprocal inhibition: A mechanism underlying oscillatory animal movements. *Neurosci Biobehav Rev* **18**:547-53.
- Gabriel JP., Scharstein H., Schmidt J. and Büschges A. (2003). Control of flexor motoneuron activity during single leg walking of the stick insect on an electronically controlled treadmill. *J Neurobiol* **56**:237-51.
- Getting PA. and Dikin MS. (1985). Mechanisms of pattern generation underlying swimming in *Tritonia*. IV. Gating of central pattern generator. *J Neurophysiol* **53**:466-80.
- Gewecke M. (1995). *Physiologie der Insekten*. Gustav Fischer Verlag, Stuttgart, Germany.
- Gordon J. (1991). Spinal mechanisms of motor coordination. In: *Principles of neural science*; E. R. Kandel, J. H. Schwartz, and T. M. Jessell (eds). Appleton and Lance, Norwalk, USA; pp. 581-95.
- Graham D. (1972). A behavioural analysis of the temporal organization of walking movements in the 1st instar and adult stick insect (*Carausius morosus*). *J Comp Physiol* **81**:23-52.
- Graham D. (1979a). The effects of circumoesophageal lesions on the behavior of the stick insect *Carausius morosus*. I. Cyclic behaviour patterns. *Biol Cybern* **32**:139-45.
- Graham D. (1979b). The effects of circumoesophageal lesions on the behavior of the stick insect *Carausius morosus*. II. Changes in walking coordination.. *Biol Cybern* **32**:147-52.
- Graham D. (1985). Pattern and control of walking in insects. *Adv Insect Physiol* **18**:31-140.
- Graham D. and Cruse H. (1981). Coordinated walking of stick insects on a mercury surface. *J Exp Biol* **92**:229-41.
- Grillner S. (1981) Control of locomotion in bipeds, tetrapods, and fish, In: Handbook of Physiology. Sect 1, Vol 2, *The Nervous System, Motor Control*. Brooks VB. (ed.). American Physiology Society, Maryland, Waverly Press; pp. 1179-236.
- Grillner S. (2003). The motor infrastructure: from ion channels to neuronal networks. *Nat Rev Neurosci* **4**:573-86.
- Grillner S, Zangger P. (1975). How detailed is the central pattern generation for locomotion? *Brain Res.* **88**:367-71.

- Grillner S., Georgopoulos AP. and Jordan LM. (1997). Selection and initiation of motor behavior. In: *Neurons, Networks, and Motor Behavior*. Stein PSG., Grillner S., Selverston AI. and Stuart DG. (eds). MIT Press, Cambridge, USA; pp 3-19.
- Halbertsma JM. (1983). The stride cycle of the cat: the modelling of locomotion by computerized analysis of automatic recordings. *Acta Physiol Scand*, Suppl.**521**:1-75.
- Heckmann CJ., Gorassini MA. and Bennet DJ. (2005). Persistent inward currents in motoneuron dendrites: implications for motor output. *Muscle Nerve* **31**:135-56.
- Hedwig B. (2000). Control of cricket stridulation by a command neuron: efficacy depends on behavioural state. *J Neurophysiol* **83**:712-22.
- Hedwig B. and Pearson KG. (1984). Patterns of synaptic input to identifies flight motoneurons in the locust. *J Comp Physiol A* **154**:745-60.
- Heinrich R. (2002). Impact of descending brain neurons on the control of stridulation, walking and flight in orthoptera. *Microsc Res Tech* **65**:292-301.
- Heinrich R., Wenzel B. and Elsner N. (2001). A role for muscarinic excitation: control of specific singing behavior by activation of the adenylate cyclase pathway in the brain of grasshoppers. *Proc Natl Acad Sci USA* **98**:9919-23.
- Henneman E., Somjen G., and Carpenter DO. (1965) Functional significance of cell size in spinal motoneurons. *J Neurophysiol* **28**:560-80.
- Hess D and Büschges A. (1997). Sensorimotor pathways involved in interjoint reflex action of an insect leg. *J Neurobiol* **33**:891-913.
- Hess D. and Büschges A. (1999) Role of proprioceptive signals from the stick insect femur-tibia joint in patterning motoneuronal activity of an adjacent leg joint. *J Neurophysiol* **81**:1856-65.
- Hill AA., Masino MA. and Calabrese RL. (2003). Intersegmental coordination of rhythmic motor patterns. *J Neurophysiol* **90**:531-8.
- Hooper SL. and DiCaprio RA. (2004). Crustacean motor pattern generator networks. *Neurosignals* **13**:50-69.
- Hounsgaard J., Hultborn H., Jespersen B. and Kiehn O. (1984). Intrinsic membrane properties causing a bistable behaviour of alpha-motoneurons. *Exp Brain Res* **55**:391-4.
- Hoyle G. and Burrows M. (1973). Neural mechanisms underlying behavior in the locust *Schistocerca gregaria*. I. Physiology of identified motoneurons in the metathoracic ganglion. *J Neurobiol* **4**:3-41.
- Johnston RM, Consoulas C, Pflüger HJ and Levine RB (1999) Patterned activation of unpaired median neurons during active crawling in manduca sexta larvae. *J Exp Biol* **202**:103–113.

- Johnston RM and Levine RB (1996) Crawling motor patterns induced by pilocarpine in isolated larval nerve cords of *Manduca sexta*. *J Neurophysiol* **76**:3178–95.
- Jordan LM. (1998). Initiation of locomotion in mammals. *Ann N Y Acad Sci* **860**:83-93.
- Kiehn O and Eken T. (1998). Functional role of plateau potentials in vertebrate motor neurons. *Curr Opin Neurobiol* **8**:746-52.
- Kiehn O., Kjaerulff O., Tresch MC. and Harris-Warrick RM. (2000). Contributions of intrinsic motor neuron properties to the production of rhythmic motor output in the mammalian spinal cord. *Brain Res Bull* **53**:649-59.
- Laurent G. and Hustert R. (1988). Motor neuronal receptive fields delimit patterns of motor activity during locomotion of the locust. *J Neurosci* **8**:4349-66.
- Le Ray D., Clarac F. and Cattaert D. (1997). Functional analysis of the sensory motor pathway of resistance reflex in crayfish. II. Integration Of sensory inputs in motor neurons. *J Neurophysiol* **78**:3144-53.
- Llinas R. and Sugimori M. (1980). Electrophysiological properties of in vitro Purkinje cell dendrites in mammalian cerebellar slices. *J Physiol* **305**:197-213.
- Lippold OCJ. (1952). The relation between integrated action potentials in a human muscle and its isometric tension. *J Physiol* **117**:492-99.
- Ludwar B. (2003). Mechanisms for intersegmental leg coordination in walking stick insects. Inaugural-Dissertation zur Erlangung des Doktorgrades der Mathematisch-Naturwissenschaftlichen Fakultät der Universität zu Köln.
- Ludwar BC, Göritz ML. and Schmidt J. (2005a) Intersegmental coordination of walking movements in stick insects. *J Neurophysiol* **93**:1255-65.
- Ludwar BC, Westmark S, Büschges A and Schmidt J. (2005b). Modulation of membrane potential in mesothoracic moto- and interneurons during stick insect front-leg walking. *J Neurophysiol* **94**:2772-84.
- Marder E. and Calabrese RL. (1996). Principles of rhythmic motor pattern generation. *Physiol Rev* **76**:687-717.
- Marquardt F. (1940). Beiträge zur Anatomie der Muskulatur und der peripheren Nerven von *Carausius (Dixippus) morosus* BR. *Zool Jahrb Abt Ont Tiere* **66**:63-128.
- McCrea DA. (2001). Spinal circuitry of sensorimotor control of locomotion. *J Physiol* **533**:41-50.
- Mendell LM. and Henneman E. (1971). Terminals of single Ia fibers: location, density, and distribution within a pool of 300 homonymous motoneurons. *J Neurophysiol* **34**:171-87.
- Newland PL. and Emptage NJ. (1996). The central connections and actions during walking of the tibial campaniform sensilla in the locust. *J Comp Physiol A* **178**:749-762.

- Nusbaum MP and Beenhakker MP. (2002). A small-systems approach to motor pattern generation *Nature* **417**:343-50.
- Nusbaum MP., El Manira A., Gossard J-P. and Rossignol S. (1997). Presynaptic mechanisms during rhythmic activity in vertebrates and invertebrates. In: *Neurons, Networks, and Motor Behavior*. Stein PSG., Grillner S., Selverston AI. and Stuart DG. (eds.). MIT Press, Cambridge, USA; pp 237-253
- Orlovsky GN., Deliagina TG. and Grillner S. (eds.). (1999). *Neuronal Control of Locomotion*. Oxford University Press, New York, USA.
- Orsal D., Perret C. and Cabelguen JM. (1986). Evidence of rhythmic inhibitory synaptic influences in hindlimb motoneurons during fictive locomotion in the thalamic cat. *Exp Brain Res* **64**:217-24.
- Paggett KC., Jackson AW. and McClellan AD. (2004). Organization of higher-order brain areas that initiate locomotor activity in larval lamprey. *Neuroscience* **125**:25-33.
- Pearson K. (1993). Common principles of motor control in vertebrates and invertebrates. *Annu Rev Neurosci* **16**:265-97.
- Pearson KG. and Gordon J. (2000). Locomotion. In: *Principles of Neural Science*, 4th edition, pp. 737-755. Kandel ER., Schwartz JH. and Jessell TM. (eds). Appleton & Lange, New York.
- Pearson KG. and Wolf H. (1987). Comparison of motor patterns in intact and deafferented flight system of the locust. *J Comp Physiol* **106**:259-68.
- Pearson KG, Reye, DN, Parsons DW., Bicker, G. (1985). Flight-initiating interneurons in the locust. *J Neurophysiol* **53**:910-25.
- Perreault MC. (2002). Motoneurons have different membrane resistance during fictive scratching and weight support. *J Neurosci* **22**:8259-65.
- Pfeiffer HJ. (1991). Kontrolle des Flexor-Tibiae-Muskels der Gespenstheuschrecke *Extatosoma tiaratum* in verschiedenen Verhaltenszuständen. Inaugural dissertation zur Erlangung des Doktorgrades, University of Kaiserslautern.
- Pinter MJ. 1990. The role of motoneuron membrane properties in the determination of recruitment order. In: *The segmental motor system*. Binder MD and Mendell LM (eds.). New York, Oxford: Oxford University Press; pp. 195-181.
- Preston, JB. and Whitlock DG. (1961). Intracellular potentials recorded from motoneurons following precentral gyrus stimulation in primate. *J Neurophysiol* **24**:91-100.
- Prochazka A. and Yakovenko S. (2001) Locomotor control: from spring-like reactions of muscles to neural prediction. In: *The Somatosensory System: Deciphering The Brain's Own Body Image*. Nelson RJ. (ed.). CRC Press, Boca Raton, USA; pp. 141-81.

- Rathmayer W. (1996). Motorische Steuerung bei Invertebraten. In: *Neurowissenschaft*; Dudel J., Menzel R. and Schmidt RF. (eds.). Springer Verlag, Heidelberg, Germany; pp. 167-90.
- Ridgel AL. and Ritzmann RE. (2005). Effects of neck and circumoesophageal connective lesions on posture and locomotion in the cockroach *J Comp Physiol A* **191**:559–73.
- Ritzmann RE., Quinn RD. and Fischer MS. (2004). Convergent evolution and locomotion through complex terrain by insects, vertebrates and robots. *Arth Struct Devel* **33**:361–79.
- Roberts A., Soffe SR. and Dale N. (1986). Spinal interneurons and swimming in frog embryos. In: *Neurobiology of vertebrate locomotion*. Grillner S., Stein PSG., Stuart DG., Forssberg H. and Herman RM. (eds.). MacMillan, London; pp. 335-52.
- Roberts A, Dale N, Evoy WH and Soffe SR. (1985). Synaptic potentials in motoneurons during fictive swimming in spinal *Xenopus* embryos. *J Neurophysiol* **54**:1-10.
- Roberts A., Soffe SR., Wolf ES., Yoshida M. and Zhao FY. (1998). Central circuits controlling locomotion in young frog tadpoles. *Ann N Y Acad Sci* **860**:19-34.
- Robertson RM. (2003). Locust flight: components and mechanisms in the motor. In: *The Handbook of Brain Theory and Neural Networks*, 2nd Edition, pp. 654-657. Arbib MA. (ed.). MIT Press, Cambridge, USA.
- Roeder K (1937) The control of tonus and locomotor activity in the praying mantis (*Mantis religiosa* L.). *J Exp Biol* **76**:353–74.
- Russell DF. and Wallén P. (1983). On the control of myotomal motoneurons during "fictive swimming" in the lamprey spinal cord in vitro. *Acta Physiol Scand* **117**:161-70.
- Sasaki K. and Burrows M. (1998). Innervation pattern of a pool of nine excitatory motor neurons in the flexor tibiae muscle of a locust hind leg. *J Exp Biol* **201**:1885-93.
- Satterlie RA. (1993). Neuromuscular organization in the swimming system of the pteropod mollusc *Clione limacina*. *J Exp Biol* **181**:119-40.
- Sauer AE., Büschges A. and Stein W. (1997). Role of presynaptic inputs to proprioceptive afferents in tuning sensorimotor pathways of an insect joint control network. *J Neurobiol* **32**:359-76.
- Sauer AE., Driesang RB., Büschges A. and Bässler U. (1996). Distributed processing on the basis of parallel antagonistic pathways. Simulation of the femur-tibia control system in the stick insect. *J Comp Neurosci* **3**:179-98.
- Schmidt J., Fischer H. and Büschges A. (2001). Pattern generation for walking and searching movements of a stick insect. II. Control of motoneuronal activity. *J Neurophysiol* **69**:1583-95.
- Schmitz J. and Stein W. (2000). Convergence of load and movement information onto leg motoneurons in insects. *J Neurobiol* **42**:424-36.

- Schmitz J., Schumann K. and von Kamp A. (2000) Mechanisms for self-adaptation of posture and movement to increased load. In: *Proc. 30th Meeting Soc. for Neuroscience*, New Orleans; p. 368.7.
- Schmitz J., Bartling C., Brunn DE., Cruse H., Dean J., Kindermann T., Schumm M. and Wagner H. (1995). Adaptive properties of "hard-wired" neuronal systems. *Verh Dtsch Zoo. Ges* **88.2**: 165-79.
- Selverston AI. (1977). Neural circuitry underlying oscillatory motor output. *J Physiol (Paris)* **73**:463-70.
- Shik ML., Severin FV. and Orlovsky GN. (1966). Control of walking and running by means of electrical stimulation of the mid-brain. *Biophysics* **11**:756-65.
- Sillar KT. and Roberts A. (1993). Control of frequency during swimming in *Xenopus* embryos: a study on interneuronal recruitment in a spinal rhythm generator. *J Physiol* **472**:557-72.
- Sirota MG., Di Prisco GV. and Dubuc R. (2000). Stimulation of the mesencephalic locomotor region elicits controlled swimming in the semi-intact lamprey. *Eur J Neurosci* **12**:4081-92.
- Soffe SR. and Roberts A. (1982). Tonic and phasic synaptic input to spinal cord motoneurons during fictive locomotion in frog embryos. *J Neurophysiol* **48**:1279-88.
- Spruston N., Jaffe DB., Williams SH and Johnston D. (1993). Voltage- and space-clamp errors associated with the measurement of electrotonically remote synaptic events. *J Neurophysiol* **70**:781-802.
- Stein PSG., Grillner S., Selverston AI. and Stuart DG. (eds.) (1997). *Neurons, Networks, and Motor Behavior*. MIT Press, Cambridge, USA.
- Stent GS., Thompson WJ. and Calabrese RL. (1979). Neural control of heartbeat in the leech and in some other invertebrates. *Physiol Rev* **59**:101-36.
- Storrer J., Bässler U. and Mayer S. (1986). Motor neurons in the meso- and metathoracic ganglia of the stick insect. *Zool Jb Physiol* **90**:359-74.
- Theophilidis G. and Burns MD. (1983). The innervation of the mesothoracic flexor tibiae muscle of the locust. *J Exp Biol* **105**:373-88.
- Trimmer BA. (1994). Characterization of a muscarinic current that regulates excitability of an identified insect motoneuron. *J Neurophysiol* **72**:1862-73.
- Trimmer BA and Weeks JC. (1993). Muscarinic acetylcholine receptors modulate the excitability of an identified insect motoneuron. *J Neurophysiol* **69**:1821-36.
- von Uckermann GBG. (2004). Untersuchungen zur Kontrolle der Extensoraktivität im Einbeinpräparat der Stabheuschrecke *Carausius morosus*. Diplomarbeit an der Universität zu Köln.

- Wallén P. Grillner S. and Feldman JL. (1985). Dorsal and ventral myotome motoneurons and their input during fictive locomotion in lamprey. *J Neurosci* **5**:654-62.
- Wallén P. Shupliakov O. and Hill RH. (1993). Origin of phasic synaptic inhibition in myotomal motoneurons during fictive locomotion in the lamprey. *Exp Brain Res* **96**:194-202.
- Wendler G. (1964). Laufen und Stehen der Stabheuschrecke *Carausius morosus*: Sinnesborstenfelder in den Beingelenken als Glieder von Regelkreisen. *Z Vergl Physiol* **48**:198-250.
- Wiersma CAG. and Ikeda K. (1964). Interneurons commanding swimmeret movements in the crayfish *Procambarus clarki* (Girard). *Comp Biochem Physiol* **12**:509-25.
- Wilson JA. 1979. The structure and function of serially homologous leg motor neurons in the locust. II. Physiology. *J Neurobiol* **10**:153-167.
- Winter DA. (1990). Biomechanics and motor control of human movement. John Wiley & Sons, New York, USA:
- Yakovenko S., McCrea DA., Stecina K. and Prochazka A. (2005). Control of locomotor cycle durations. *J Neurophysiol* **94**:1057-65.
- Zill S., Schmitz J. and Büschges A. (2004). Load sensing and control of posture and locomotion. *Arth Struct Devel* **33**:237-86.

Appendix

Erklärung

Ich versichere, dass ich die von mir vorgelegte Dissertation selbständig angefertigt, die benutzten Quellen und Hilfsmittel vollständig angegeben und die Stellen der Arbeit - einschließlich Tabellen, Karten und Abbildungen -, die anderen Werken im Wortlaut oder dem Sinn nach entnommen sind, in jedem Einzelfall als Entlehnung kenntlich gemacht habe; dass diese Dissertation noch keiner anderen Fakultät oder Universität zur Prüfung vorgelegen hat; dass sie - abgesehen von unten angegebenen Teilpublikationen - noch nicht veröffentlicht worden ist sowie, dass ich eine solche Veröffentlichung vor Abschluss des Promotionsverfahrens nicht vornehmen werde. Die Bestimmungen dieser Promotionsordnung sind mir bekannt. Die von mir vorgelegte Dissertation ist von Prof. Dr. Ansgar Büschges betreut worden.

Jens Peter Gabriel

Teilpublikationen:

Articles:

Gabriel JP., Scharstein H., Schmidt J. and Büschges A. (2003). Control of flexor motoneuron activity during single leg walking of the stick insect on an electronically controlled treadmill. *J Neurobiol* **56**:237-251.

Posters and Abstracts:

v. Uckermann G., **Gabriel JP** and Büschges A. (2005). The local control of tibial motoneuron activity during single leg stepping in the stick insect. *98th Annual Meeting of the Deutsche Zoologische Gesellschaft, Bayreuth 2005; 7_Po_02.*

Gabriel JP. and Schmidt J. (2005). Synaptic drive to leg motoneurons during walking movements of the stick insect. *Proceedings of the 30th Goettingen Neurobiology Conference 2005*, 87A.

Westmark S., Ludwar BC., **Gabriel J.P.** and Schmidt J. (2004). Tonic input to leg motoneurons during walking in stick insects. Program No. 658.12. *2004 Abstract Viewer/Itinerary Planner*. Washington, DC: Society for Neuroscience.

Gabriel JP. and Schmidt J. (2003). Neural control of locomotion – intrinsic and extrinsic factors determining motoneuron activity in the stepping cycle. *Neuro-Visions: Brain Research in the 21st century. Düsseldorf, Germany 2003*, 18.

Gabriel JP., Scharstein H. and Schmidt J. (2003). Recruitment of flexor tibiae motoneurons during walking-like movements of the stick insect. *Proceedings of the 29th Goettingen Neurobiology Conference 2003*, 268.

Gabriel JP., Scharstein H., Schoenemann HD., Schmidt J. and Büschges, A. (2002). Locomotor movements of the stick insect single leg preparation on an ‘active’ treadmill. *95th Annual Meeting of the Deutsche Zoologische Gesellschaft, Halle (Saale) 2002. Supplement V*, 67.

Lebenslauf

Name: Jens Peter Gabriel

Gurtsdatum/-ort: 25. November 1975; Bielefeld

Nationalität: deutsch

<u>Anschrift (Büro):</u> Institut für Zoologie Universität zu Köln Weyertal 119 50931 Köln Deutschland	<u>Anschrift (privat):</u> Vintervägen 107 19464 Upplands-Väsby Schweden	<u>Telefon/Email:</u> Tel. privat: 0177-2632952 Email: jensgabriel@web.de Web: www.uni-koeln.de/math-nat-fak/zoologie/tierphysiologie/bueschges
--	--	---

Ausbildung

- Jun.-Aug. 2004 Teilnahme am Sommerkurs „Neural Systems & Behavior“ am Marine Biological Laboratory in Woods Hole, USA.
- Feb. 2002-Okt. 2005 Doktorarbeit im Fach Zoologie im Labor von Prof. Dr. A. Büschges an der Universität zu Köln mit dem Thema „Activity of leg motoneurons during single leg walking of the stick insect: From synaptic inputs to motor performance“.
- Jan. 2001-Jan. 2002 Diplomarbeit im Fach Zoologie im Labor von Prof. Dr. A. Büschges an der Universität zu Köln mit dem Thema „Die Schreitbewegungen des Einbeinpräparates der Stabheuschrecke auf einem ‚aktiven‘ Laufband“. **Abschluss als Diplom-Biologe**, Endnote 1.0 (sehr gut).
- Okt. 1996-Jan. 2002 Studium der Biologie an der Universität zu Köln.
- 1995 – 1996 Zivildienst bei der „Gemeinschaft für Naturschutz Senne und Ostwestfalen e.V.“ (GNS).
- 1986 – 1995 Hans-Ehrenberg Gymnasium, Bielefeld. Erwerb der **allgemeinen Hochschulreife** (Abitur); Endnote 1.6.
- 1982 – 1986 Hans-Christian-Andersen Grundschule, Bielefeld

Berufliche Tätigkeiten

- Feb. 2002-Sep. 2005 Wissenschaftlicher Mitarbeiter im Labor von Prof. Dr. A. Büschges an der Universität zu Köln.
- Okt.-Nov. 2000 Studentische Hilfskraft im Labor von Prof. Dr. W. Walkowiak an der Universität zu Köln.

Mitgliedschaften

- Mitglied der *Deutsche Zoologische Gesellschaft*
Mitglied der *Neurowissenschaftliche Gesellschaft*

Stipendien

- Reisestipendium, *Boehringer Ingelheim Fonds* (2004).

Jens Peter Gabriel

Acknowledgements

I would like to thank my supervisor Prof. Ansgar Büschges for excellent and friendly support as well as Drs. Joachim Schmidt, Hans Scharstein, Örjan Ekeberg, Scott Hooper, Tim Mentel and Matthias Gruhn for many thorough revisions of manuscripts, helpful comments and good insights. Many thanks also to the rest of the lab: Hans-Peter Bollhagen, Christa Graef, Sharon Meyen-Southard, Sherylane Marasigan, Ming-Ching Eckert and Lydia Berlingen for continuous technical help and lots of paperwork; Michael Dübbert and Michael Schöngen for valuable help with a large variety of computer problems; Christoph Guschlbauer, Géraldine v. Uckermann, Sandra Westmark, Markus Blümel, Anke Borgmann and Alexander Krause for many discussions and a great and friendly atmosphere.

I am thankful to my parents for their continuous support.

But I am most grateful to my wife Jennifer, who through many years has provided me with love, encouragement and also the distraction that was necessary in the course of this work.

Jens Peter Gabriel